

## Improved Conditioning and Testing Procedures for HMA Moisture Susceptibility

### DETAILS

---

69 pages | | PAPERBACK

ISBN 978-0-309-42169-0 | DOI 10.17226/23153

### AUTHORS

---

BUY THIS BOOK

FIND RELATED TITLES

### Visit the National Academies Press at [NAP.edu](http://NAP.edu) and login or register to get:

---

- Access to free PDF downloads of thousands of scientific reports
- 10% off the price of print titles
- Email or social media notifications of new titles related to your interests
- Special offers and discounts



Distribution, posting, or copying of this PDF is strictly prohibited without written permission of the National Academies Press. (Request Permission) Unless otherwise indicated, all materials in this PDF are copyrighted by the National Academy of Sciences.

---

---

**NCHRP REPORT 589**

---

---

**Improved Conditioning  
and Testing Procedures  
for HMA Moisture Susceptibility**

**Mansour Solaimanian**

PENNSYLVANIA STATE UNIVERSITY  
University Park, PA

**Ramon F. Bonaquist**

ADVANCED ASPHALT TECHNOLOGIES, LLC  
Sterling, VA

**Vivek Tandon**

THE UNIVERSITY OF TEXAS AT EL PASO  
El Paso, TX

*Subject Areas*

Materials and Construction

---

Research sponsored by the American Association of State Highway and Transportation Officials  
in cooperation with the Federal Highway Administration

---

**TRANSPORTATION RESEARCH BOARD**

WASHINGTON, D.C.

2007

[www.TRB.org](http://www.TRB.org)

## **NATIONAL COOPERATIVE HIGHWAY RESEARCH PROGRAM**

Systematic, well-designed research provides the most effective approach to the solution of many problems facing highway administrators and engineers. Often, highway problems are of local interest and can best be studied by highway departments individually or in cooperation with their state universities and others. However, the accelerating growth of highway transportation develops increasingly complex problems of wide interest to highway authorities. These problems are best studied through a coordinated program of cooperative research.

In recognition of these needs, the highway administrators of the American Association of State Highway and Transportation Officials initiated in 1962 an objective national highway research program employing modern scientific techniques. This program is supported on a continuing basis by funds from participating member states of the Association and it receives the full cooperation and support of the Federal Highway Administration, United States Department of Transportation.

The Transportation Research Board of the National Academies was requested by the Association to administer the research program because of the Board's recognized objectivity and understanding of modern research practices. The Board is uniquely suited for this purpose as it maintains an extensive committee structure from which authorities on any highway transportation subject may be drawn; it possesses avenues of communications and cooperation with federal, state and local governmental agencies, universities, and industry; its relationship to the National Research Council is an insurance of objectivity; it maintains a full-time research correlation staff of specialists in highway transportation matters to bring the findings of research directly to those who are in a position to use them.

The program is developed on the basis of research needs identified by chief administrators of the highway and transportation departments and by committees of AASHTO. Each year, specific areas of research needs to be included in the program are proposed to the National Research Council and the Board by the American Association of State Highway and Transportation Officials. Research projects to fulfill these needs are defined by the Board, and qualified research agencies are selected from those that have submitted proposals. Administration and surveillance of research contracts are the responsibilities of the National Research Council and the Transportation Research Board.

The needs for highway research are many, and the National Cooperative Highway Research Program can make significant contributions to the solution of highway transportation problems of mutual concern to many responsible groups. The program, however, is intended to complement rather than to substitute for or duplicate other highway research programs.

## **NCHRP REPORT 589**

Project 9-34  
ISSN 0077-5614  
ISBN: 978-0-309-09906-6  
Library of Congress Control Number 2007907446

© 2007 Transportation Research Board

### **COPYRIGHT PERMISSION**

Authors herein are responsible for the authenticity of their materials and for obtaining written permissions from publishers or persons who own the copyright to any previously published or copyrighted material used herein.

Cooperative Research Programs (CRP) grants permission to reproduce material in this publication for classroom and not-for-profit purposes. Permission is given with the understanding that none of the material will be used to imply TRB, AASHTO, FAA, FHWA, FMCSA, FTA, or Transit Development Corporation endorsement of a particular product, method, or practice. It is expected that those reproducing the material in this document for educational and not-for-profit uses will give appropriate acknowledgment of the source of any reprinted or reproduced material. For other uses of the material, request permission from CRP.

### **NOTICE**

The project that is the subject of this report was a part of the National Cooperative Highway Research Program conducted by the Transportation Research Board with the approval of the Governing Board of the National Research Council. Such approval reflects the Governing Board's judgment that the program concerned is of national importance and appropriate with respect to both the purposes and resources of the National Research Council.

The members of the technical committee selected to monitor this project and to review this report were chosen for recognized scholarly competence and with due consideration for the balance of disciplines appropriate to the project. The opinions and conclusions expressed or implied are those of the research agency that performed the research, and, while they have been accepted as appropriate by the technical committee, they are not necessarily those of the Transportation Research Board, the National Research Council, the American Association of State Highway and Transportation Officials, or the Federal Highway Administration, U.S. Department of Transportation.

Each report is reviewed and accepted for publication by the technical committee according to procedures established and monitored by the Transportation Research Board Executive Committee and the Governing Board of the National Research Council.

The Transportation Research Board of the National Academies, the National Research Council, the Federal Highway Administration, the American Association of State Highway and Transportation Officials, and the individual states participating in the National Cooperative Highway Research Program do not endorse products or manufacturers. Trade or manufacturers' names appear herein solely because they are considered essential to the object of this report.

*Published reports of the*

### **NATIONAL COOPERATIVE HIGHWAY RESEARCH PROGRAM**

*are available from:*

Transportation Research Board  
Business Office  
500 Fifth Street, NW  
Washington, DC 20001

*and can be ordered through the Internet at:*

<http://www.national-academies.org/trb/bookstore>

Printed in the United States of America

# THE NATIONAL ACADEMIES

*Advisers to the Nation on Science, Engineering, and Medicine*

The **National Academy of Sciences** is a private, nonprofit, self-perpetuating society of distinguished scholars engaged in scientific and engineering research, dedicated to the furtherance of science and technology and to their use for the general welfare. On the authority of the charter granted to it by the Congress in 1863, the Academy has a mandate that requires it to advise the federal government on scientific and technical matters. Dr. Ralph J. Cicerone is president of the National Academy of Sciences.

The **National Academy of Engineering** was established in 1964, under the charter of the National Academy of Sciences, as a parallel organization of outstanding engineers. It is autonomous in its administration and in the selection of its members, sharing with the National Academy of Sciences the responsibility for advising the federal government. The National Academy of Engineering also sponsors engineering programs aimed at meeting national needs, encourages education and research, and recognizes the superior achievements of engineers. Dr. Charles M. Vest is president of the National Academy of Engineering.

The **Institute of Medicine** was established in 1970 by the National Academy of Sciences to secure the services of eminent members of appropriate professions in the examination of policy matters pertaining to the health of the public. The Institute acts under the responsibility given to the National Academy of Sciences by its congressional charter to be an adviser to the federal government and, on its own initiative, to identify issues of medical care, research, and education. Dr. Harvey V. Fineberg is president of the Institute of Medicine.

The **National Research Council** was organized by the National Academy of Sciences in 1916 to associate the broad community of science and technology with the Academy's purposes of furthering knowledge and advising the federal government. Functioning in accordance with general policies determined by the Academy, the Council has become the principal operating agency of both the National Academy of Sciences and the National Academy of Engineering in providing services to the government, the public, and the scientific and engineering communities. The Council is administered jointly by both the Academies and the Institute of Medicine. Dr. Ralph J. Cicerone and Dr. Charles M. Vest are chair and vice chair, respectively, of the National Research Council.

The **Transportation Research Board** is one of six major divisions of the National Research Council, which serves as an independent adviser to the federal government and others on scientific and technical questions of national importance. The National Research Council is jointly administered by the National Academy of Sciences, the National Academy of Engineering, and the Institute of Medicine. The mission of the Transportation Research Board is to provide leadership in transportation innovation and progress through research and information exchange, conducted within a setting that is objective, interdisciplinary, and multimodal. The Board's varied activities annually engage about 7,000 engineers, scientists, and other transportation researchers and practitioners from the public and private sectors and academia, all of whom contribute their expertise in the public interest. The program is supported by state transportation departments, federal agencies including the component administrations of the U.S. Department of Transportation, and other organizations and individuals interested in the development of transportation. [www.TRB.org](http://www.TRB.org)

[www.national-academies.org](http://www.national-academies.org)

# COOPERATIVE RESEARCH PROGRAMS

## **CRP STAFF FOR NCHRP REPORT 589**

**Christopher W. Jenks**, *Director, Cooperative Research Programs*  
**Crawford F. Jencks**, *Deputy Director, Cooperative Research Programs*  
**Edward T. Harrigan**, *Senior Program Officer*  
**Eileen P. Delaney**, *Director of Publications*  
**Ellen M. Chafee**, *Assistant Editor*

## **NCHRP PROJECT 09-34 PANEL**

### **Field of Materials and Construction—Area of Bituminous Materials**

**Timothy B. Aschenbrener**, *Colorado DOT (Chair)*  
**Phillip B. Blankenship**, *Asphalt Institute, Lexington, KY*  
**German J. Claros**, *Texas DOT*  
**Ronald Cominsky**, *Pennsylvania Asphalt Pavement Association*  
**Karl W. Frick**, *Oregon DOT*  
**Wade McClay**, *Freeport, ME*  
**Gale C. Page**, *Florida DOT*  
**Richard E. Root**, *Consultant, Scottsdale, AZ*  
**Judie Ryan**, *Wisconsin DOT*  
**John D'Angelo**, *FHWA Liaison*  
**Frederick Hejl**, *TRB Liaison*

## **AUTHOR ACKNOWLEDGMENTS**

The research reported herein was performed under NCHRP Project 9-34 by the Pennsylvania Transportation Institute at Pennsylvania State University, the University of Texas at El Paso, Advanced Asphalt Technologies, LLC, and PaveTex Engineering and Testing, Inc. The Pennsylvania Transportation Institute was the primary contractor.

Dr. Mansour Solaimanian, Director of the Northeast Center of Excellence for Pavement Technology at Pennsylvania State University, served as principal investigator for the project. Work at Advanced Asphalt Technologies, LLC, was performed under the direction of Dr. Ramon Bonaquist, Chief Operating Officer, who also served as the project manager. Dr. Vivek Tandon, Associate Professor of Civil Engineering, University of Texas, El Paso, was responsible for the work performed at the University of Texas at El Paso. Mr. Maghsoud Tahmoressi, President, PaveTex Engineering and Testing, Inc., oversaw the work performed at PaveTex. Dr. Charles Antle, Professor Emeritus, Pennsylvania State University, provided statistical advice to the research team.

Several graduate students were involved with testing and contributed significantly to the success of this project. Dr. Ali Soltani was instrumental in providing the data acquisition program. Mr. Darin Hunter, Senior Technician at Pennsylvania State University, and David Fedor, former Pennsylvania State University graduate student, made important contributions toward conducting the quality testing program for this research.

# FOREWORD

By Edward T. Harrigan

Staff Officer

Transportation Research Board

This report presents the findings of a research project to investigate whether combining the environmental conditioning system with the simple performance test would provide a superior procedure for determining the moisture susceptibility of hot-mix asphalt (HMA). The report will be of particular interest to materials engineers in state highway agencies, as well as to materials suppliers and paving contractor personnel who are responsible for the design and evaluation of HMA.

---

Moisture susceptibility is a primary cause of distress in hot-mix asphalt (HMA) pavements. There is good evidence that moisture susceptibility is influenced by aggregate mineralogy, aggregate surface texture, asphalt binder chemistry, and the interaction between asphalt binder and aggregate. The great number of different aggregate mineralogies and the numerous types of unmodified and modified asphalt binders used across the United States, coupled with varied environmental conditions, traffic levels, and construction practices, have made testing to accurately predict HMA moisture susceptibility a difficult task.

Under NCHRP Project 9-34, "Improved Conditioning Procedure for Predicting the Moisture Susceptibility of HMA Pavements," the Pennsylvania Transportation Institute was tasked with developing an improved method for determining the moisture susceptibility of HMA. The method would be based on the use of the Strategic Highway Research Program (SHRP) environmental conditioning system (ECS) combined with the dynamic modulus procedure developed as a simple performance test for HMA in NCHRP Projects 9-19 and 9-29; the measure of moisture susceptibility would be the ratio of dynamic modulus before conditioning to the dynamic modulus after conditioning in the ECS. At a minimum, the improved conditioning and testing procedure would be sensitive to the effects of normal variability in material and mix properties expected during laboratory mix design and field construction and exhibit acceptable levels of repeatability and reproducibility compared with current methods for moisture susceptibility testing.

In Phase I of the project, Pennsylvania Transportation Institute evaluated the three HMA performance tests developed in NCHRP Project 9-19 and determined that the dynamic modulus test method combined with the ECS conditioning procedure provided the best accuracy and precision compared with ASTM D4867, *Standard Test Method for Effect of Moisture on Asphalt Concrete Paving Mixtures*. In the following Phase IA, a preliminary ECS/dynamic modulus method was applied to laboratory specimens prepared from materials used in the construction of eight pavements of known field moisture susceptibility. The ECS/dynamic modulus procedure was shown to provide the best correlation with field performance compared with the results of both ASTM D4867 and the Hamburg wheel tracking test. However, despite this demonstrated ability to discriminate between mixes that

perform well and mixes that perform poorly in resisting moisture damage, it is unlikely that the ECS/dynamic modulus procedure would be adopted for routine use in its present form. Specifically, further work would be needed to reduce the duration of water and load conditioning and to better define the temperature at the time of conditioning and the magnitude of the required conditioning load.

This final report includes (1) detailed descriptions of the conditioning and test equipment, the laboratory experiments, and the data analysis procedures; (2) a discussion of the research results and their limitations; and (3) a summary of the key findings, conclusions, and recommendations. The following appendixes are available online at [http://trb.org/news/blurb\\_detail.asp?id=8113](http://trb.org/news/blurb_detail.asp?id=8113):

- Appendix A ECS/Dynamic Modulus Procedure for Phase IA
- Appendix B Test Specimen Identification and Air Void Content
- Appendix C HWTD Data and Graphs
- Appendix D ECS/Dynamic Modulus Results
- Appendix E Visual Inspection
- Appendix F Statistical Analysis of Dynamic Modulus Results.

# CONTENTS

1	<b>Summary</b>
3	<b>Chapter 1 Introduction and Research Approach</b>
3	1.1 Background and Problem Statement
3	1.2 Laboratory Tests for Moisture Damage Prediction
4	1.3 Objective and Scope
5	1.4 Report Organization
6	<b>Chapter 2 Experimental Program</b>
6	2.1 Phase I Experimental Program and Findings
8	2.2 Phase IA Experiment Design
9	2.3 Materials Selection
10	2.4 Laboratory Testing Program
27	<b>Chapter 3 Findings</b>
27	3.1 Mix Design Verification
30	3.2 ASTM D4867 Results
41	3.3 The Hamburg Wheel Tracking Test
43	3.4 Dynamic Modulus Testing
52	3.5 Statistical Analysis of Dynamic Modulus Test Results
61	<b>Chapter 4 Interpretation, Appraisal, and Applications</b>
61	4.1 Interpretation of the Results
61	4.2 Appraisal of the ECS/Dynamic Modulus Test Procedure
62	4.3 Applications
64	4.4 Cost of the ECS/Dynamic Modulus Set-Up
65	<b>Chapter 5 Conclusions and Recommendations</b>
65	5.1 Conclusions
65	5.2 Recommendations
67	<b>References</b>
69	<b>Appendixes</b>



## S U M M A R Y

# Improved Conditioning and Testing Procedures for HMA Moisture Susceptibility

Moisture damage continues to be one of the major causes of premature failure of hot-mix asphalt (HMA) pavements. Moisture damage in HMA occurs due to a loss of adhesion and/or cohesion, resulting in reduced strength or stiffness of the HMA and the development of various forms of pavement distress.

Numerous laboratory tests have been developed over the years to identify the moisture sensitivity of HMA. A general consensus in the industry is that laboratory tests performed on compacted HMA have the potential to be better indicators of moisture sensitivity than tests on loose mixture samples or the component asphalt binder or aggregate. Research documented by R. P. Lottman in *NCHRP Report 192: Predicting Moisture-Induced Damage to Asphaltic Concrete* (Transportation Research Board, National Research Council, Washington, D.C., 1978) with further modifications by D. G. Tunnicliff and R. Root (“Antistripping Additives in Asphalt Concrete—State-of-the-Art 1981,” *Proceedings, Association of Asphalt Paving Technologists*, Volume 51, 1982, pp. 265–293) resulted in the laboratory test that currently has the widest acceptance in the paving industry, AASHTO T283/ASTM D4867. Some state highway agencies have used alternatives such as the Hamburg Wheel Tracking Device (HWTD) and the Asphalt Pavement Analyzer (APA).

Under NCHRP Project 9-34, research was undertaken to develop an improved laboratory test procedure for predicting asphalt concrete susceptibility to moisture damage through integrating the Environmental Conditioning System (ECS) and Superpave simple performance tests. The ECS was developed under the Strategic Highway Research Program (SHRP) for predicting the moisture sensitivity of asphalt concrete under conditions of temperature, moisture saturation, and dynamic loading similar to those found in pavements. Several modifications were made to the ECS based on Post-SHRP evaluations at the University of Texas at El Paso.

Specific Superpave simple performance tests were researched and recommended under NCHRP Project 9-19. These tests included flow time (static creep), flow number (repeated load permanent deformation), and dynamic modulus. The objective of NCHRP Project 9-34 was to investigate whether an improved moisture sensitivity test could be developed by combining the ECS conditioning procedure with one of the NCHRP Project 9-19 simple performance tests.

The scope of work for NCHRP Project 9-34 was divided into two Phases. Phase I focused on the development and execution of a limited experiment to evaluate the potential for combining the NCHRP Project 9-19 simple performance tests with the ECS conditioning procedure to produce an improved moisture sensitivity test. Phase IA focused on further investigation of the ability of the selected simple performance test in combination with the ECS conditioning procedure to predict the moisture sensitivity of a larger number of mixes with documented field performance.

The primary conclusion from the Phase I study was that the dynamic modulus test was the most suited of the three simple performance tests for possible use with the ECS in an improved moisture sensitivity test. In Phase IA, the dynamic modulus test was the only test used under the ECS. The combined system was referred to as ECS/dynamic modulus procedure. Under Phase IA, the results from ECS/dynamic modulus tests were compared with those from the HWTD and ASTM D4867 tests. Two broad categories of mixes were included in the experiment: those mixes reported to perform poorly in the field and those mixes reported to perform well in the field.

The degree of success of the developed ECS/dynamic modulus procedure was not measured based on how well the results from this procedure compared with those from HWTD or ASTM D4867. Rather, the measure of success was based on the capability of the procedure to predict the reported field performance for each mix. The ECS/dynamic modulus procedure appeared to best match the reported field performance for each mix among the presented procedures.

Procurement of detailed information regarding construction and performance of selected mixes for this study was a great challenge. In most cases, lack of detailed performance information prevented reliable ranking of the mixtures in terms of moisture damage resistance. Furthermore, construction data and in-place density information were not available for use in interpreting results. Three of the mixes selected for this study that were reported to perform poorly had been historically poor performers in regard to moisture damage, regardless of in-place air voids. However, for two of the mixes, reported moisture damage problems were associated with specific projects, and in-place density information for these projects could have been of value in interpreting results.

In spite of the advantages of the ECS/dynamic modulus procedure, there are several shortcomings that need to be addressed before the ECS/dynamic modulus procedure can be used as a routine mix design test to identify the moisture damage susceptibility of a mix. These problems are mostly associated with the duration of water/load conditioning, temperature at the time of conditioning, and the magnitude of the conditioning load.

The developed ECS/dynamic modulus testing procedure has the potential to be used in the HMA design phase. A great benefit to this testing system is that it is focused on measuring a widely used engineering property, i.e., asphalt modulus. The technicians and engineers who will be conducting Superpave mix design will need to get familiar with the dynamic modulus test once it becomes part of the Superpave mix design system. As a result, it makes reasonable sense to utilize this testing with water/load conditioning to evaluate moisture damage.

Another important application of the results from this testing system will be with the developed mechanistic empirical pavement design guide (MEPDG) used for pavement performance predictions. The pavement response models in the design guide utilize the dynamic modulus as one of the important input parameters. The modulus of the unconditioned specimen as well as the retained modulus after the ECS/dynamic modulus testing could be used in the models to determine the impact of moisture damage on developed distresses (rutting and fatigue cracking).

Distilled water was used for conditioning of specimens in this study. The researchers for this study are not aware of any study that has investigated mix behavior after the mix has been conditioned with different types of water containing various dissolved chemicals and salts. This may be important to research since rain water and underground water, major contributors to asphalt moisture damage, could contain different types of salts in different parts of the country.

---

## CHAPTER 1

# Introduction and Research Approach

### 1.1 Background and Problem Statement

Moisture damage continues to be one of the major causes of premature failure of hot-mix asphalt (HMA) pavements. Moisture damage in HMA occurs due to a loss of adhesion and/or cohesion (1), resulting in reduced strength or stiffness of the HMA and the development of various forms of pavement distress (2).

Several mechanisms have been cited as causes of moisture damage, including detachment, displacement, spontaneous emulsification, film rupture, pore pressure, and hydraulic scouring (3). The proposed mechanisms are not well understood, and there is lack of agreement regarding the level of impact of individual or combined mechanisms on the moisture sensitivity of a given mixture. However, there is good evidence that moisture damage is influenced by aggregate mineralogy, aggregate surface texture, asphalt binder chemistry, and the interaction between the asphalt binder and aggregate (1, 3).

A general consensus in the industry is that laboratory tests performed on compacted HMA have the potential to be better indicators of moisture sensitivity than tests on loose mixture samples or the component asphalt binder or aggregate. Today, it remains a challenge to asphalt pavement technologists to develop a highly reliable and practical test procedure for determination of moisture damage. The challenge has been made more evident in research by Epps et al. that showed that the most widely used test procedure, AASHTO T283, has some problems (4). That research included five different mixtures from various states, and the results indicated that the sensitivity of the mixtures to moisture damage, as described by the state highway agencies, did not satisfactorily match the observed behavior of the mixtures for a number of data groups in the study.

An important consideration in the development and acceptance of a test procedure for moisture damage should be calibration of the test to the conditions for which it will be applied. Some tests have been calibrated and implemented on

a local basis (a region within a state). No test has been successfully calibrated and implemented across a wide spectrum of conditions. Factors for this have been a lack of correlation with field performance, a lack of good field performance databases, and difficulties with the tests, such as variability and difficulty of operation.

### 1.2 Laboratory Tests for Moisture Damage Prediction

Numerous laboratory tests have been developed over the years to identify the moisture sensitivity of HMA. The tests for identifying the moisture damage potential of an asphalt/aggregate mixture can be classified into two major categories: (1) those performed on loose mixtures, such as the static immersion test and the boil test, and (2) those performed on compacted mixtures, such as the immersion compression, indirect tensile strength, and modulus tests.

The immersion compression test was introduced in the late 1940s and was the first test to become an ASTM standard in the mid-1950s. Research in the 1960s brought considerable awareness to asphalt pavement technologists of the significant impact of climate and traffic on moisture damage. The significance of these factors was emphasized through the work of researchers such as Johnson (5), Schmidt and Graf (6), Jimenez (7), and Lottman (8). Jimenez developed a laboratory test simulating the effect of repeated water pressure on the behavior of saturated HMA. Extensive work by Lottman, with further modifications by Tunnicliff and Root (9), resulted in the laboratory test that currently has the widest acceptance in the paving industry, AASHTO Designation T283 (also known as ASTM D4867).

A survey of 55 agencies (including 50 states) compiled by Aschenbrener in 2002 indicated that 39 agencies used a tensile strength ratio obtained from specimens tested with and without moisture conditioning to evaluate moisture sensitivity. Methods that were used included the original Lottman

procedure (10), AASHTO T283, and ASTM D4867. According to Aschenbrener's survey, AASHTO T283 was by far the most popular, with 30 agencies using this method. State highway agencies have reported mixed success with AASHTO T283, resulting in continued research to refine the procedures and to investigate other alternatives. Examples of such alternatives include the Hamburg Wheel Tracking Device (HWTd) and the Asphalt Pavement Analyzer (APA), which were introduced in the early 1990s. The HWTd has gained popularity as a moisture sensitivity test and has been the subject of several research projects (11–14).

As part of the Strategic Highway Research Program (SHRP), the mechanisms responsible for moisture damage were investigated and a system, known as the Environmental Conditioning System (ECS), was developed for predicting the moisture sensitivity of HMA (15–17). It was subsequently standardized as AASHTO TP34, "Determining Moisture Sensitivity of Compacted Bituminous Mixtures Subjected to Hot and Cold Climate Conditions." This procedure was designed to determine the moisture sensitivity of compacted HMA specimens under conditions of temperature, moisture saturation, and dynamic loading similar to those found in pavements. Although the ECS showed promise, it gave results that were not significantly more precise or accurate than those of AASHTO T283. For this reason, AASHTO T283 was included as part of the standard practice for "Superpave Volumetric Mix Design," AASHTO R35. Post-SHRP evaluations of the ECS at the University of Texas at El Paso recommended several modifications to the system to improve its repeatability (18–21). These improvements focused on the conditioning process and the measurement of the specimen resilient modulus, which serves as the measure of moisture-induced damage in AASHTO TP34.

During the last several years, parallel to efforts for improving moisture damage tests, there has been significant research effort toward the development of a simple performance test to complement the Superpave volumetric mix design method. *NCHRP Report 465: Simple Performance Test for Superpave Mix Design* recommended three candidate methods for testing cylindrical specimens in uniaxial or triaxial loading: flow time (static creep), flow number (repeated load permanent deformation), and dynamic modulus (22). All three tests were shown to correlate to observed rutting in field test pavements (22). The dynamic modulus was also shown to have potential as a simple performance test for fatigue cracking. In work completed in NCHRP Project 1-37A, "Development of the 2002 Guide for the Design of New and Rehabilitated Pavement Structures: Phase II," the dynamic modulus was recommended as the primary material characterization test of HMA for pavement structural design. The use of this test for both mixture evaluation and structural design provides a link between mixture design and structural design that was one of the goals of the original Superpave Mixture Design and Analysis System.

This research project considers and evaluates candidate simple performance tests under the ECS for predicting the susceptibility of asphalt concrete to moisture damage.

### 1.3 Objective and Scope

The objective of NCHRP Project 9-34 was to investigate whether an improved moisture sensitivity test could be developed by combining the ECS procedure with one of the NCHRP Project 9-19 simple performance tests. To be an improvement over existing tests, the resulting procedure must

1. Reliably identify and rank the moisture sensitivity of HMA mixture, and
2. Exhibit acceptable levels of repeatability and reproducibility.

It is also desirable for the test to be extendable to quantify the effect of moisture sensitivity on pavement life. The product envisioned as a result of NCHRP Project 9-34 is an integrated system with capabilities of performing one or more of the NCHRP Project 9-19 simple performance tests on unconditioned and moisture-conditioned test specimens. The main advantage of such an integrated system would be the use of the same test to judge the expected performance of the mixture and its sensitivity to moisture damage. Such an integrated system also has the potential to allow moisture sensitivity to be considered in flexible pavement performance models. Finally, the cost of an integrated system could be potentially lower than that of separate systems for performance and moisture sensitivity testing.

The scope of work for NCHRP Project 9-34 was divided into two phases. Phase I focused on the development and execution of a limited experiment to evaluate the potential for combining the NCHRP Project 9-19 simple performance tests with the ECS procedure to produce an improved moisture sensitivity test. Following successful completion of Phase I, Phase II would then be directed at refining the combined test procedure, developing a Draft Standard Method of Test, and recommending moisture sensitivity specification limits for the ranges of U.S. climate and traffic.

Findings from Phase I were presented to the project panel in the Interim Report. The Interim Report and the Phase I findings were also discussed in detail with the project panel during a meeting in April 2003. Based on the findings from Phase I, the project panel made a series of recommendations revising the direction of NCHRP Project 9-34. The primary recommendation was that the remainder of the project should focus on further investigation of the ability of the dynamic modulus test, in combination with the ECS, to predict the moisture sensitivity of a larger number of mixes with documented field performance. This new work was referred to as Phase IA because it was an expansion of some of the experimental work conducted in Phase I.

## 1.4 Report Organization

This report documents the results of the research completed under NCHRP Project 9-34. Results from Phase I are briefly presented since details were reported in the Interim Report. This report is mostly allocated to Phase IA of the

project. The report is organized in five chapters. Chapters 1 and 2 cover the background information and experimental program, respectively. Results and findings are discussed in Chapter 3. Interpretation of results, appraisal, and applications are covered in Chapter 4. Finally, conclusions and recommendations are presented in Chapter 5.

---

## CHAPTER 2

# Experimental Program

### 2.1 Phase I Experimental Program and Findings

Details of the Phase I experimental program and its findings were documented in the Interim Report submitted on January 5, 2004. A summary of Phase I work is presented here. Table 1 presents the experimental matrix for the Phase I study. In this design, three aggregate sources with different levels of moisture sensitivity based on past research were tested using the three NCHRP Project 9-19 simple performance tests, ASTM D4867, and the HWTD. For the simple performance tests, specimens were tested unconditioned and after the ECS moisture procedure. The ASTM D4867 testing also included tests on unconditioned and conditioned specimens. The HWTD testing used submerged specimens only.

The aggregates included in the Phase I experiment were selected based on their performance in previous studies. The Texas limestone aggregate had historically exhibited good resistance to moisture damage. Mixtures produced with the sandstone aggregate typically had AASHTO T283 tensile strength ratios in the range of 0.83 to 0.86, which were lower than the typical results obtained for the limestone aggregate. Mixtures produced with the Virginia granite had poor resistance to moisture damage without the aid of an anti-stripping agent.

The same asphalt source (PG 70-22) was used to produce the mixtures for the Phase I experiment. The binder source used in the moisture-sensitive Virginia granite mixture was selected for the Phase I evaluation.

The mixtures for the Phase I evaluation were laboratory reproductions of actual project mixtures made from the three aggregate sources, with the exception of using the same binder for all mixtures. Table 2 provides a summary of the mixtures used in the Phase I experiment.

Table 3 presents a summary of the interpretation of the findings from the Phase I experiment. This table includes the ratings from past studies upon which the selection of the

three aggregates was based, moisture sensitivity results and ratings from the five tests conducted in Phase I, and the criteria used in the ratings.

The primary conclusion from Phase I of NCHRP Project 9-34 was that the dynamic modulus test was the most suited of the three simple performance tests for possible use with the ECS in an improved moisture sensitivity test. The ECS/Dynamic Modulus test was able to differentiate between mixes made with stripping resistant aggregates (such as Texas limestone) and those with aggregates prone to stripping (such as Virginia granite). The Phase I testing showed that the dynamic modulus decreases significantly when a moisture-sensitive material is conditioned using the ECS conditioning procedure. For the three materials tested in Phase I, the ratio of the conditioned to unconditioned dynamic modulus correctly identified the known moisture-insensitive and the known moisture-sensitive aggregates. The ratio of the conditioned to the unconditioned dynamic modulus ranked a suspected marginal aggregate as insensitive; however, based on ASTM D4867 and the HWTD, it appears that mixtures made with this aggregate and the specific binder used in Phase I are, in fact, moisture insensitive. The ECS/dynamic modulus test ranked the three Phase I mixtures the same way as ASTM D4867 ranked them.

In contrast to the dynamic modulus test, when the ECS was combined with the two flow tests, the results were generally irrational. Strains and strain rates were consistently lower in ECS specimens than strains and strain rates in unconditioned specimens. The repeated loading in the ECS conditioning procedure hardens the conditioned specimens, making it impossible to use the flow time test on unconditioned specimens and specimens conditioned with the ECS. The flow number test could possibly be used if the ECS conditioning procedure were modified to perform the flow number test during the conditioning process. However, this was not the case with this research since flow number tests were conducted after the ECS conditioning procedure. Although it appears feasible to

**Table 1. Phase I test matrix.**

Aggregate Source		Resistance to Moisture Damage	NCHRP Project 9-19 Simple Performance Tests			ASTM D4867	HWTD
Type	Location		Flow Time	Flow Number	Dynamic Modulus		
Limestone	Hunter, TX	Good	X	X	X	X	X
Sandstone	Sawyer, OK	Marginal	X	X	X	X	X
Granite	Richmond, VA	Poor	X	X	X	X	X

**Table 2. Summary of aggregate sources used in the Phase I experiment.**

Material Type	Source	Resistance to Moisture Damage	Nominal Maximum Aggregate Size (mm)	Design Asphalt Content
Limestone	Hunter, TX	Good	12.5	5.4%
Sandstone	Sawyer, OK	Moderate	19.0	5.3%
Granite	Richmond, VA	Poor	19.0	4.5%

conduct the flow number test during the ECS conditioning process, the flow number test has been shown to have a high level of variability in other studies. This high level of variability results in the test having poor sensitivity to changes caused by moisture conditioning. With four specimens per test and the current level of variability reported for the flow number test, the flow number for conditioned specimens must

decrease by approximately 40 percent for the conditioned and unconditioned tests to be considered significantly different. The high level of variability in the flow number test is a result of the flat slope of the permanent deformation curve for a large number of cycles prior to flow. This flat slope makes it very difficult to detect the exact point at which flow occurs in most mixtures. It is unlikely that the further development

**Table 3. Interpretation of Phase I findings.**

Test	Criteria	Resistance to Moisture Damage		
		Texas Limestone	Oklahoma Sandstone	Virginia Granite <sup>1</sup>
	Expected Performance from Previous Studies	Good	Moderate	Poor
ASTM D4867	Minimum TSR= 80% <sup>2</sup>	Pass	Pass	Fail
	TSR	87%	89%	66%
HWTD	Stripping Inflection Point (SIP)	Good	Good	Good
	SIP	> 20,000 passes	> 20,000 passes	>16,000 passes
	TxDOT Maximum Impression Depth	Pass	Pass	Pass
	Impression Depth at 20,000 passes	4.9 mm	2.2 mm	6.5 mm
ECS/Flow Time	Significant Difference in Flow Time	No Flow	No Flow	Pass
ECS/Flow Number	Significant Difference in Flow Number	No Flow	No Flow	No Flow
ECS/Dynamic Modulus	Significant Difference in Dynamic Modulus	Pass	Pass	Fail
	Modulus Ratio	0.92	0.95	0.66

<sup>1</sup> All three mixes were prepared using the binder for the Virginia granite mix, and, therefore, the mixes for Texas limestone and Oklahoma sandstone were not prepared using specific binders from the sources identified in the mix design.

<sup>2</sup> TSR = Tensile strength ratio.

planned for this test will decrease the variability to a level where it can be acceptable in a moisture sensitivity test.

## 2.2 Phase IA Experiment Design

### 2.2.1 Testing Program

The research conducted during Phase IA included ECS/dynamic modulus testing, ASTM D4867 tests, and HWTD tests. A total of eight different mixes was selected. Two broad categories of mixes were included in the experiment: (1) those reported to have poor field performance with respect to moisture damage and (2) those reported to have good field performance with respect to moisture damage. Selection of materials was skewed toward poorly performing mixes since it is crucial to properly identify these mixes before construction. Thus, the work plan included five mixes reported to perform poorly and three mixes reported to perform well.

For each mix, ASTM D4867 and HWTD tests required six and four test specimens, respectively. ASTM D4867 tests were conducted at Advanced Asphalt Technologies, LLC (AAT). The HWTD specimens were tested at Pavetex Engineering and Testing (Pavetex). For the ECS/dynamic modulus testing, six replicate specimens for each mix were considered. The ECS/dynamic modulus testing was conducted at the materials laboratories of the Northeast Center of Excellence for Pavement Technologies (NECEPT) at Pennsylvania State University (PSU), as well as the materials laboratories of the University of Texas at El Paso (UTEP). Therefore, there were a total of 12 ECS/dynamic modulus specimens for each mix—six for each laboratory. Table 4 presents the Phase IA testing matrix and location of tests.

### 2.2.2 Selection of Proper Sample Size for ECS/Dynamic Modulus Testing

An important consideration for Phase IA of this study was the selection of the sample size for testing conducted with the ECS/dynamic modulus test. Reasonable estimates of the required sample size were determined considering confidence intervals for the mean and standard deviation, as discussed below.

In general, the authors consider  $n$  specimens to be fabricated for each mix and each specimen to be tested for dynamic modulus before and after moisture conditioning with the ECS/dynamic modulus system. The property of interest is the percentage of the dynamic modulus retained after conditioning (i.e., the ratio of modulus after conditioning to modulus before conditioning), designated as *Retained %*. Thus

$$\text{Retained \%} = \left[ \frac{(\text{Dyn. Modulus After ECS})}{(\text{Dyn. Modulus Before ECS})} \right] \times 100\%$$

The values of the *Retained %* for the  $n$  specimens will provide information regarding the moisture susceptibility for the material. After consideration of possible outliers, the average of the remaining values will be the estimate of the ability of the mixtures to resist moisture-induced damage.

In Phase I of this study, it was found that the estimated standard deviation for a single measured *Retained %* was 5.7 percent. With this as the assumed true standard deviation for a single measured *Retained %*, the standard deviation for the average of  $n$  such measurements would be  $5.7\% / \sqrt{n}$ . The values for this standard deviation of the average are given in Table 5 for values of  $n$  from 1 to 10.

It is clear that additional samples beyond approximately six samples will not provide sufficient benefit to justify the added cost with respect to the estimation of the *Retained %*.

It should be noted that the standard deviation of the average of the measurements for each cell presented in Table 5 is the quantity that determines the power of the test and the precision of the confidence intervals.

The accuracy of the estimation of the standard deviation of a single measured *Retained %* is the second important question when a sample size is being considered. This estimation is important as one is considering the properties of the testing process and the measurements in a given cell for the combination of test device and test procedures of interest. It would be desirable to have a testing process for which the standard deviation is known to be small. For each cell of interest, a good estimate of the standard deviation of the measured values in the cell will be required. A useful approach is to consider the length of the confidence interval for the standard deviation that will result as a function of the number of samples. The 90-percent confidence interval for the true standard deviation

**Table 4. Phase IA testing matrix and location of tests.**

Test	Location	Number of Superpave Gyrotory Compactor (SGC) Specimens Per Mix	Number of Conditioned Specimens
HWTD	Pavetex	4	4
ASTM D4867	AAT	6	3
ECS/dynamic modulus	PSU and UTEP	12 (6 for each lab)	12 (6 for each lab)



**Table 5. Standard deviations of the average retained modulus for different sample sizes.**

Value of $n$	1	2	3	4	5	6	7	8	9	10
Std. Dev. of Mean (%)	5.7	4.0	3.3	2.9	2.5	2.3	2.2	2.0	1.9	1.8

of a single measured value of *Retained %* is a function of sample size and standard deviation. The sample size function,  $F(n)$ , is determined using chi square distribution with  $n - 1$  degrees of freedom for the selected level of confidence. The values of  $F(n)$  are given in Table 6 for  $n$  between 2 and 10.

It is clear from Table 6 that for the purpose of estimating the standard deviation of the measured values in a given cell, it would be good to have at least nine samples. However, considering that the data from the two laboratories for a given cell can be pooled (resulting in 12 observations), the common standard deviation can be reasonably estimated considering six replicates per mix for each laboratory.

### 2.3 Materials Selection

The most important criterion in selecting a specific mix for Phase IA was that the mix should have a known field performance record. The authors' best estimate of field performance was qualitative rather than rigorously quantitative. The best approach was to consider the two general categories of mixes, those that performed poorly and those that performed well, rather than sequential ranking of all the mixes. The performance of a mix will vary when it is exposed to different traffic, climatic, and construction conditions in the field. Therefore, comparing the performance of two mixes on tests in a controlled laboratory environment will not yield the most useful information on mix performance in the field. A mix might have failed severely in a short period of time in one project because it was exposed to a considerable amount of rain and heavy loads, drainage problems, and possibly had high air-void contents resulting from either poor mix design or poor compaction. A different mix might have exhibited marginal moisture damage just because it was well constructed and was located in an environment with less rain, lighter traffic, and good drainage. For these reasons, it was difficult to identify mixes that might be referred to as "marginal." Quantitative ranking of different mixes in different environments is a difficult task unless accurate traffic and environment and construction data are available and consid-

ered in conducting such a ranking. Qualitative data was the best type of information that could be obtained as the basis for the comparisons of mixtures in Phase IA.

Selection of specific mixes for this project was based on the following factors:

- Feedback from the project panel members,
- Feedback from other experts regarding the history of moisture damage and field performance of candidate mixes,
- Available creditable literature on previous research on moisture damage, and
- Feedback from state personnel in the areas where the mixes/aggregates were commonly used.

Five mixes reported to perform poorly and three mixes reported to perform well were identified for Phase IA of this research. Materials and pertinent mix designs for these mixes were received from materials producers. For each mix, the corresponding asphalt binder was also received from the pertinent asphalt producer. The sections that follow discuss the materials used in this phase of the project.

#### 2.3.1 Georgia Granite

Georgia granite, widely available in Georgia, has very good frictional properties. However, this material has demonstrated poor resistance to moisture damage. Most of the problems noticed with this aggregate in Georgia date back to the 1980s; attempts to solve these problems led to most of the research regarding moisture damage in the state (23). Since detecting moisture damage problems with this material, Georgia DOT has been using 1 percent lime in mixes containing Georgia granite. Georgia granite was also used in one of the mixes placed in the Pavement Test Track of the National Center for Asphalt Technology (NCAT) and was included in 1995 research conducted by Tunncliff and Root (24). Conversations with past and present Georgia DOT personnel resulted in the selection of Georgia granite from a specific source for use in this study.

**Table 6. Sample size function  $F(n)$  for determination of 90-percent confidence interval for standard deviation.**

Value of $n$	2	3	4	5	6	7	8	9	10
$F(n)$	15.29	3.83	2.3	1.72	1.42	1.23	1.09	0.99	0.92

### 2.3.2 Pennsylvania Dolomite

Pennsylvania dolomite, a dolomitic limestone, has been used in many projects throughout the Commonwealth of Pennsylvania with no apparent signs of stripping. The good historical performance of this aggregate along with the fact that it has been used without any antistripping agent made it an excellent source to be included in the project.

### 2.3.3 Mississippi Chert

Widely available in Mississippi, Mississippi chert has generally shown poor moisture damage resistance in the field. The moisture susceptibility of this aggregate resulted in significant change to the mixes used in the state in the early 1990s. The improvements included limiting natural sand, reducing the ratio of material passing the #200 sieve to the binder content, and using lime and liquid antistripping agents. The chert rock from one of the available sources has shown stripping problems with one source of binder and good resistance to moisture damage when the binder source was changed. The poor resistance to moisture damage has been observed with plant mixes even with lime added to the mix. The chert rock from one of the sources in Mississippi was also among the aggregates exhibiting poor performance in Tunncliffe and Root's 1995 laboratory evaluation of antistripping additives in asphaltic concrete mixtures (24). Chert rock from the same source has been used in one of the sections in the NCAT Pavement Test Track.

### 2.3.4 Kentucky Limestone

This crushed limestone aggregate is from a quarry in Kentucky. The aggregate has shown stripping problems at the pavement surface in the field after 1 to 2 years of service. The material has also exhibited severe failure in the HWTD when used with the local natural sand and with a PG 64 binder. The performance, however, has been good with a polymer-modified PG 76 binder. The mix with a PG 64 binder was selected as one of the candidates for this research.

### 2.3.5 Arkansas Gravel

Mixes prepared with gravel from one of the quarries in Arkansas have resulted in several pavement failures in Texas due to moisture damage. The mix design information for these mixes was available. The failed mixes had been prepared with a specific source of binder that is graded as a PG 64-22. The mix also failed when tested in the HWTD. The data from the completed ECS study at UTEP provided important information for this mix (19). In that research, the mix clearly demonstrated poor resistance to moisture damage. The performance of the mix had been reported to be excellent both

in the field and in the HWTD when a PG 76-22 polymer-modified binder with 1 percent lime was used with this aggregate. The mix with the PG 64-22 binder that exhibited failure in the field (see above) was included in this study.

### 2.3.6 Oklahoma Sandstone

The Oklahoma sandstone used in Phase IA of this research has been used with a PG 76-22 binder to make a mix that performs well. This mix was placed on IH-20 in the Atlanta District of Texas in 2001 and exhibited excellent performance based on measurements in 2003. This mix also demonstrated very little deformation in the HWTD (3 to 4 mm) when subjected to 20,000 passes at 50°C. The IH-20 study is a 5-year field/laboratory moisture damage research project that will be a valuable source of information for this mix. Therefore, this mix was selected as mix that performs well for this project.

### 2.3.7 Wisconsin Gravel

Materials and mix design were received from a gravel source in Wisconsin that, historically, has shown excellent resistance to moisture damage. The gravel for the selected mix has been used with no lime or liquid antistripping agent. This mix utilizes a PG 58-28 binder and is the softest mix used in this research.

### 2.3.8 Wyoming Gravel

Wyoming gravel, which has a high silica ( $\text{SiO}_2$ ) content, has been known as a highly moisture-sensitive aggregate if no hydrated lime is used. Various laboratory studies on this aggregate during SHRP and in the post-SHRP period have proven the moisture sensitivity of this aggregate with a range of different binders. As a result of this well-documented poor behavior, a specific mix design for this material, with known poor field performance, was requested and received from the Wyoming Department of Transportation (DOT) for use in this research.

## 2.4 Laboratory Testing Program

The mixtures procured for Phase IA of the research were subjected to three types of tests: ASTM D4867, HWTD, and dynamic modulus before and after the ECS conditioning procedure. Prior to preparation of the specimens for the tests, a procedure was followed to verify the mix designs.

### 2.4.1 Mix Design Information and Verification

As discussed previously, eight mixtures were used in Phase IA of NCHRP Project 9-34. For each mixture, detailed

mix design information was requested from both the responsible highway agency and the hot-mix supplier. Production quality control data and acceptance data were also requested, but none of the agencies or suppliers provided these data. Table 7 summarizes the mix design data that were provided for each of the eight mixtures. Detailed mix design data were provided for seven of the eight mixtures used. For the Arkansas gravel, only the gradation, optimum binder content, and design compaction level were provided.

The date that each mixture design was prepared is presented in Table 7 along with the date that samples were received for NCHRP Project 9-34. The time between the mixture design and the verification ranged from less than 1 month to 4.25 years.

The findings from the mix design verification study are discussed in Chapter 3.

## 2.4.2 Specimen Preparation

All specimens for Phase IA of NCHRP Project 9-34 were fabricated by AAT using standard procedures. The sections that follow discuss procedures used in the specimen fabrication process for:

- Handling of binders and aggregates;
- Laboratory mixing, aging, and compaction;
- Fabrication of specimens for the ECS/dynamic modulus tests; and
- Shipping of test specimens.

### 2.4.2.1 Binder Handling

Samples of the binder used in each mixture were shipped to AAT by the respective material supplier in either 1-gal or 5-gal metal cans. Upon receipt at AAT, the binder samples were divided into quart containers by heating the original container in an oven set at 135°C, stirring with a mechanical stirrer, and pouring the binder into the individual quart containers. A representative sample was obtained from one of the quart containers, and viscosities were determined at 135°C, 150°C, and 165°C—in accordance with AASHTO T316—to determine appropriate mixing and compaction temperatures. The quart containers were then used in the preparation of laboratory mixture batches. Quart containers were heated only once. Excess binder in the quart containers was discarded. The Phase IA testing program required approximately 7.5 l (2 gal) of binder for each mixture.

### 2.4.2.2 Aggregate Handling

Representative samples of the aggregates used in each mixture were shipped to AAT by the respective suppliers in sam-

ple bags, plastic containers, and metal cans of varying sizes. The procedures described in the appendix of *Mix Design Methods for Asphalt Concrete and Other Hot-Mix Types (25)* were used to prepare the aggregate samples for laboratory batching. Coarse aggregate samples were separated into individual sizes, while individual samples of fine aggregate were mixed together to produce a homogeneous supply for subsequent batching.

Specimen batches were made assuming that the proportions given in the mixture design were based on washed gradations analyses. The research team attempted to verify that all of the mixture designs were based on washed gradation analyses; however, the team was unable to achieve this verification. The gradation of the blends was verified by performing washed sieve analysis on one of the batches. The results of these sieve analyses are discussed in Chapter 3.

### 2.4.2.3 Mixing, Aging, and Compaction

Four different size gyratory specimens were used in Phase IA. Specimens for mixture verification were 150 mm (5.90 in.) in diameter by 115 mm (4.53 in.) high. Specimens for the ASTM D4867 testing were 100 mm (3.94 in.) in diameter by 65 mm (2.5 in.) high. Specimens for the HWTD were 150 mm (5.90 in.) in diameter by 62 mm (2.44 in.) high. Specimens for the ECS/dynamic modulus tests before sawing and coring were 150 mm (5.90 in.) in diameter by 165 mm (6.5 in.) high. After sawing and coring, the ECS/dynamic modulus specimens were 100 mm (4.0 in.) in diameter by 150 mm (5.9 in.) high. All gyratory specimens were prepared to a target air void content in accordance with AASHTO T312. The reported air void contents are those for the final test specimen, which is the complete specimen for the verification, ASTM D4867 and HWTD tests, and the sawed and cored specimen for the ECS/dynamic modulus tests. An Interlaken compactor meeting the requirements of AASHTO T312 was used to prepare the HWTD and ECS/dynamic modulus test specimens. An Invelop Oy compactor meeting the requirements of AASHTO T312 was used to prepare the ASTM D4867 specimens.

Mixing and compaction temperatures for the binders were determined from viscosities measured at 135°C, 150°C, and 165°C—in accordance with ASTM D316. These viscosities were converted to kinematic viscosities using the binder specific gravity measured at 25°C and the specific gravity temperature correction factors given in Annex A1 of AASHTO T201. Table 8 presents mixing and compaction temperatures for each mixture. Prior to compaction, materials for all specimens were short-term oven-aged in accordance with AASHTO R30 for 2 h at the compaction temperature. Again, the research team attempted to verify, but ultimately was unable to verify, that the volumetric properties of

Table 7. Summary of mix design data provided for the mixtures used in Phase IA.

Property	GA Granite	AR Gravel	WI Gravel	MS Chert	KY Limestone	OK Sandstone with Lime	PA Dolomite	WY Gravel
Mixture Design Date	5/3/2000	10/3/2003	7/8/2003	4/14/2003	5/7/2003	3/20/2001	7/13/2000	4/24/2002
Sample Receipt Date	8/5/2003	10/20/2003	12/1/2003	12/1/2003	5/24/2004	6/23/2004	10/15/2004	12/21/2004
Time between Design and Verification, yrs	3.26	0.05	0.40	0.63	1.05	3.26	4.26	2.66
AASHTO M323 Nominal Max Size, mm	12.5	19.0	12.5	12.5	9.5	12.5	19.0	12.5
AASHTO M323 Gradation Classification	Coarse	Fine	Fine	Fine	Coarse	Coarse	Coarse	Fine
Binder Grade	PG 67-22	PG 64-22	PG 58-28	PG 67-22	PG 64-22	PG 76-22	PG 64-22	PG 64-22
Design Compaction	Gyratory	Gyratory	Gyratory	Gyratory	Gyratory	Gyratory	Gyratory	Marshall
Compaction Level, $N_{design}$ /Blows	75	100	100	68	100	125	75	75
Gradation, % passing	Sieve Size, mm							
	25	100	100	100	100	100	100	100
	19	100	100	100	100	100	100	100
	12.5	99	88	97	95	100	92	95
	9.5	83	80	89	89	95	79	77
	4.75	50	60	70	65	64	49	53
	2.36	36	48	53	47	42	29	39
	1.18	27	36	38	35	29	22	25
	0.6	20	27	27	27	21	19	20
	0.3	15	16	14	14	11	15	9
0.15	9	7	7	7	6	10	6	
0.075	5.1	4.3	4.8	5.3	4.5	6.5	4.0	6.4
Asphalt Content, wt %	4.7	5.0	5.4	5.4	5.4	5.1	4.6	5.0
Air Voids, vol %	4.0	4.0	4.0	4.0	4.0	4.0	3.8	5.0
Maximum Specific Gravity of Mix	2.592	NA <sup>1</sup>	2.504	2.371	2.458	2.373	2.597	2.452
Bulk Specific Gravity of Specimen	2.477	NA	2.404	2.276	2.360	2.278	2.498	2.329
Bulk Specific Gravity of Aggregate	2.795	NA	2.684	2.513	2.640	2.541	2.772	2.577
Bulk Specific Gravity of Binder	<b>1.030</b> <sup>2</sup>	<b>1.030</b>	1.031	1.038	1.030	1.030	1.030	1.030
Effective Specific Gravity of Aggregate	2.802	NA	2.726	2.559	2.669	2.552	2.803	2.644
Absorbed Asphalt, wt % aggregate basis	0.086	NA	0.597	0.735	0.427	0.172	0.406	1.015
Effective Binder Content, wt %	4.6	NA	4.8	4.7	5.0	4.9	4.2	4.0
Voids in Mineral Aggregate, vol %	15.5	NA	15.3	14.3	15.4	14.9	14.0	14.1
Voids Filled with Asphalt, %	74.3	NA	73.8	72.1	74.1	73.2	72.9	64.6
Effective Binder Content, vol %	11.5	NA	11.3	10.3	11.4	10.9	10.2	9.1
Dust to Effective Binder Content, %	1.1	NA	1.0	1.1	0.9	1.3	0.9	1.6
Tensile Strength Ratio, %	NA	NA	87.0	NA	81.0	NA	90.0	16.9

<sup>1</sup>NA = data not available.<sup>2</sup>Binder specific gravity data in bold was assumed.

**Table 8. Mixing and compaction temperatures for the mixes used in the study.**

Source	Mixing Temperature (°C)	Compaction Temperature (°C)
GA Granite	163	152
AR Gravel	159	156
WI Gravel	150	135
MS Chert	158	148
KY Limestone	148	130
OK Sandstone with Lime	166	155
PA Dolomite	157	145
WY Gravel	165	145

mixture designs that were provided were based on specimens that were short-term oven-aged.

#### 2.4.2.4 Sawing and Coring of ECS/Dynamic Modulus Test Specimens

The ECS/dynamic modulus test specimens were manufactured by coring and sawing test specimens 100 mm (3.94 in.) in diameter by 150 mm (5.90 in.) in height from the middle of gyratory compacted specimens that were 150 mm (5.90 in.) in diameter by 165 mm (6.5 in.) in height. The procedure for preparing dynamic modulus specimens is described in AASHTO TP62. There are three reasons for using smaller test specimens obtained from larger gyratory specimens in the dynamic modulus test. The first is to obtain an appropriate aspect ratio for the test specimens. Research performed under NCHRP Project 9-19 found that a minimum height-to-diameter ratio of 1.5 was needed for the dynamic modulus test (26). The second reason is to eliminate areas of high air voids in the gyratory specimens. Gyratory compacted specimens typically have high air voids near the ends and the circumference of the specimen. The third reason is to obtain relatively smooth, parallel ends for testing. Dynamic modulus test specimens were prepared to the dimensional tolerances listed in Table 9. These tolerances are somewhat different from those specified in AASHTO TP62 and are the result of a study performed under NCHRP Project 9-29 to determine practical tolerances for dynamic modulus specimen preparation (27).

Several laboratories have adapted equipment for preparing dynamic modulus test specimens. The various approaches range from elaborate feed-control drills combined with sophisticated holders and double-bladed saws to standard drills and single-bladed saws with simple clamping arrangements. For this project, specimens meeting the tolerances listed in Table 9 were prepared using a portable core-drilling machine and a double-bladed saw. As shown in Figure 1, the portable core-drilling machine was mounted to a heavy stand on the laboratory floor to facilitate vertical drilling of the

**Table 9. NCHRP Project 9-29 specimen dimension tolerances (27).**

Item	Specification	Remarks
Average Diameter	100 mm to 104 mm (3.94 in to 4.09 in)	See Note 1
Standard Deviation of Diameter	0.5 mm (0.02 in)	See Note 1
Height	147.5 mm to 152.5 mm (5.81 in to 6.00 in)	See Note 2
End Flatness	0.5 mm (0.02 in)	See Note 3
End Perpendicularity	1.0 mm (0.40 in)	See Note 4

<sup>1</sup>Measure the diameter at the center and third points of the test specimen along axes that are 90 deg apart. Record each of the six measurements to the nearest 0.1 mm. Calculate the average and the standard deviation of the six measurements. The standard deviation shall be less than 0.5 mm. The average diameter, reported to the nearest 0.1 mm, shall be used in all material property calculations.

<sup>2</sup>Measure the height of the test specimen in accordance with Section 6.1.2 of ASTM D3459. Record the average height.

<sup>3</sup>Using a straightedge and feeler gauges, measure the flatness of each specimen end. Place a straightedge across the diameter at three locations approximately 120 deg apart and measure the maximum departure of the specimen end from the straightedge using tapered-end feeler gauges. For each end, record the maximum departure along the three locations as the end flatness.

<sup>4</sup>Using a combination square and feeler gauges, measure the perpendicularity of each end. At two locations approximately 90 deg apart, place the blade of the combination square in contact with the specimen along the axis of the cylinder and place the head in contact with the highest point of the end of the cylinder. Measure the distance between the head of the square and the lowest point on the end of the cylinder using tapered-end feeler gauges. For each end, record the maximum measurement from the two locations as the end perpendicularity.

**Figure 1. Portable core-drilling machine and stand.**

specimen. The gyratory compacted specimen of 150 mm (5.90 in.) in diameter by 165 mm (6.50 in.) high was held in place under the drill by blocks of wood cut to provide a tight fit between the gyratory specimen and the stand. A sophisticated clamp for holding the gyratory specimen is not needed to obtain the tolerances on the specimen diameter listed in Table 9. Figure 2 shows the 100-mm (3.94-in.) diameter core and the waste portion of the gyratory specimen.

Reasonably smooth, parallel ends for the test specimen were then provided by trimming the 100-mm-diameter (3.94-in.) core using the double-bladed saw shown in Figure 3. This step is more critical than the coring step and requires the 100-mm-diameter (3.94-in.) core to fit tightly in the saw clamp and sufficient waste material on each end to keep the saw blades from bending.

All coring and sawing was done using water to cool the cutting tools. After all cutting was complete, the bulk specific gravity of the finished specimen was determined, in accordance with AASHTO T166, by first measuring the immersed mass, then the saturated surface dry mass, and finally the dry mass. A completed test specimen is shown in Figure 4.

### 2.4.3 Testing Sequence

The mixtures were tested in the order given in Table 10. For each mixture, the verification was completed first. The order for the remaining tests depended on the workload in each laboratory. Generally, the ASTM D4867 specimens were fabricated and tested first, followed by the specimens for the HWTD testing, which were shipped to PaveTex. The 12 dynamic modulus test specimens were usually prepared last. These 12 specimens were ranked based on their air void contents, then separated into two groups to provide approximately the same average and standard deviation of air void contents within each group. One group was shipped to PSU, and the other was shipped UTEP for ECS/dynamic

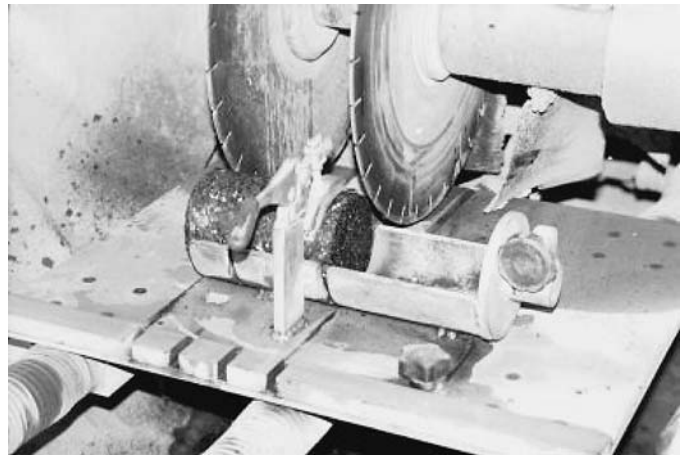


**Figure 3. Double-bladed saw with 100-mm core.**

modulus testing. Appendix B presents specimen identification numbers and air void contents for the specimens that were tested.

All specimens that were shipped for either the HWTD or the ECS/dynamic modulus testing were packaged as a set of four specimens per box in cardboard boxes. Voids in the boxes were filled with packaging materials to minimize the potential for damage to the specimens. Upon receipt of the specimens at PaveTex, PSU, or UTEP, the boxes and specimens were inspected for damage during shipping.

### 2.4.4 ASTM D4867

This testing was performed at AAT in accordance with ASTM D4867. Six specimens, three conditioned and three unconditioned, were prepared and tested for each mixture. Briefly, the test includes compaction and preparation of at least six specimens. The compacted specimens should have



**Figure 2. 100-mm-diameter core and waste ring.**



**Figure 4. Final dynamic modulus test specimen.**

**Table 10. Sequence of mixture testing.**

Order	Mixture
1	Georgia Granite
2	Arkansas Gravel
3	Wisconsin Gravel
4	Mississippi Chert
5	Kentucky Limestone
6	Oklahoma Sandstone with Lime
7	Pennsylvania Dolomite
8	Wyoming Gravel

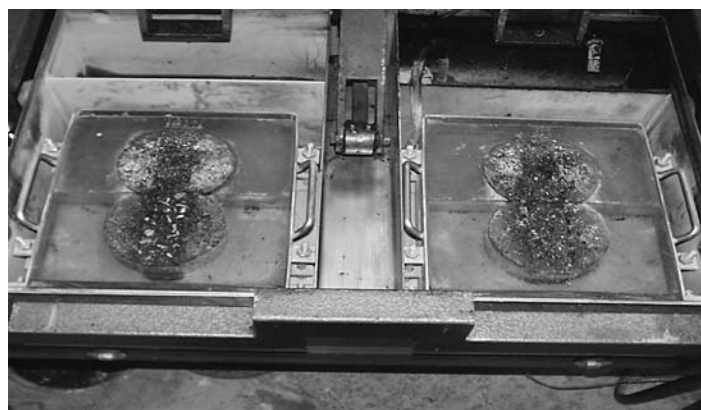
air void contents between 6.0 and 8.0 percent. Half of the compacted specimens are conditioned through a freeze cycle (optional) followed by water bath. First, a vacuum level of approximately 525 mm of mercury (Hg) is applied to partially saturate specimens to a level between 55 and 80 percent. Vacuum-saturated samples are kept in a  $-18^{\circ}\text{C}$  freezer for 16 h and then placed in a  $60^{\circ}\text{C}$  water bath for 24 h. After this period, the specimens are considered conditioned. The other three samples remain unconditioned. All of the samples are brought to a constant temperature, and the indirect tensile strength is measured on both dry (unconditioned) and conditioned specimens. The test method used in this research included the freeze cycle. Results from the ASTM D4867 tests are presented and analyzed in Chapter 3.

#### 2.4.5 Hamburg Wheel Tracking Device (HWTD)

The HWTD measures the combined effects of rutting and moisture damage by rolling a steel wheel across the surface of an asphalt concrete test specimen that is immersed in hot water (see Figure 5).

Rutting, as a function of number of passes, is recorded and used to compute the following test parameters:

- Maximum impression depth,
- Creep slope,



- Stripping slope, and
- Stripping inflection point.

Figure 6 presents a schematic of a typical rutting curve from the HWTD and the definition of the test parameters.

The test was performed for all eight mixtures using cylindrical specimens in accordance with TxDOT test method Tex-242-F. The testing was performed at  $50^{\circ}\text{C}$  for a total of 20,000 wheel passes. The mix is considered a failing mix if the measured rutting after a specified number of passes exceeds 12.5 mm. The number of passes at which the rutting pass/fail criterion is applied depends on the binder grade. For mixes with a high performance grade (PG) of 64, 70, and 76, the number of passes for rutting consideration is 5,000, 10,000, and 20,000, respectively. A summary of test method Tex-242-F is provided in Table 11.

The test was also conducted on specimens prepared in the form of slabs for two of the mixtures. This was done for a comparison of results from testing Superpave gyratory specimens with results from slabs. Results from the HWTD tests are presented and discussed in Chapter 3.

#### 2.4.6 Dynamic Modulus and Environmental Conditioning System

The environmental conditioning system that was developed during SHRP was used for accelerated conditioning of the specimens. During development stages, this system was the subject of several research projects (15–17). The system was further researched and modified later (18, 20). This modified version was used in the current research. The change in dynamic modulus as a result of water/load conditioning under the ECS is used as a measure of moisture damage in the test.

##### 2.4.6.1 Water Conditioning

The ECS water flow control device presented in Figure 7 was used to provide the accelerated water conditioning. This



**Figure 5. Submerged specimens in the HWTD and the associated testing.**

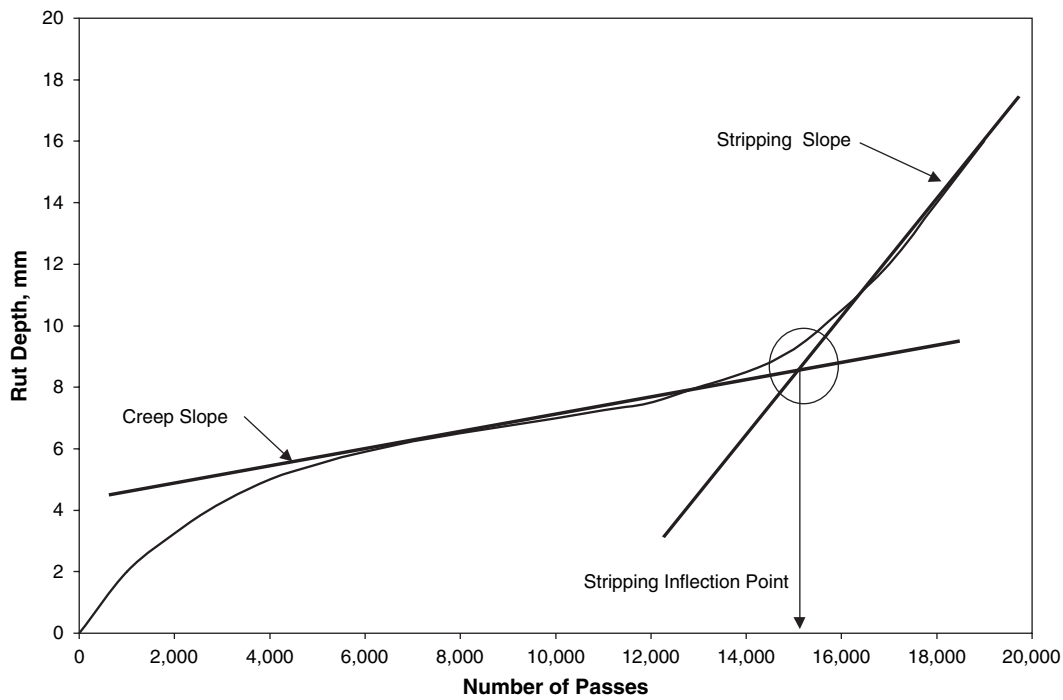


Figure 6. Schematic of HWTD test results.

Table 11. Summary of test method Tex-242-F as used in this research.

<b>Apparatus:</b>	
<i>HWTD</i>	
The load applied by the wheel is $158 \pm 5$ lb. ( $705 \pm 22$ Newtons [N])	
The wheel shall make approximately 50 passes across the test specimen per min.	
The maximum speed of the wheel must be approximately 1.1 ft/sec (0.305 m/s) and will be reached at the midpoint of the slab.	
<i>Temperature Control System</i>	
A water bath capable of controlling the test temperature within $\pm 4^\circ\text{F}$ ( $2^\circ\text{C}$ ) over a range of 77 to 158°F (25 to 70°C).	
<i>Rut Depth Measurement System</i>	
A Linear Variable Differential Transducer (LVDT) device capable of measuring the rut depth induced by the steel wheel within 0.0004 in (0.01 mm), over a minimum range of 0.8 in (20 mm).	
The system shall be mounted to measure the rut depth at the midpoint of the wheel's path on the slab.	
Rut depth measurements must be taken at least every 100 passes of the wheel.	
<b>Specimen:</b>	
Specimen diameter shall be 6 in (150 mm) and specimen height should be $2.4 \pm 0.1$ in ( $62 \pm 2$ mm).	
Air void of test specimens must be $7 \pm 1\%$ .	
<b>Procedure:</b>	
Test requires two cylindrically molded specimens with the Superpave Gyrotory Compactor.	
Place a specimen in the cutting template mold and use a masonry saw to cut it along the edge of the mold. The cut across the specimen should be approximately 5/8 in (16 mm) deep.	
Place the high-density polyethylene molds in the mounting tray and fit specimens into each one.	
Secure the molds in the mounting tray.	
Test temperature shall be $122 \pm 2^\circ\text{F}$ ( $50 \pm 1^\circ\text{C}$ ) for all hot-mix asphalt specimens. Fill the water bath until the water temperature is at the desired test temperature. The temperature of the water can be monitored on the computer screen.	
Start the test after the test specimens have been in the water for 30 min at the desired test temperature. The testing device automatically stops the test when the device applies the desired number of passes or when the maximum allowable rut depth has been reached.	
<b>Report:</b>	
For each specimen, report the air void content, antistripping additive used, number of passes to failure, and rut depth at the end of the test.	



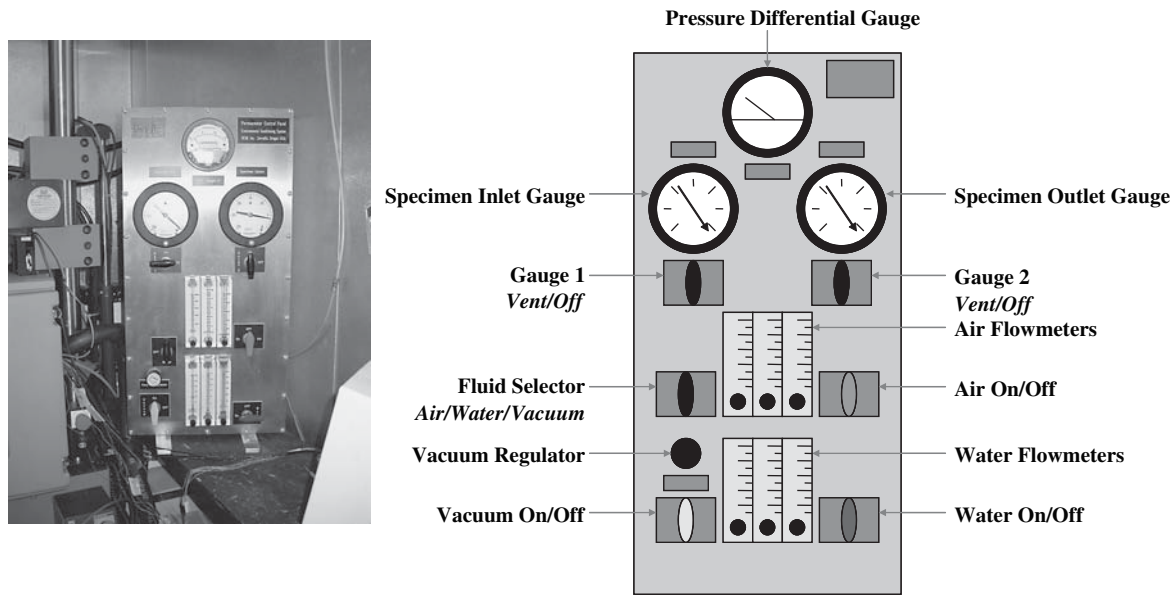


Figure 7. Water flow control device for the ECS.

device consists of a vacuum pump, a water source, valves, pressure gauges, and flow meters. The system was used to apply and monitor the flow of water. Constant flow of air or water can be achieved through suction applied by the vacuum pump. The water supply tank (not shown) was positioned approximately 1.5 m (5 ft) above the specimen to provide sufficient water head. The water was guided through spiraled pipes in a controlled hot water bath (not shown) before permeating through the specimen to ensure proper temperature. The 60°C water was run through the encapsulated specimen

from the top for 18 h. The water flow rate was approximately 8 cm<sup>3</sup>/min (0.5 in.<sup>3</sup>/min).

#### 2.4.6.2 Load Conditioning

A repeated haversine load was applied simultaneously with water conditioning (see Figure 8). Every pulse of the load had a duration of 0.1 sec followed by a rest period of 0.9 sec. This loading on the specimen continued for 18 h. The load level during conditioning was selected based on the temperature

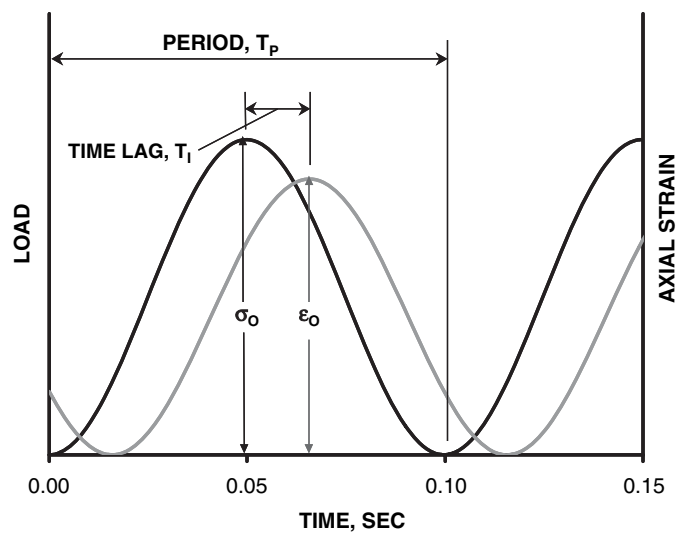


Figure 8. The specimen set-up for testing and the corresponding sinusoidal load.

of the site at which the mix was constructed and varied between 670 and 930 N (150 and 210 lb) depending on the site. An experiment was conducted to establish the load level, as discussed later in this chapter. Load and water conditioning parameters are shown in Table 12.

### 2.4.6.3 Dynamic Modulus Testing

The ECS/dynamic modulus tests were conducted at the laboratories of both PSU and UTEP. For each mix, a total of 12 replicate specimens were tested, with 6 at each laboratory. Dynamic modulus tests were conducted on the same specimen three times. The first test was on the dry unconditioned specimen, followed by a second test after the specimen was exposed to vacuum partial saturation with distilled water for 30 min at 25°C. The last dynamic modulus test was conducted after the specimen was exposed to full load/water conditioning for 18 h at 60°C in the ECS.

The dynamic modulus testing was conducted with a uniaxial sinusoidal load inducing approximately 100  $\mu$ strain in the specimen (see Figure 8). All dynamic modulus tests were conducted at 25°C. Selection of the 25°C test temperature was based on the findings of research under NCHRP Project 9-29, which concluded that dynamic modulus testing at moderate temperatures close to 25°C produced less variability in results than tests at extreme temperatures such as -10°C or 40°C, respectively. Specimen set-up and temperature control are also more easily managed at moderate temperatures. The loading frequencies for each specimen were 10, 5, 2, and 1 Hz, applied in decreasing order. Some of the earlier mixes, tested at PSU, were also the subject of a 25-Hz loading frequency. The 25-Hz frequency was dropped later for consistency with testing at UTEP.

The dynamic modulus and phase angle are defined by Equations 1 and 2, respectively.

$$|E^*| = \frac{\sigma_0}{\epsilon_0} \quad (1)$$

$$\phi = \left( \frac{T_i}{T_p} \right) \times 360 \quad (2)$$

where

- $|E^*|$  = dynamic modulus,
- $\sigma_0$  = amplitude of applied sinusoidal loading,
- $\epsilon_0$  = amplitude of resulting sinusoidal strain,
- $\phi$  = phase angle in degrees,
- $T_i$  = time lag in seconds, and
- $T_p$  = period of sinusoidal loading in seconds.

At PSU laboratories, three Linear Variable Displacement Transducers (LVDTs) were used at 120° to capture deformation of the specimen during both dynamic modulus testing and repeated loading of the conditioning phase (see Figure 9). At UTEP, two LVDTs were used to measure deformation during the dynamic modulus test, and no deformation data were captured during the conditioning phase. Dynamic modulus testing parameters are presented in Table 13.

### 2.4.6.4 Modifications to the Dynamic Modulus Test System of Phase I

Work in Phase II of NCHRP Project 9-29 indicated that the dynamic modulus test could be very repeatable, with the coefficient of variation for a single dynamic modulus test to be 13 percent. This value was based on pooling data on 576 dynamic modulus measurements made in two laboratories using two test devices. This level of test variability compares well with data from NCHRP Project 9-19 that showed coefficients of variation ranging from 13 to 16 percent (26, 28). For the six specimens planned for each cell of the ECS/dynamic modulus testing during Phase IA, the coefficient of variation of the average of the modulus measurements should be approximately  $13/\sqrt{6} = 5.3$  percent, a reasonable value for this type of mechanical test. The data on the dynamic modulus testing variability were used as a guide in Phase IA for identifying outliers and assessing the quality of the collected data. In addition to establishing benchmark variability data for the dynamic modulus test, NCHRP Project 9-29 identified the following factors that were carefully considered in the dynamic modulus testing of Phase IA:

- Specimen temperature,
- Gauge length for measuring strains,

**Table 12. Load and water conditioning parameters used in this research.**

Item	Temperature	Duration/ Frequencies	Magnitude	Loading Type
Short-Term Conditioning (Static Vacuum Saturation)	25 °C	30 min	625 mm Hg	
Long-Term Conditioning (ECS)	Temperature	60 °C	18 h	—
	Load	60 °C	18 h	Site Specific Haversine (0.1 sec loading and 0.9 sec rest)
	Vacuum		18 h	100 mm Hg
	Water Flow	60 °C	18 h	8 cm <sup>3</sup> /min

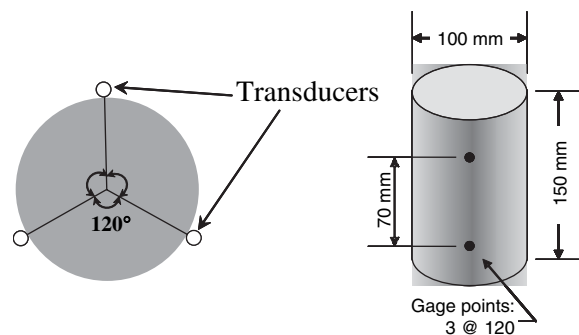


**Figure 9. Schematics showing configuration of LVDTs on the specimen.**

- Strain level used in the testing,
- End friction reducer, and
- Data analysis and quality of raw data collected.

Modifications that were made to the dynamic modulus to reduce variability during Phase IA follow.

**Specimen Temperature.** A very important consideration in dynamic modulus testing is control of the specimen temperature. The NCHRP Project 9-19 test protocols require controlling temperature to  $\pm 0.5^\circ\text{C}$  and recommend using dummy specimens with embedded thermocouples to monitor specimen temperatures. In lieu of dummy specimens, the protocols recommend specific equilibrium times that appear to be too short based on work completed in an FHWA pooled-fund study (29). For ECS/dynamic modulus testing, the problem of temperature control is further complicated by the partial saturation and membrane used in the testing. For Phase IA, equilibrium times for the initial unconditioned dynamic modulus, the dynamic modulus after saturation, and the dynamic modulus after conditioning were determined using specimens instrumented with thermocouples. These equilibrium times were then used in the subsequent testing. Later in this chapter, the experiment followed to ensure proper temperature equilibrium will be discussed.

**Gauge Length.** In Phase I, strains were measured over a 100-mm gauge length as specified in the NCHRP Project 9-19

test protocols. For this gauge length on a 150-mm-high specimen, the strain measuring system is mounted 25 mm from the end of the specimen. One of the issues identified in NCHRP Project 9-29 is the parallelism and flatness of the sawed specimens used in the dynamic modulus testing. To reduce errors associated with end effects, the NCHRP Project 9-29 research recommended reducing the gauge length to 70 mm based on previous research conducted in NCHRP Project 9-19 (26). The reduction in gauge length increases the reproducibility of data from the two deformation sensors mounted on the specimen. Side-to-side differences in measured strains were generally less than 20 percent in NCHRP Project 9-29 compared to 50 percent or more in NCHRP Project 9-19. For Phase IA, a 70-mm gauge length was used.

**Strain Level.** The NCHRP Project 9-19 dynamic modulus test protocol specifies controlling the strain on the specimen between 50 and 150  $\mu\text{strain}$ . Due to possible nonlinear effects, particularly at high temperatures, as reported by Pellinen (28), these tolerances were reduced to 75 to 125  $\mu\text{strain}$  in NCHRP Project 9-29. Strain data for Phase I were generally collected below the NCHRP Project 9-19 minimum values, resulting in more variable data. For Phase IA, the NCHRP Project 9-29 limits of 75 to 125  $\mu\text{strain}$  were used.

**End Friction Reducer.** An end friction reducer was not used in the Phase I testing. The double latex membrane recommended by the NCHRP Project 9-19 test protocols was deemed impractical for use with the ECS conditioning procedure. This system was also considered impractical by the NCHRP Project 9-29 researchers for use in production mixture design testing. Teflon sheets with a thickness of 0.28 mm were found to be an acceptable alternative in NCHRP Project 9-29 and were used as end friction reducers in the Phase IA testing. The sheets were perforated to allow permeation of water through the specimen.

#### 2.4.6.5 Data Analysis and Quality of Raw Data

The NCHRP Project 9-19 dynamic modulus test protocol permits various data analysis methods to be used to calculate the dynamic modulus from the measured stresses and strains.

**Table 13. Description of parameters for dynamic modulus testing.**

Parameter	Value/Type
Temperature	$25 \pm 0.5^\circ\text{C}$
Load Pattern	Sinusoidal
Frequencies	25 <sup>1</sup> , 10, 5, 2, and 1 Hz
Load Level	Variable
Displacement Measurement	3 LVDTs at $120^\circ$ Axial Direction
Measurement Span in Axial Direction	70 mm
Strain Level	$100 \pm 25 \mu\text{strain}$

<sup>1</sup>25-Hz frequency applied to a limited number of specimens at PSU.

In NCHRP Project 9-29, such latitude for data analysis was considered unacceptable for mixture specification testing. Standard data collection and analysis algorithms were developed in NCHRP Project 9-29 and implemented in the first article simple performance test devices evaluated in the project. The standard methods are based on regression analysis of sinusoidal data and, in addition to the modulus and phase angle data, produce data quality statistics that indicate to the testing technician the acceptability of the test data. The data quality statistics and the recommended criteria levels for good quality data (based on NCHRP Project 9-29) are summarized in Table 14.

The standard errors of the load and deformations indicate how closely the applied loading and the measured deformations reproduce sinusoidal forms. The dynamic modulus analysis is only applicable to sinusoidal loading. Poor loading waveforms, both in shape and frequency, and noisy deformations will increase these standard errors. Both are less than 10 percent. The deformation drift is a measure of the permanent strain that accumulates during the dynamic modulus test. It is expressed as a percentage of the measured strain amplitude and is limited to 4 times the measured strain amplitude, or roughly 400  $\mu$ strain. The deformation uniformity and phase uniformity measure how close responses from the individual sensors on the specimen are to each other. These are essentially the coefficient of variation for the deformation and the standard deviation of the phase angle and are less than 20 percent and 3 degrees, respectively. An Excel spreadsheet was developed in NCHRP Project 9-29 to process raw data and to compute the dynamic modulus, phase angle, and data quality statistics. This spreadsheet was modified to include deformation measurements from three LVDTs and was used by the technicians performing the tests in Phase IA to quickly assess the quality of the dynamic modulus test data and repeat testing as needed.

#### 2.4.6.6 Establishing Temperature Control Procedure at Various Stages

During Phase IA, significant attention was paid to controlling temperature during various stages of the test. This was specifically important because different temperatures were used during dynamic modulus testing and conditioning. To

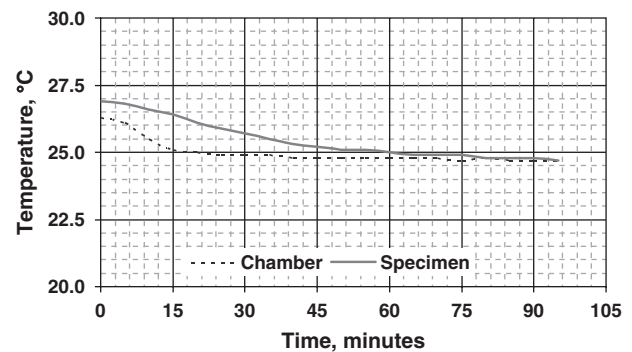
**Table 14. NCHRP Project 9-29 recommended data quality statistics.**

Statistic	Criteria for Good Quality Data
Standard Error of the Load	< 10 percent
Standard Error of the Deformations	< 10 percent
Deformation Drift	< 400 percent
Deformation Uniformity	< 20 percent
Phase Angle Uniformity	< 3 degrees

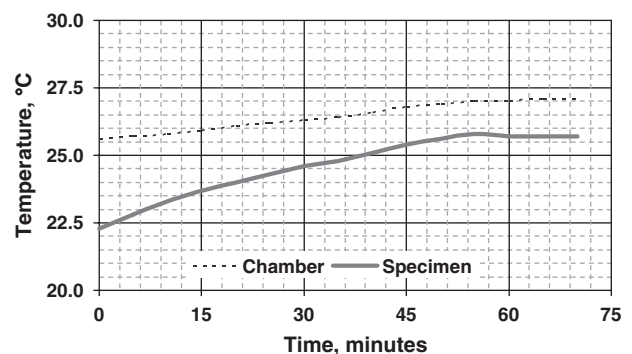
ensure that the specimen temperature was maintained at 60°C during conditioning and that dynamic modulus measurements were performed at 25°C, an experiment was conducted at UTEP that consisted of installing a thermocouple inside the specimen and subjecting the specimen to the temperature conditioning procedure. The only exception was that the dynamic modulus measurements were not performed. A datalogger was used to record the temperature of the specimen every 5 min. The specimen temperature monitored during various steps is presented in Figures 10 through 13. Figure 10 shows that approximately 1 h is required to reach equilibrium after placement of the specimen inside the chamber, which is maintained at 25°C.

Figure 11 shows the equilibrium time required before the dynamic modulus measurement of the vacuum-saturated specimen is taken. The figure shows that the specimen initially has a lower temperature and reaches equilibrium after approximately 1 h inside the chamber. Therefore, at least a 1-h waiting period is required to conduct vacuum-saturated dynamic modulus measurements after placement of the specimen inside the chamber maintained at 25°C.

A typical result of the specimen temperature during conditioning is shown in Figure 12. The results summarized in Figure 12 suggest that the specimen reaches a temperature of



**Figure 10. Equilibrium time for unconditioned dynamic modulus measurements (Tests at UTEP).**



**Figure 11. Establishing equilibrium time for vacuum-saturated dynamic modulus measurements (tests at UTEP).**

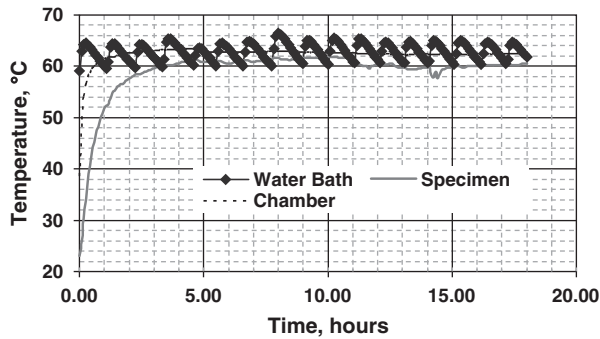


**Figure 12. Specimen temperature during conditioning (tests at UTEP).**

60°C between 2.5 and 3 h of conditioning and remains constant during the remaining conditioning period. The figure also suggests that the chamber temperature and water bath temperature must be set at a level higher than 60°C to ensure the specimen temperature is maintained at 60°C.

To measure the conditioned dynamic modulus, the specimen temperature needs to be reduced from 60°C to 25°C. To expedite the temperature drop, the chamber temperature is initially set at 15°C for 1.25 h and then raised to 25°C. The specimen and chamber temperature measurements are presented in Figure 13. The results suggest that approximately

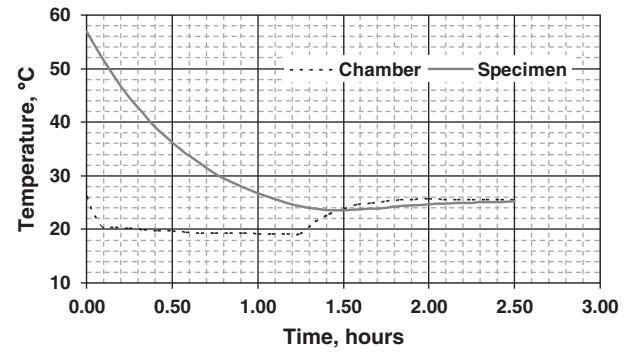


**Figure 13. Equilibrium time for conditioned dynamic modulus measurements (tests at UTEP).**

2.25 h of equilibrium time is needed after the temperature drop from 60°C is initiated.

In a separate experiment at PSU, the evaluation of the temperature condition was conducted using nine thermocouples on the surface of the specimen and at the center of a dummy specimen, and it was found that the temperature is well controlled within the specified range. During each actual test, temperature was monitored using a thermocouple at the center of the dummy specimen. A temperature example for one of the specimens is shown in Figures 14 and 15. The figures indicate the time it takes for the temperature to rise from 25°C to 60°C

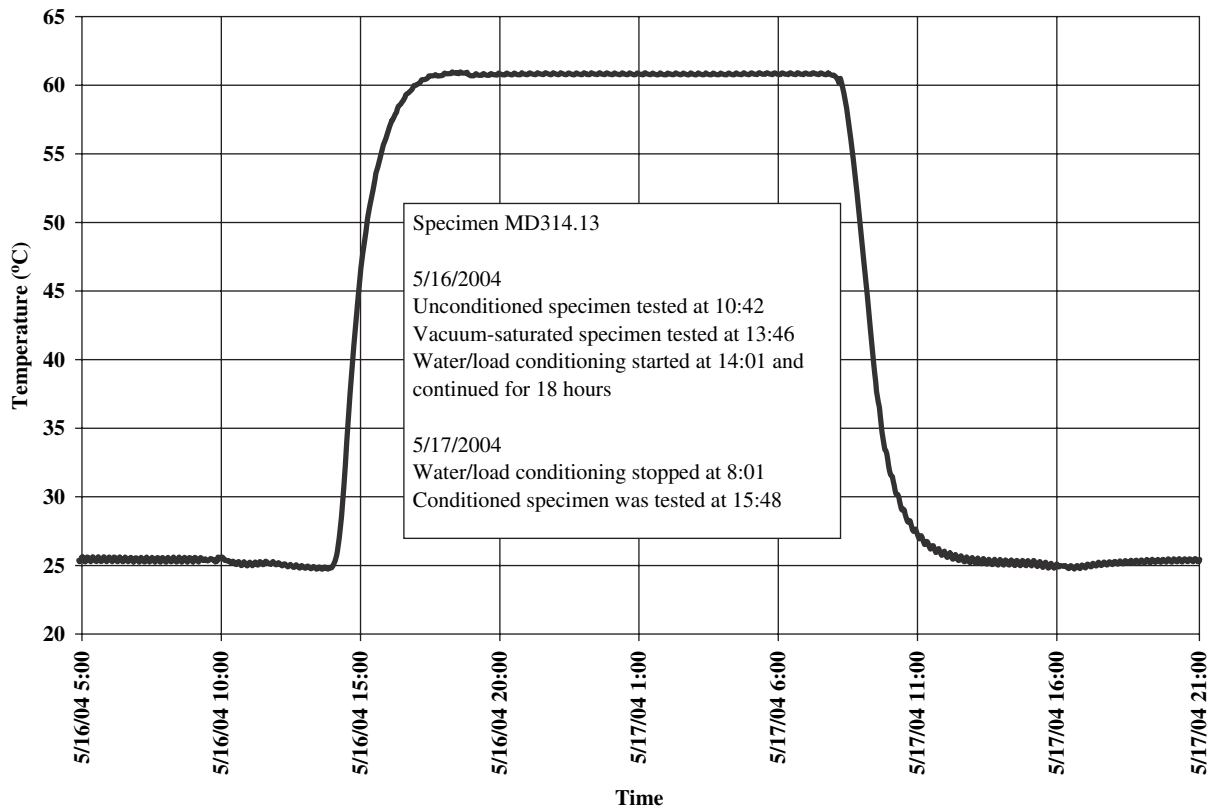


**Figure 14. Temperature measured at the center of a dummy specimen during an actual test (tests at PSU).**

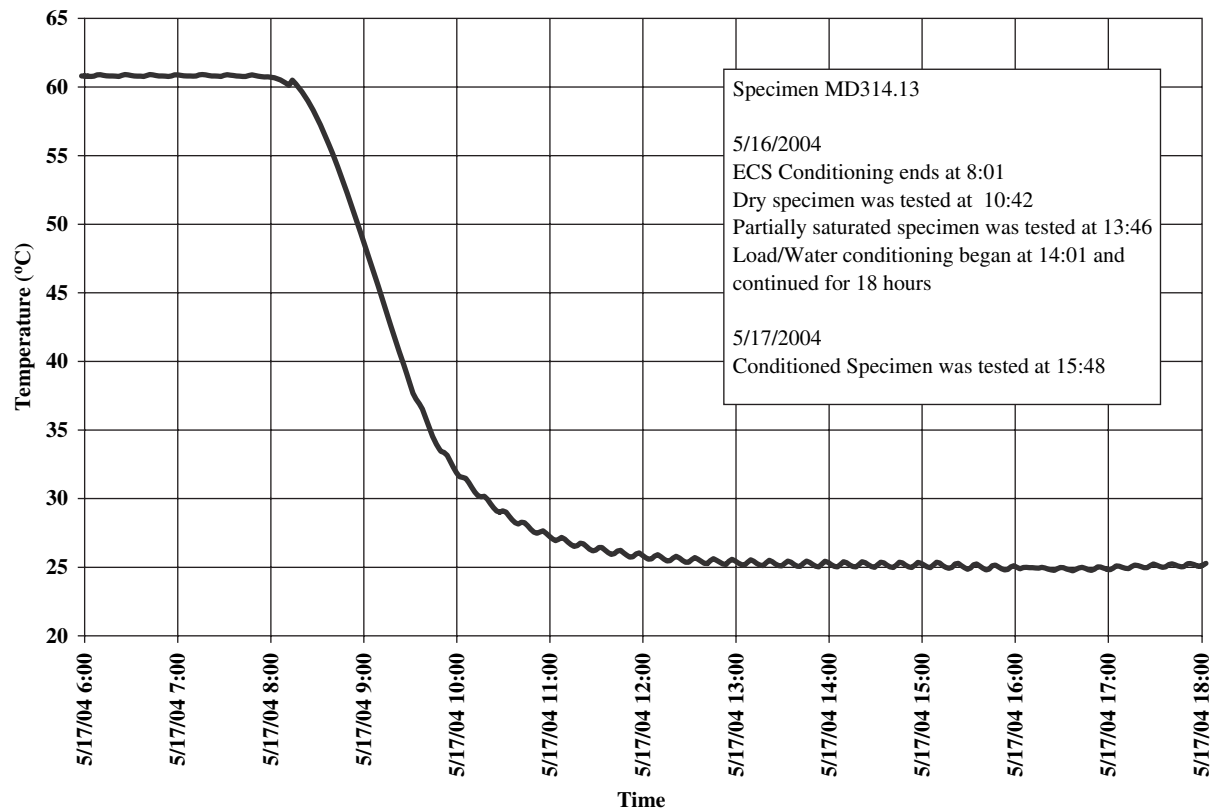


**Figure 15. Evaluating the time it takes for the temperature to decrease from 60°C to 25°C (tests at PSU).**

and the time it takes for the temperature to drop from 60°C to 25°C. The times needed to reach equilibrium at PSU were longer than the times at UTEP, perhaps due to differences in the equipment used. During the PSU experiments, it was observed that after completion of 18-h, 60°C conditioning, it took 6 to 7 h before the specimen temperature became suitable for testing dynamic modulus at 25°C. Times for different events during the test are shown in Figure 14. A close-up of the time it takes for the temperature to drop from 60°C to 25°C is shown in Figure 15. It should be mentioned again that the temperature of the chamber is first dropped from 60°C to 15°C and maintained at this level for about 1.5 h before setting it at 25°C. Also, in all experiments for establishing equilibrium time, a dummy specimen was partially saturated along with actual test specimens.

The significance of proper testing temperature control for dynamic modulus is evident from Figure 16. This simple experiment conducted at PSU indicates that, for a typical mixture, a deviation of 2°C from 25°C results in a modulus decrease or increase of 10 percent (for testing at 25 Hz) and 18 percent (for testing at 1 Hz).

#### 2.4.6.7 Establishing Load Levels during Conditioning

In the original ECS conditioning procedures developed under SHRP at Oregon State University and those developed at UTEP during the 1990s, the haversine load during condi-

tioning was maintained at a constant peak of 200 lb (890 N). The selection of this conditioning load level is not well documented in SHRP Report A-403 (30). The report states, “[t]his loading level was selected from others (not reported here) to be moderate enough to minimize permanent deformation.” The report presents data from a mixture composed of Materials Reference Library (MRL) asphalt AAG-1 and MRL aggregate RB at air void levels of 5 and 8 percent. The total accumulated permanent axial strain for the 8-percent air void mixture was approximately 2.5 percent; for the 5-percent air void mixture, it was approximately 1.5 percent.

Maintaining the same temperature (60°C) and the same load (890 N) during the conditioning procedure for all mixes has some deficiencies, as site conditions are not properly taken into account when mixes are used in different areas with different pavement temperatures. Since the temperature is maintained at a constant 60°C during the ECS procedure, the magnitude of load needs to be adjusted for different mixes to account for differences in the site temperature and binder grades. In Phase IA, a study was undertaken to address this issue and to establish the conditioning load levels for different pavement temperatures.

**Alternatives to Establishing the Load Level.** There are three alternatives for the conditioning load—constant load, constant dynamic strain, and constant mechanical damage. These are discussed below:

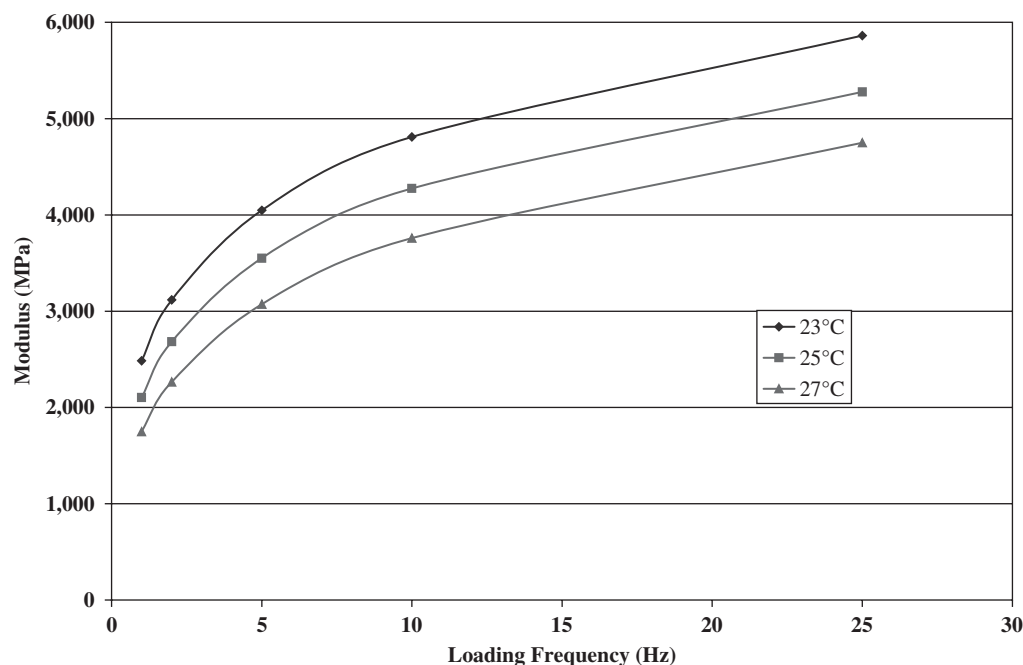


**Figure 16. Effect of deviation from 25°C temperature on the measured dynamic modulus at different frequencies (tests at PSU).**

- Constant Load.** This is the approach used currently in AASHTO TP34 and the Texas modified ECS conditioning procedure. The conditioning load is 890 N (200 lb). This is the easiest approach to implement, but the strain in the specimen and the level of non-moisture-induced damage varies with mixture stiffness, particularly binder grade. Greater dynamic strains and levels of non-moisture-induced damage will occur in mixtures made with softer grades of binder. This approach probably biases the test results in favor of stiffer binders.
- Constant Dynamic Strain.** The second approach is to adjust the load level to obtain constant dynamic strains in the specimen. In this case, the load level would be adjusted, based on the grade of the binder, such that the dynamic strains induced in the specimens remain constant. Stiffer mixtures would be tested at higher loads to maintain constant dynamic strain.
- Constant Mechanical Damage.** The third approach is to adjust the load level to obtain a constant level of non-moisture-induced mechanical damage in the specimens at the end of conditioning. In this case, the load levels would be adjusted such that the permanent deformation in the test without moisture would be constant. Again, this would result in stiffer mixtures being tested at higher loads to maintain constant mechanical damage.

**Initial Assessment of Load Level.** An initial assessment of the load level was based on the grade of binder used in the mixture. The rationale behind this effort was to maintain approximately the same level of non-moisture-induced mechanical damage in the specimens. For mixtures that are

moisture sensitive, additional moisture-induced damage would occur. Since the ECS conditioning procedure is performed at 60°C regardless of the grade of binder used in the mixture, stiffer binders should be tested at higher load levels to maintain a constant amount of mechanical damage in the test.

Research reported by Kaloush, (31), has shown that permanent strains can be predicted from resilient strains using the following model:

$$\log\left(\frac{\epsilon_p}{\epsilon_r}\right) = -3.1555 + 0.3994 \log(N) + 1.7340 \log(T) \quad (3)$$

where

$\epsilon_p$  = accumulated permanent strain,

$\epsilon_r$  = resilient strain,

$N$  = number of load cycles, and

$T$  = temperature in °F.

Rearranging Equation 3 to solve for the permanent strains produces

$$\epsilon_p = \epsilon_r \left[ 10^{(-3.1555 + 0.3994 \log(N) + 1.7340 \log(T))} \right] \quad (4)$$

For a particular temperature and number of load cycles, which is the case in the ECS conditioning procedure, Equation 4 shows that the accumulated permanent strain is proportional to the resilient strain. Based on Equation 4, conditions resulting in the same resilient strain should produce the same accumulated permanent strain. The resilient strain is proportional to the modulus of the material, so when testing materials with different moduli, the load level should be adjusted to maintain a constant resilient strain level.

Resilient strains can be estimated by dividing the applied load by the mixture modulus. Mixture modulus values for different binder stiffnesses can be estimated using the Witczak predictive equation (32):

$$\log E = -1.249937 + 0.029232\rho_{200} - 0.001767(\rho_{200})^2 - 0.002841\rho_4 - 0.058097V_a - 0.802208\left(\frac{V_{\text{beff}}}{V_{\text{beff}} + V_a}\right) + \frac{3.871977 - 0.0021\rho_4 + 0.003958\rho_{38} - 0.000017(\rho_{38})^2 + 0.005470\rho_{34}}{1 + e^{(-0.6033 \cdot 3 - 0.313351 \log(f) - 0.393532 \log(\eta))}} \quad (5)$$

where

- $E$  = dynamic modulus,  $10^5$  psi;
- $\eta$  = bitumen viscosity,  $10^6$  Poise;
- $f$  = frequency, Hz;
- $V_a$  = air void content, %;
- $V_{\text{beff}}$  = effective bitumen content, % by volume;
- $\rho_{34}$  = cumulative % retained on 19-mm sieve;
- $\rho_{38}$  = cumulative % retained on 9.5-mm sieve;
- $\rho_4$  = cumulative % retained on 4.76-mm sieve; and
- $\rho_{200}$  = % passing 0.075-mm sieve.

For the AAG-1 mixture used in the original SHRP ECS research, the following parameters are used in the dynamic modulus predictive equation to obtain the modulus representative of the ECS conditioning procedure at 60°C:

- $\eta = 0.003253$ ,  $10^6$  Poise;
- $f = 10$  Hz;
- $V_a = 8\%$ ;
- $V_{\text{beff}} = 10.75\%$  by volume;
- $\rho_{34} = 5\%$ ;
- $\rho_{38} = 32\%$ ;
- $\rho_4 = 52\%$ ; and
- $\rho_{200} = 5.5\%$ .

This results in a modulus at 60°C of 47,000 psi. Moduli for the same mix can be estimated using Equation 5 and 60°C viscosity values representative of various binder grades. In NCHRP Project 1-37A, representative viscosity temperature parameters were developed to predict viscosity values for various binder grades using the ASTM viscosity-temperature susceptibility relationship:

$$\log \log \eta = A + VTS \log T_R \quad (6)$$

where

- $\eta$  = viscosity, cP;
- $T_R$  = temperature, Rankine;
- $A$  = regression intercept; and
- $VTS$  = regression slope of viscosity temperature susceptibility.

These binder grades are summarized in Table 15 along with the representative viscosity at 60°C for that grade, the modulus from Equation 5 assuming the volumetric parameters representative of the mix used in the original ECS research, and the estimated loading to produce equivalent resilient strains at 60°C. The estimated load is the ratio of the modulus for the given binder grade to the standard modulus of 47,000 psi multiplied by the standard ECS conditioning procedure load of 200 lb.

Both the constant dynamic strain approach and the constant mechanical damage approach would yield the same load adjustment factors since the Kaloush permanent deformation equation reduces, for a specific temperature and number of load cycles, to the permanent strain being proportional to the resilient or dynamic strain.

#### 2.4.6.8 Laboratory Study for Establishing the Conditioning Load Level

Following the initial assessment, a laboratory study was undertaken to verify the load levels by conducting repeated load permanent deformation tests on a limited number of samples made with different grades of binder. This testing was used to confirm that similar resilient and permanent strains were obtained at 60°C when the load was varied with binder grade (binder grades were as given in Table 15). An experiment was designed to confirm these load levels using a single mixture with three different binders.

Table 16 summarizes volumetric properties of the mixture selected for this study. It was a 12.5-mm mixture that used crushed limestone coarse aggregate and a blend of manufactured and natural sand. The natural sand was used at 14.0 percent of the total aggregate. This represented approximately 41.0 percent of the fine aggregate fraction. Specimens for the load level study were prepared using three binders: a

**Table 15. Estimated loads for ECS procedure by binder grade.**

Grade	VTS	A	60 ° Viscosity (cP)	Modulus 10 Hz (psi)	Estimated Load (lb)
52-34	-3.602	10.707	105,210	31,371	133
58-28	-3.701	11.010	227,151	42,031	179
64-22	-3.680	10.980	521,740	57,804	246
70-22	-3.426	10.299	1,123,552	77,534	330
76-22	-3.208	9.715	2,285,502	101,500	432
82-22	-3.019	9.209	4,403,607	129,670	552



**Table 16. Volumetric properties of the mixture used in the load level study.**

Nominal Maximum Aggregate Size	12.5 mm
N <sub>design</sub>	75
Coarse Aggregate Angularity, One Face/ Two Face	100/100
Fine Aggregate Angularity	47.2
Flat & Elongated, % (Ratio 5:1)	3.0
Sand Equivalent, %	55
Binder Content, %	4.75%
Gyratory Compaction, % Gmm	
N <sub>ini</sub>	86.4%
N <sub>des</sub>	96.0%
N <sub>max</sub>	97.3%
Voids in Mineral Aggregate (VMA), %	14.6
Voids in Total Mixture (VTM), %	4.0
Voids Filled with Asphalt (VFA), %	72.6
Fines to Effective Binder Ratio (F/A)	1.2
Gradation, % passing sieve size, mm	
37.5	100
25	100
19	100
12.5	97
9.5	75
4.75	39
2.36	30
1.18	24
0.6	18
0.3	11
0.15	7
0.075	5.6

neat PG 58-28, a neat PG 64-22, and an elastomeric modified PG 76-22.

The experimental design for the load level study consisted of performing permanent deformation tests without moisture at 60°C using three load levels for each binder grade. The load levels bracket the estimates presented in Table 15. Replicate specimens were tested for each binder/load level combination. Table 17 summarizes the experimental design. The experiment required fabricating and testing 18 specimens. Table 18 summarizes the air void content of these specimens.

Each specimen was tested under repeated haversine load at UTEP at 60°C without water conditioning. The load period

**Table 17. Experimental design for the load level verification study.**

Binder	Load Level (lb)	Repeated Load Permanent Deformation Test on Dry Unconditioned Specimens at 60°C	
		Replicate 1	Replicate 2
PG 58-28	130	X	X
	168	X	X
	180	X	X
PG 64-22	190	X	X
	210	X	X
	240	X	X
PG 76-22	240	X	X
	280	X	X
	410	X	X

for each cycle was 0.1 sec with the rest period being 0.9 sec. To simulate the effect of confinement during the ECS conditioning procedure, the specimens were encapsulated in a membrane and tested while a partial vacuum of 2.5 in. (8.5 kPa) of Hg was applied. The conditioning load pulses were applied for 3 h (9,500 cycles), and resilient strains and permanent strains were recorded. The strain measurement set-up was modified to measure the strains during conditioning while the membrane was on the specimen. This was achieved by placing the targets on the specimens and affixing the LVDT mounting system outside the membrane. The mounting targets were modified to add a screw that passes through the membrane and is connected to the LVDT mounting system. The hole was plugged using Super Glue to make sure that the vacuum level was maintained.

The results of this experimental program are presented in Chapter 3.

#### 2.4.6.9 Resolving Testing System Differences between the Two Laboratories

One concern that needed to be addressed was ensuring that the testing systems at the PSU and UTEP laboratories produced comparable results. This was accomplished by

**Table 18. Air void content of load level verification study specimens.**

PG 58-28		PG 64-22		PG 76-22	
Specimen	Air Voids	Specimen	Air Voids	Specimen	Air Voids
MD 310.1	6.2	MD 309.1	6.3	MD 308.1	6.7
MD 310.2	6.4	MD 309.2	6.2	MD 308.2	6.6
MD 310.3	7.2	MD 309.3	6.7	MD 308.3	6.8
MD 310.4	6.5	MD 309.4	6.8	MD 308.4	6.4
MD 310.5	6.8	MD 309.5	6.5	MD 308.5	6.3
MD 310.6	6.3	MD 309.6	7.3	MD 308.6	6.4
Average	6.6	Average	6.6	Average	6.5
Standard Deviation	0.36	Standard Deviation	0.40	Standard Deviation	0.20

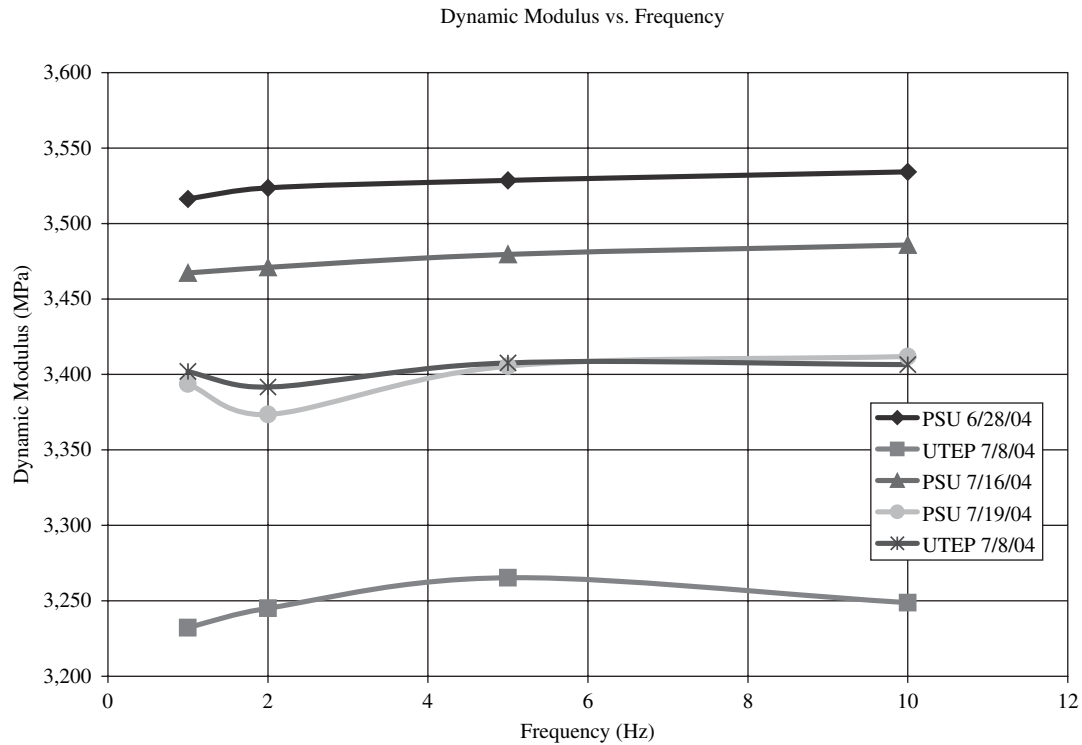


**Figure 17. Comparison of results from dynamic modulus tests on a synthetic specimen from laboratories at PSU and UTEP.**

conducting dynamic modulus tests on a specimen made from Polyethylene Terephthalate (PET) at 25°C and at different frequencies. The tests were first conducted at PSU, and then the specimen was shipped to UTEP for testing. The synthetic specimen was again tested at PSU after completion of UTEP

tests. The results are shown in Figure 17. This graph indicates that the modulus results from the tests at both laboratories are considerably close. The difference between the average modulus values from the two laboratories is about 4 percent of the overall average.

## CHAPTER 3

# Findings

### 3.1 Mix Design Verification

As discussed in Chapter 2, the design of each mix was verified prior to preparation of the test specimens. A wide range of mixtures is represented in Table 7 (see Chapter 2). One was a 9.5-mm mixture, five were 12.5-mm mixtures, and two were 19.0-mm mixtures. Half of the mixtures are classified as coarse-graded based on the AASHTO M323 primary control sieve. Seven of the 8 mixtures were designed using gyratory compaction, with the design gyration level varying from 68 to 125. One mixture was designed using 75-blow Marshall compaction. One mixture used neat PG 58-28 binder, four mixtures used neat PG 64-22 binder, two mixtures used neat PG 67-22 binder, and one mixture used polymer-modified PG 76-22 binder. Design asphalt contents varied from 4.6 to 5.4 percent of the total mixture weight, with effective binder contents varying from 9.1 to 11.5 percent by volume.

Since production data were not available for any of the mixtures, the mixture designs were used as the basis for preparing the laboratory specimens. Four options were considered for adjusting the mixtures based on the volumetric properties of verification specimens:

1. Make no adjustment to the mixture and use only mixtures in which the volumetric properties in the verification specimens are the same as those from the mixture design.
2. Adjust the asphalt content of the mixtures to obtain volumetric properties in the verification specimens that are the same as those from the mixture design.
3. Adjust the gradation of the mixtures to obtain volumetric properties in the verification specimens that are the same as those from the mixture design.
4. Adjust both the gradation and the asphalt content of the mixtures to obtain volumetric properties in the verification specimens that are the same as those from the mixture design.

Changes, within tolerance limits, are typically made to mixtures during production to keep volumetric properties within the specification tolerances. The binder content is often increased or decreased if mixture air voids are too high or too low. The typical allowable deviation for binder content from the design value is  $\pm 0.4$  percent. If the necessary change in volumetric properties cannot be made by changing the binder content, or if the producer does not want to change the binder content, then the gradation can be adjusted within specified tolerances to keep the mixture volumetric properties in compliance with the specifications. Although it is likely that field production of the mixtures used in this study deviated from the mixture designs given in Table 7, there were no data available to support any changes. Therefore, it was decided to fabricate all specimens using the proportions given in the mix design but to only include mixtures in which the volumetric properties of verification specimens were the same as those in the mixture design.

As discussed in Chapter 2, it was assumed that the gradation data provided in the mixture designs were based on washed gradations. Since in some cases, the mixture designs were several years old, the research team was not able to verify that all of the mixture designs were based on washed gradation analyses.

Each mixture was verified by compacting replicate specimens to the design compaction level and comparing the air void content, bulk specific gravity, and maximum specific gravity to the data provided in the mix design. The objective of this verification was to screen the mixtures for inconsistency with the mixture design on which the field performance was based. Multilaboratory precision data from NCHRP Project 9-26 (33) and the AASHTO Materials Reference Laboratory (AMRL) proficiency sample program (PSP) (34) were used to assess the significance of differences between the NCHRP Project 9-34 verifications and the submitted mixture designs. Table 19 presents single operator and multilaboratory precision statements for selected properties of hot-mix

**Table 19. Precision statements (33).**

Test	Mix	Single Operator Precision difference two-sigma limit (d2S)			Multilaboratory Precision d2S		
		NCHRP 9-26 Experiment	85% of AMRL PSP Sample 9 & 10 Data	100% of AMRL PSP Sample 9 & 10 Data	NCHRP 9-26 Experiment	85% of AMRL PSP Sample 9 & 10 Data	100% of AMRL PSP Sample 9 & 10 Data
Bulk Specific Gravity AASHTO T166	12.5 mm	0.023	0.037	0.047	0.042	0.070	0.088
	19.0 mm	0.037	NA	NA	0.042	NA	NA
Maximum Specific Gravity ASTM D2041	12.5 mm	0.006	0.008	0.011	0.011	0.016	0.021
	19.0 mm	0.006	NA	NA	0.011	NA	NA
Relative Density at $N_{design}$	12.5 mm	0.9	1.5	1.8	1.7	2.8	3.5
	19.0 mm	1.4	NA	NA	1.7	NA	NA

asphalt concrete made with nonabsorptive aggregates. This table includes precision statements for three sets of data:

1. The NCHRP Project 9-26 multilaboratory study that included 27 laboratories (33),
2. A subset of data from AMRL gyratory sample proficiency sample pair 9 and 10 representing 85 percent of the data, and
3. The entire AMRL gyratory sample proficiency sample pair 9 and 10.

As shown in Table 19, the precision of the test method depends upon the level of control. The NCHRP Project 9-26 multilaboratory study was a carefully controlled study using a small number of laboratories with qualified technicians and equipment meeting the specification requirements. On the other hand, the AMRL proficiency sample program includes over 270 laboratories and may include data generated by untrained technicians or data generated using equipment that does not meet the specification requirements. The subset of the AMRL proficiency sample data used in NCHRP Project 9-26 was selected to screen the most extreme data from the AMRL proficiency sample data set. Since the qualifications of the laboratories that performed the original mixture designs were unknown, the multilaboratory precision statement for the complete AMRL proficiency data set was used. The mixtures were accepted for use in this project if the difference between the verification test results and the submitted mixture design was less than the d2S value given in the last column of Table 19.

Specimens for all mixture verifications except the Wyoming gravel were prepared using the procedures described in the next section. The verification specimens for the Wyoming gravel were compacted using a mechanical Marshall hammer in accordance with AASHTO T245. The mixture verification results are summarized in Table 20.

Figures 18, 19, 20, and 21 present differences in volumetric properties between the submitted mixture design and the mixture verification specimens with the multilaboratory d2S values given in Table 19. As shown, the verification data for all of the mixtures are within the multilaboratory d2S value obtained from complete AMRL gyratory proficiency sample data for gyratory proficiency samples 9 and 10. The data for most mixtures are also within the range of multilaboratory d2S values from the NCHRP Project 9-26 controlled interlaboratory study. These comparisons indicate that the mixtures used in this study are representative of the submitted mixture designs. The largest differences in maximum specific gravity occur for the Oklahoma sandstone with lime and Wyoming gravel mixtures (see Figure 18). Both of these contain aggregates with high absorption. The mix design data for the Oklahoma sandstone with lime mixture have a low asphalt absorption of 0.17 percent, suggesting that the maximum specific gravity tests during the mix design may have been performed before all of the absorption was complete. The largest difference in the bulk specific gravity occurs for the Mississippi chert (see Figure 19). Since the maximum specific gravity for this mixture shows good agreement, it appears that this difference is probably due to differences in compaction equipment or procedure between laboratories. Finally, the largest differences in air voids occur for the Mississippi chert and Arkansas gravel mixtures. The difference in air voids for the Mississippi chert is a product of the difference in bulk specific gravity discussed above. A complete mix design was not submitted for the Arkansas gravel, and it was assumed that the design air void content was 4 percent.

Figure 21 shows differences in gradation between the submitted mixture designs and the verification data. As discussed previously, the verification specimens were batched

Table 20. Summary of mixture verification results.

Property	GA Granite			AR Gravel			WI Gravel			MS Chert		
		Lab			Lab			Lab			Lab	
Mixing Temperature, °C		163			159			150			158	
Compaction Temperature, °C		152			156			135			148	
Gradation, % passing												
Sieve Size, mm	Design	Lab	Diff	Design	Lab	Diff	Design	Lab	Diff	Design	Lab	Diff
25	100	100	0	100	100	0	100	100	0	100	100	0
19	100	100	0	100	100	0	100	100	0	100	100	0
12.5	99	99	0	88	87	1	97	98	-1	95	95	0
9.5	83	82	1	80	79	1	89	88	1	89	89	0
4.75	50	50	0	60	59	1	70	70	0	65	65	0
2.36	36	35	1	48	50	-2	53	53	0	47	46	1
1.18	27	27	0	36	37	-1	38	38	0	35	35	0
0.6	20	22	-2	27	27	0	27	30	-3	27	27	0
0.3	15	15	0	16	16	0	14	15	-1	14	14	0
0.15	9	9	0	7	7	0	7	7	0	7	7	0
0.075	5.1	5.1	0.0	4.3	4.3	0.0	4.8	4.7	0.1	5.3	5.3	0.0
Asphalt Content, %	4.7	4.7	0.0	5.0	5.0	0.0	5.4	5.4	0.0	5.4	5.4	0.0
Maximum Specific Gravity	2.592	2.601	0.009	NA	2.436	NA	2.504	2.512	0.008	2.371	2.374	0.003
Gmb at Design Compaction	2.487	2.466	-0.021	NA	2.289	NA	2.404	2.41	0.006	2.276	2.203	-0.073
Air Voids at Design Compaction, %	4.0	5.2	1.2	4.0	6.0	2.0	4.0	4.1	0.1	4.0	7.2	3.2
Gradation, % passing												
Property	KY Limestone			OK Sandstone with Lime			PA Dolomite			WY Gravel		
		Lab			Lab			Lab			Lab	
Mixing Temperature, °C		148			166			157			165	
Compaction Temperature, °C		130			155			145			145	
Gradation, % passing												
Sieve Size, mm	Design	Lab	Diff	Design	Lab	Diff	Design	Lab	Diff	Design	Lab	Diff
25	100	100	0	100	100	0	100	100	0	100	100	0
19	100	100	0	100	100	0	100	100	0	100	100	0
12.5	100	100	0	92	90	2	82	79	3	95	93	2
9.5	95	94	1	79	79	0	66	65	1	77	76	1
4.75	64	63	1	49	48	1	40	38	2	53	51	2
2.36	42	41	1	29	29	0	26	26	0	39	36	3
1.18	29	31	-2	22	22	0	16	17	-1	25	26	-1
0.6	21	22	-1	19	19	0	12	11	1	20	19	1
0.3	11	9	2	15	14	1	9	8	1	13	14	-1
0.15	6	5	1	10	10	0	6	5	1	10	10	0
0.075	4.5	4.5	0.0	6.5	6.6	-0.1	4.0	4.1	-0.1	6.4	6.7	-0.3
Asphalt Content, %	5.4	5.4	0.0	5.1	5.1	0.0	4.6	4.6	0.0	5.0	5.0	0.0
Maximum Specific Gravity	2.458	2.465	0.007	2.373	2.394	0.021	2.597	2.604	0.007	2.452	2.436	-0.016
Gmb at Design Compaction	2.360	2.353	-0.007	2.278	2.284	0.006	2.498	2.461	0.037	2.329	2.289	-0.040
Air Voids at Design Compaction, %	4.0	4.5	0.5	4.0	4.6	0.6	3.8	5.5	1.7	5.0	6.0	1.0

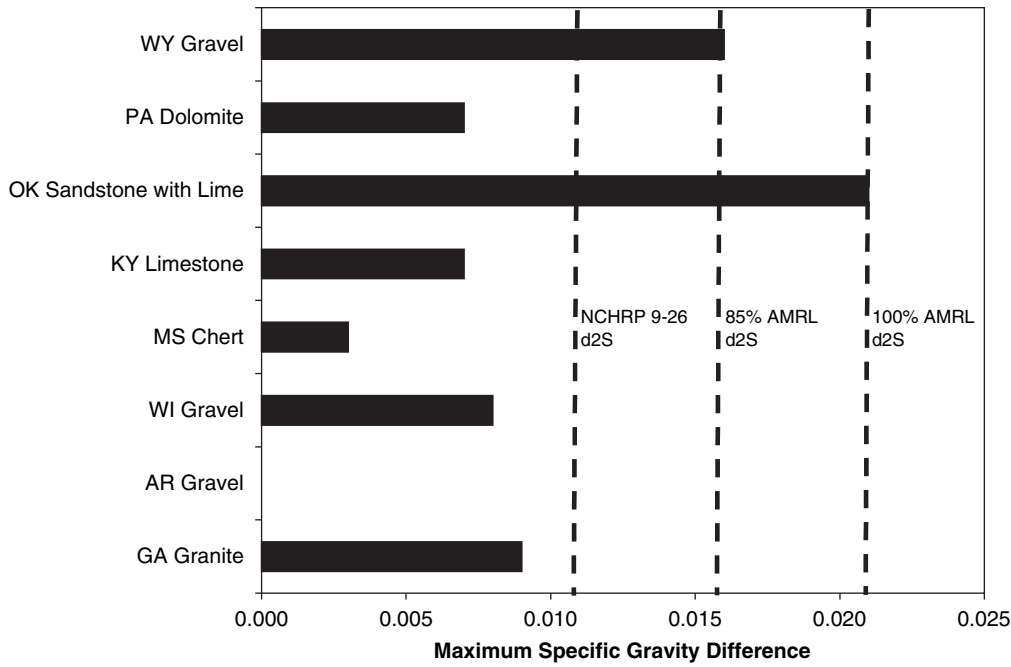


**Figure 18. Difference between maximum specific gravity of mix design and mixture verification samples.**

assuming that washed gradation was used. The mixtures used in the verifications reasonably reproduced the submitted mixture design gradations, with coarse and fine aggregates typically being within  $\pm 2$  percent of the mixture design and the mineral filler being within  $\pm 0.3$  percent of the mixture design.

### 3.2 ASTM D4867 Results

Tensile strength ratios and estimates of visual damage from the ASTM D4867 testing are summarized in Table 21 along with the reported field performance of the mixture and available tensile strength ratios from the mixture designs that were

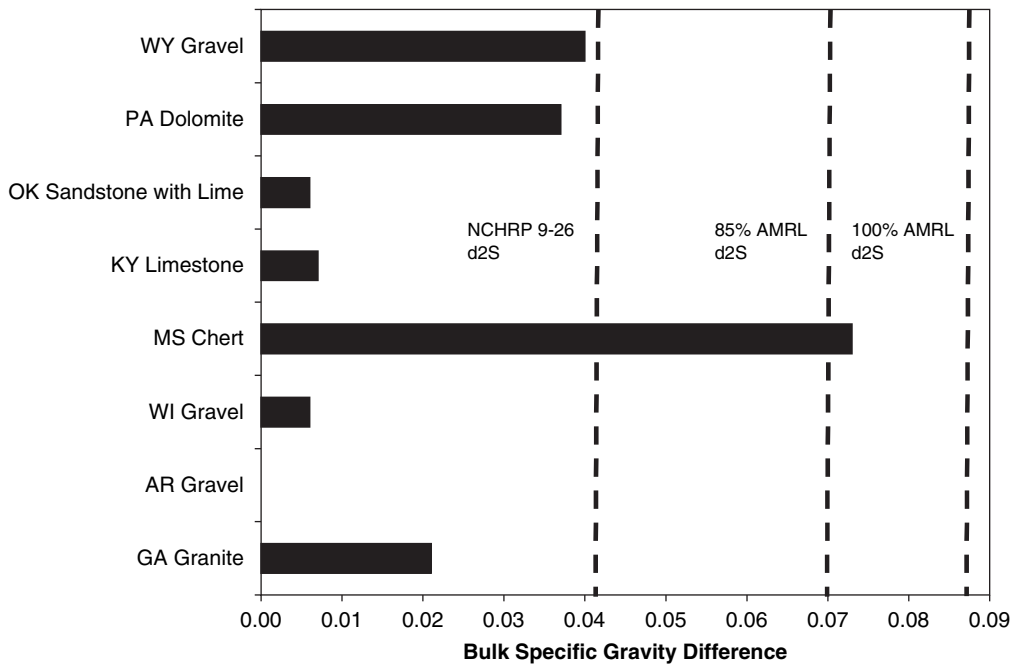


**Figure 19. Difference between bulk specific gravity of mix design and the mixture verification samples.**

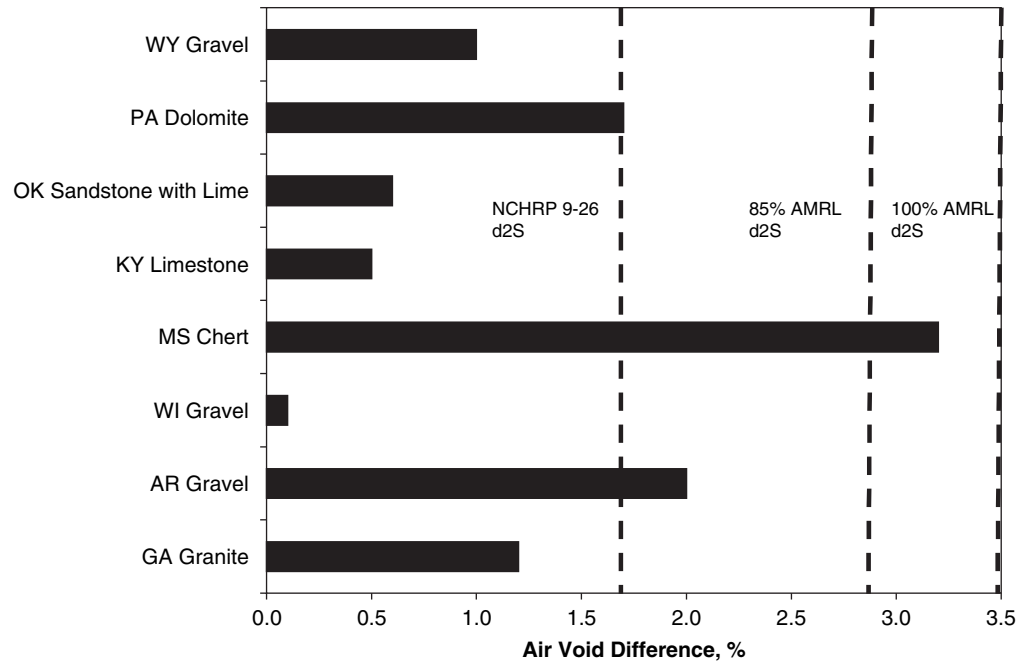


**Figure 20. Difference between air void content of mix design and the mixture verification samples.**

submitted. For convenience, the data in Table 21 are organized based on the reported field performance.

Figure 22 compares the tensile strength ratios with the AASHTO M323 minimum criterion of 80 percent. Using the AASHTO M323 criterion of 80 percent, ASTM D4867 correctly identified the performance of five of the eight mixtures tested.

It incorrectly identified the reportedly good-performing Oklahoma sandstone with lime as being susceptible to moisture damage. More importantly, however, it identified the reportedly poor-performing Kentucky limestone and Arkansas gravel mixtures as having acceptable resistance to moisture damage. Using a criterion of 75 percent would increase the number of

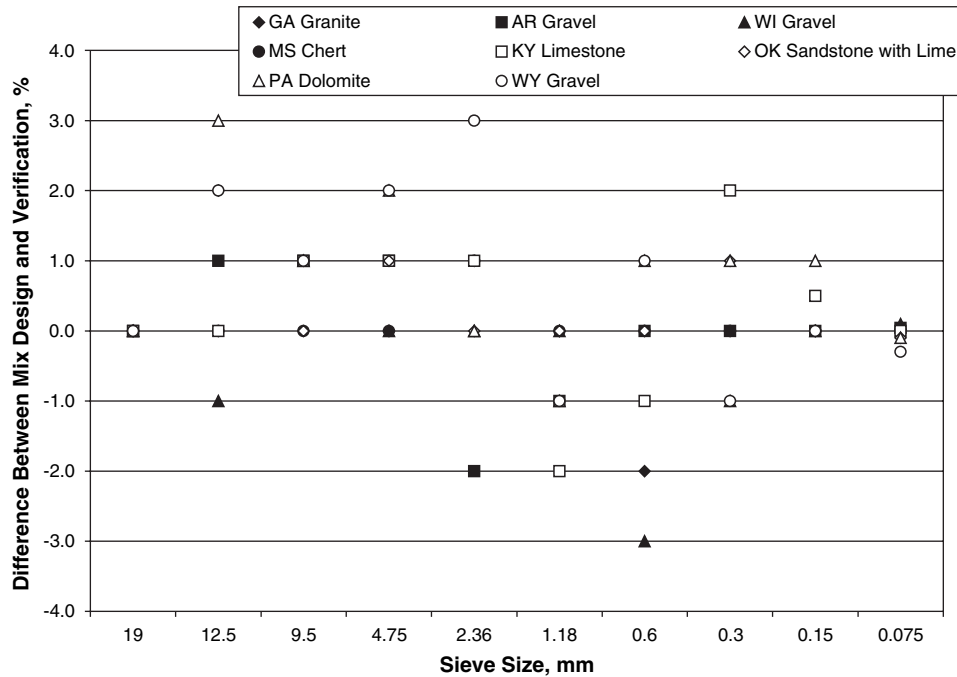


**Figure 21. Difference in gradations between submitted mixture designs and mixture verification data.**

**Table 21. Summary of ASTM D4867 test results.**

Mixture	Visual Damage, % Area	Tensile Strength Ratio		Reported Field Performance
		NCHRP Project 9-34 ASTM D4867	Mix Design	
Georgia Granite	25	39.3	NA	Poor
Arkansas Gravel	10	85.5	NA	Poor
Mississippi Chert	25	73.4	NA	Poor
Kentucky Limestone	10	85.6	81.0	Poor
Wyoming Gravel	30	56.6	16.9	Poor
Wisconsin Gravel	10	82.7	87.0	Good
Oklahoma Sandstone with Lime	30	78.8	NA	Good
Pennsylvania Dolomite	5	89.2	90.0	Good

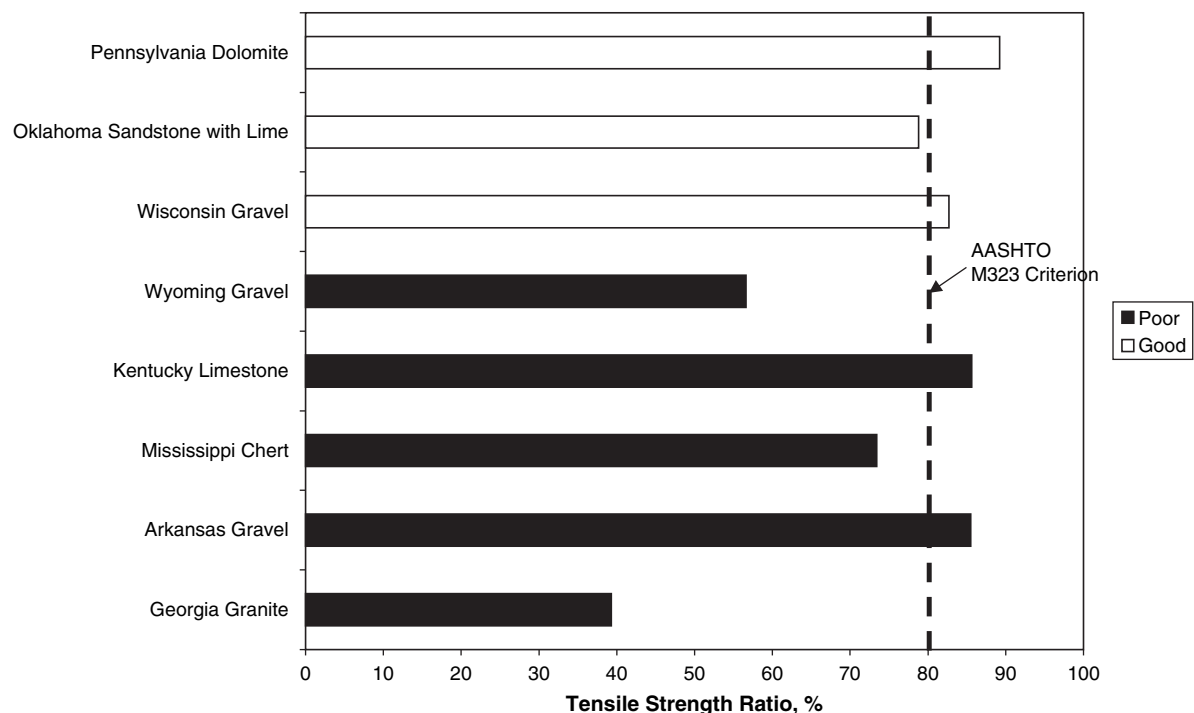
correctly identified mixtures to six by correctly identifying the Oklahoma sandstone with lime as acceptable. But this criterion would still incorrectly identify the reportedly poor-performing Kentucky limestone and Arkansas gravel mixtures as having acceptable resistance to moisture damage. The agreement of the NCHRP Project 9-34 data with those reported in the submitted mixture designs is generally good except for the Wyoming gravel, which exhibited severe moisture sensitivity. The reproducibility of data between labs is likely much poorer for highly moisture-sensitive mixtures.

All of the mixtures exhibited visual evidence of damage. Figures E.1 through E.8 in Appendix E document the extent of visual damage in each mixture. Each of these figures includes an unconditioned specimen on the left and a conditioned specimen on the right to show the amount of aggregate that fractured during the test. Aggregate fracture was small

except for the Oklahoma mixture. Damage was confined to the coarse aggregate fraction in Pennsylvania, Oklahoma, and Kentucky mixtures. Damage was evident in both the coarse and fine aggregate fractions of the remaining mixtures.

Stuart suggested visual damage greater than or equal to 10 percent indicated moisture sensitivity (35). Figure 23 compares the visual damage with this criterion. This criterion correctly identifies the five reportedly poor-performing mixtures and one of the mixtures that was reported to perform well. This criterion, however, incorrectly identifies the Oklahoma sandstone with lime and the Wisconsin gravel mixtures, both reported to perform well, as being moisture sensitive.

Figure 24 shows that there is a weak correlation between visual damage and the tensile strength ratio. The tensile strength ratio is affected by changes in binder stiffness and strength as well as the adhesive failure identified by the visual damage

**Figure 22. Comparison of ASTM D4867 test results with the AASHTO M323 criterion.**



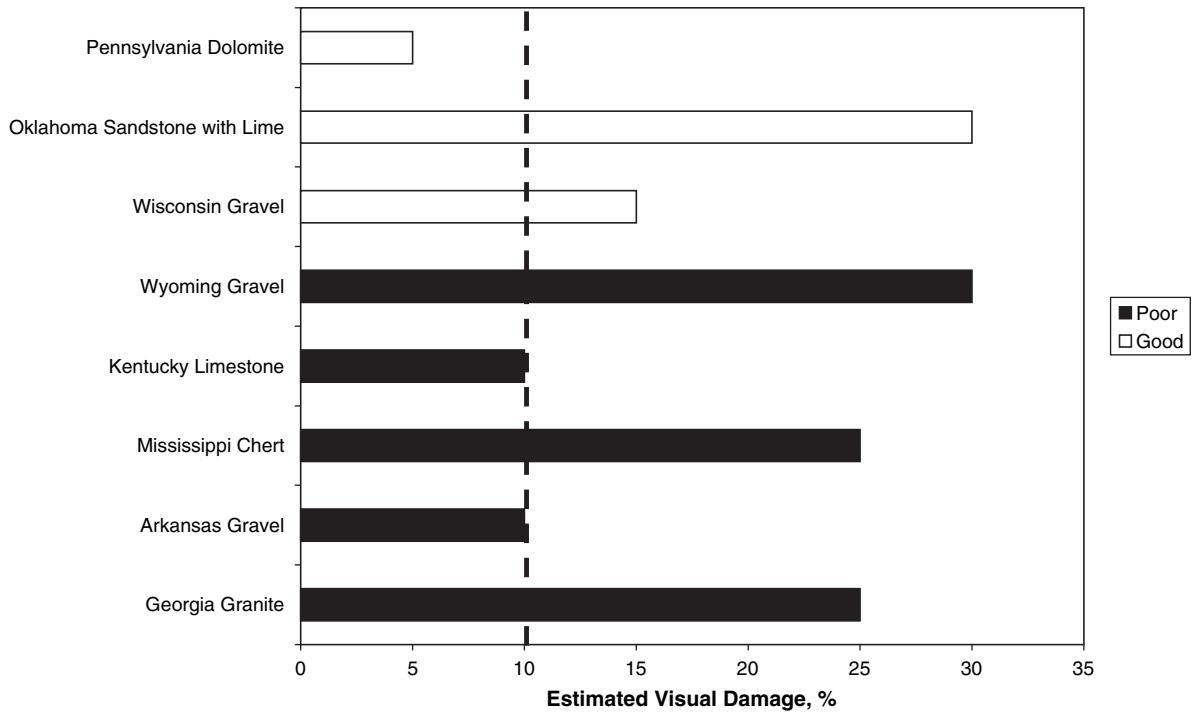


**Figure 23. Comparison of ASTM D4867 estimated visual damage with criterion suggested by Stuart (35).**

estimate. For this data set, combining the AASHTO M323 tensile strength ratio criterion and the visual damage criterion produces results that are the same as those described above for the visual damage criterion: all of the mixtures reported to perform poorly are correctly identified, but the Oklahoma sandstone with lime and Wisconsin gravel mixtures, reported to

perform well, are identified as being moisture sensitive due to the amount of visual damage evident in these mixtures.

Tables 22 through 29 present the test results for each of the mixtures. These tables include data obtained from individual specimens and averages and standard deviations for air voids, saturation, and tensile strength. Additional analyses of the

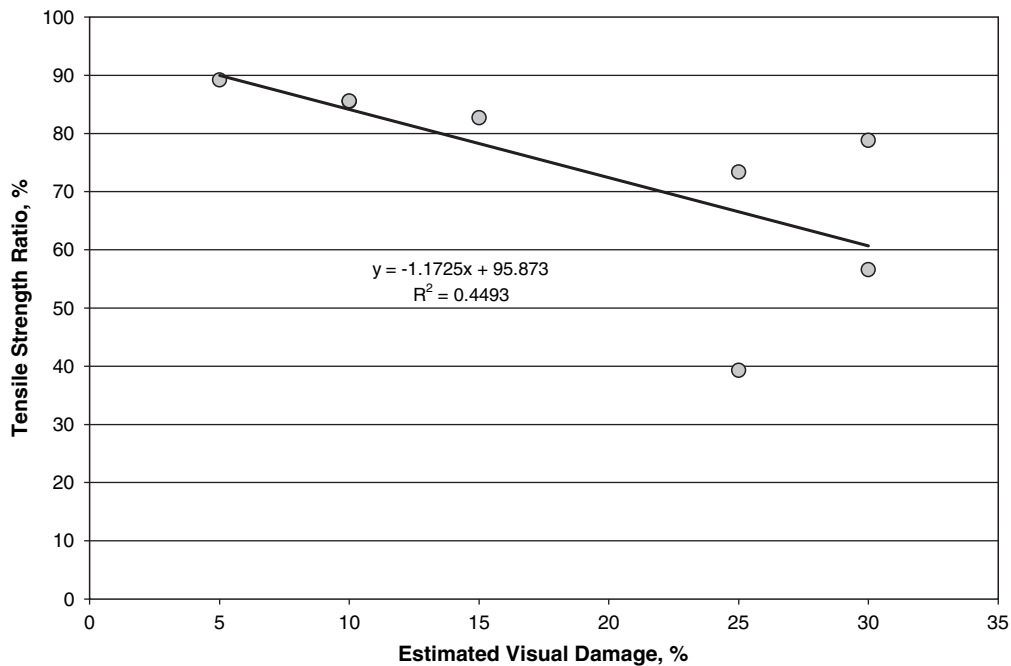


**Figure 24. Comparison of visual damage and tensile strength ratio.**

**Table 22. ASTM D4867 test data for the Georgia granite mixture.**

Condition	Sample ID	Air Voids, %	Vacuum		Saturation, %	Tensile Strength, kPa
			Level, mm	Time, min		
Conditioned	MD307.04	7.5	508	5	79.7	443.3
	MD307.05	7.4	508	5	78.7	411.6
	MD307.08	6.8	508	5	78.8	442.6
	Average	7.2	NA <sup>1</sup>	NA	79.1	432.5
	Standard Deviation	0.38	NA	NA	0.55	18.1
Unconditioned	MD307.03	7.6	NA	NA	NA	1111.5
	MD307.06	6.8	NA	NA	NA	1148.7
	MD307.07	6.8	NA	NA	NA	1041.1
	Average	7.1	NA	NA	NA	1100.4
	Standard Deviation	0.46	NA	NA	NA	54.6
					<b>Tensile Strength Ratio</b>	<b>39.3%</b>
					<b>Estimated Visual Damage</b>	<b>25 %</b>

<sup>1</sup>NA = not applicable.**Table 23. ASTM D4867 test data for the Arkansas gravel mixture.**

Condition	Sample ID	Air Voids, %	Vacuum		Saturation, %	Tensile Strength, kPa
			Level, mm	Time, min		
Conditioned	MD311.04	7.3	508	5	62.8	1045.3
	MD311.06	7.1	533	5	64.2	968.0
	MD311.08	7.1	533	5	62.5	952.2
	Average	7.2	NA	NA	63.2	988.5
	Standard Deviation	0.12	NA	NA	0.91	49.8
Unconditioned	MD311.03	7.6	NA	NA	NA	1119.1
	MD311.05	7.1	NA	NA	NA	1137.0
	MD311.07	7.1	NA	NA	NA	1212.1
	Average	7.3	NA	NA	NA	1156.1
	Standard Deviation	0.29	NA	NA	NA	49.4
					<b>Tensile Strength Ratio</b>	<b>85.5 %</b>
					<b>Estimated Visual Damage</b>	<b>10 %</b>

<sup>1</sup>NA = not applicable.**Table 24. ASTM D4867 test data for the Wisconsin gravel mixture.**

Condition	Sample ID	Air Voids, %	Vacuum		Saturation, %	Tensile Strength, kPa
			Level, mm	Time, min		
Conditioned	MD313.03	7.0	508	5	63.0	534.4
	MD313.06	7.0	533	5	65.0	537.8
	MD313.08	7.3	559	5	67.4	500.6
	Average	7.1	NA	NA	65.1	524.2
	Standard Deviation	0.17	NA	NA	2.20	20.6
Unconditioned	MD313.04	6.7	NA	NA	NA	664.7
	MD313.05	7.1	NA	NA	NA	657.8
	MD313.07	7.3	NA	NA	NA	579.2
	Average	7.0	NA	NA	NA	633.9
	Standard Deviation	0.30	NA	NA	NA	47.5
					<b>Tensile Strength Ratio</b>	<b>82.7%</b>
					<b>Estimated Visual Damage</b>	<b>15%</b>

<sup>1</sup>NA = not applicable.

**Table 25. ASTM D4867 test data for the Mississippi chert mixture.**

Condition	Sample ID	Air Voids, %	Vacuum		Saturation, %	Tensile Strength, kPa
			Level, mm	Time, min		
Conditioned	MD314.04	7.4	508	5	61.6	996.3
	MD314.05	7.2	559	5	65.4	903.2
	MD314.07	7.2	559	5	67.7	989.4
	Average	7.3	NA	NA	64.9	963.0
	Standard Deviation	0.12	NA	NA	3.08	51.9
Unconditioned	MD314.03	7.5	NA	NA	NA	1271.4
	MD314.05	7.0	NA	NA	NA	1328.0
	MD314.07	7.2	NA	NA	NA	1337.6
	Average	7.2	NA	NA	NA	1312.3
	Standard Deviation	0.25	NA	NA	NA	35.8
					<b>Tensile Strength Ratio</b>	<b>73.4%</b>
					<b>Estimated Visual Damage</b>	<b>25%</b>

<sup>1</sup>NA = not applicable.**Table 26. ASTM D4867 test data for the Kentucky limestone mixture.**

Condition	Sample ID	Air Voids, %	Vacuum		Saturation, %	Tensile Strength, kPa
			Level, mm	Time, min		
Conditioned	MD315.04	6.8	510	5	58.3	797.8
	MD315.05	6.7	610	5	73.2	708.1
	MD315.08	6.9	585	5	67.9	702.6
	Average	6.8			66.5	736.2
	Standard Deviation	0.1			7.6	53.4
Unconditioned	MD315.03	6.5	NA	NA	NA	876.4
	MD315.06	7.0	NA	NA	NA	848.1
	MD315.07	6.8	NA	NA	NA	855.0
	Average	6.8	NA	NA	NA	859.8
	Standard Deviation	0.3	NA	NA	NA	14.7
					<b>Tensile Strength Ratio</b>	<b>85.6%</b>
					<b>Estimated Visual Damage</b>	<b>10%</b>

<sup>1</sup>NA = not applicable.**Table 27. ASTM D4867 test data for the Oklahoma sandstone with lime mixture.**

Condition	Sample ID	Air Voids, %	Vacuum		Saturation, %	Tensile Strength, kPa
			Level, mm	Time, min		
Conditioned	MD316.08	6.5	510	5	72.8	1128.0
	MD316.09	6.6	510	5	68.4	936.3
	MD316.12	6.5	510	5	67.9	1009.4
	Average	6.5			69.7	1024.6
	Standard Deviation	0.1			2.7	96.7
Unconditioned	MD316.08	6.6	NA	NA	NA	1273.5
	MD316.10	6.4	NA	NA	NA	1338.3
	MD316.11	6.7	NA	NA	NA	1289.4
	Average	6.6				1300.4
	Standard Deviation	0.2				33.8
					<b>Tensile Strength Ratio</b>	<b>78.8%</b>
					<b>Estimated Visual Damage</b>	<b>30%</b>

<sup>1</sup>NA = not applicable.

**Table 28. ASTM D4867 test data for the Pennsylvania dolomite mixture.**

Condition	Sample ID	Air Voids, %	Vacuum		Saturation, %	Tensile Strength, kPa
			Level, mm	Time, min		
Conditioned	MD317.19	7.3	510	5	58.6	684.0
	MD317.22	6.7	560	5	65.2	734.3
	MD317.23	7.0	560	5	65.1	650.2
	Average	7.0			63.0	689.5
	Standard Deviation	0.3			3.8	42.3
Unconditioned	MD317.20	6.5	NA	NA	NA	777.1
	MD317.21	7.3	NA	NA	NA	816.4
	MD317.24	7.1	NA	NA	NA	725.4
	Average	7.0	NA	NA	NA	772.9
	Standard Deviation	0.4	NA	NA	NA	45.6
					<b>Tensile Strength Ratio</b>	<b>89.2%</b>
					<b>Estimated Visual Damage</b>	<b>5%</b>

<sup>1</sup>NA = not applicable.

ASTM D4867 data were conducted to determine whether there was bias in the testing that may have influenced the results and to further analyze the tensile strength data for comparison with the data from other tests.

The data were first checked against the tensile strength precision statement published in ASTM D4867. The within-laboratory standard deviation for tensile strengths on dry and conditioned specimens is 55 kPa. An appropriate statistical test to check the standard deviation of the measured tensile strengths against this standard is summarized below (36):

$$\begin{aligned}
 \text{Null Hypothesis:} & \quad \sigma^2 = \sigma_0^2 \\
 \text{Alternative Hypothesis:} & \quad \sigma^2 > \sigma_0^2 \\
 \text{Test Statistic:} & \quad \chi^2 = \frac{(n-1)s^2}{\sigma_0^2} \quad (7) \\
 \text{Rejection Region:} & \quad \chi^2 > \chi^2_U \text{ for } a = \alpha \text{ and } n - 1 \text{ degrees} \\
 & \quad \text{of freedom}
 \end{aligned}$$

where

$$\begin{aligned}
 \sigma_0 &= \text{specified standard deviation,} \\
 s &= \text{sample standard deviation,} \\
 n &= \text{number of samples,} \\
 \chi^2 &= \text{value of chi-square distribution,} \\
 \chi^2_U &= \text{limiting value of chi-square,} \\
 a &= \text{rejection area, and} \\
 \alpha &= \text{level of significance.}
 \end{aligned}$$

The results, summarized in Table 30, show that in all cases except the conditioned strengths for the Oklahoma sandstone with lime mixture, the standard deviations are not significantly greater than the within-laboratory precision value of 55 kPa. For the conditioned Oklahoma sandstone with lime tests, an outlier cannot be identified by inspection of the data in Table 27. The strength of one specimen is near the average. The other two strengths are about equally higher and lower

**Table 29. ASTM D4867 test data for the Wyoming gravel mixture.**

Condition	Sample ID	Air Voids, %	Vacuum		Saturation, %	Tensile Strength, kPa
			Level, mm	Time, min		
Conditioned	MD318.09	7.4	510	5	63.7	548.8
	MD318.11	7.0	510	5	66.4	544.7
	MD318.12	6.7	560	5	68.2	575.0
	Average	7.0			66.1	556.2
	Standard Deviation	0.4			2.2	16.5
Unconditioned	MD318.08	7.4	NA	NA	NA	1006.7
	MD318.10	7.4	NA	NA	NA	970.1
	MD318.13	6.5	NA	NA	NA	968.7
	Average	7.1	NA	NA	NA	981.8
	Standard Deviation	0.5	NA	NA	NA	21.5
					<b>Tensile Strength Ratio</b>	<b>56.6%</b>
					<b>Estimated Visual Damage</b>	<b>30%</b>

<sup>1</sup>NA = not applicable.

**Table 30. Hypothesis test on tensile strength variance.**

Mix	Condition	n	$\chi^2$	$\chi^2_u$ for $\alpha = 0.05$	Conclusion
Georgia Granite	Conditioned	3	0.216	5.995	$\sigma \leq 55$ kPa
	Unconditioned	3	1.971	5.995	$\sigma \leq 55$ kPa
Arkansas Gravel	Conditioned	3	1.640	5.995	$\sigma \leq 55$ kPa
	Unconditioned	3	1.606	5.995	$\sigma \leq 55$ kPa
Wisconsin Gravel	Conditioned	3	0.280	5.995	$\sigma \leq 55$ kPa
	Unconditioned	3	1.492	5.995	$\sigma \leq 55$ kPa
Mississippi Chert	Conditioned	3	1.781	5.995	$\sigma \leq 55$ kPa
	Unconditioned	3	0.847	5.995	$\sigma \leq 55$ kPa
Kentucky Limestone	Conditioned	3	1.885	5.995	$\sigma \leq 55$ kPa
	Unconditioned	3	0.145	5.995	$\sigma \leq 55$ kPa
Oklahoma Sandstone with Lime	<b>Conditioned</b>	<b>3</b>	<b>6.182</b>	<b>5.995</b>	<b><math>\sigma &gt; 55</math> kPa</b>
	Unconditioned	3	0.755	5.995	$\sigma \leq 55$ kPa
Pennsylvania Dolomite	Conditioned	3	1.183	5.995	$\sigma \leq 55$ kPa
	Unconditioned	3	1.375	5.995	$\sigma \leq 55$ kPa
Wyoming Gravel	Conditioned	3	0.180	5.995	$\sigma \leq 55$ kPa
	Unconditioned	3	0.305	5.995	$\sigma \leq 55$ kPa

than the average. For computation of the tensile strength ratios previously presented in Table 21, the entire data set was used in all cases in spite of the conditioned Oklahoma sandstone with lime data exceeding the ASTM D4867 precision statement.

The next analysis that was performed was a two-way analysis of variance to investigate the significance of differences in air voids between mixtures and conditioned and unconditioned subsets for each mixture. The results, summarized in Table 31, show that there is a mixture effect, but there is not a condition or interaction effect. Thus, air void contents for conditioned and unconditioned subsets were approximately equal, as required by ASTM D4867, but the air void level was different for different mixtures. Figure 25 is a graphical representation of these results. It shows average air voids for conditioned and unconditioned specimens for each mixture. The error bars shown in Figure 25 are 95-percent confidence intervals for the mean air void content using the pooled standard deviation for all of the test data. From Figure 25, it appears that the only significant air void difference is between the Oklahoma sandstone with lime which had the lowest average air void content (6.6 percent) and the Mississippi chert which had the highest air void content (7.2 percent).

This was confirmed by performing multiple comparisons using the Scheffé test (36). At a significance level of 5 percent, this test found the only difference in air voids to be between the Oklahoma sandstone with lime and the Mississippi chert. Figure 26 presents a plot of tensile strength ratio as a function of air void content. The correlation between the air void content and the tensile strength ratio is poor, indicating that differences in air void content between mixtures did not influence the ASTM D4867 test results.

The next analysis was a one-way analysis of variance for the saturation level to see if the level of saturation was significantly different between mixtures. The results, summarized in Table 32, show a greater between-mixture variation compared to within-mixture variation, indicating that the saturation level was not the same for the eight mixtures. Figure 27 is a graphical representation of these results. It shows average degrees of saturation for each mixture. The error bars shown in Figure 27 are 95-percent confidence intervals for the mean saturation level using the pooled standard deviation for all of the test data. From Figure 28, it appears that the saturation level in the Georgia granite mixture was higher than all other mixtures. This was confirmed by performing multiple comparisons using the Scheffé test

**Table 31. Two-way analysis of variance for air voids in the ASTM D4867 testing.**

Source	Degrees of Freedom	Sum of Squares	Mean Squares	F Statistic	Critical F 5% Significance Level ( $\alpha$ )	Conclusion
Mixture	7	2.34000	0.334286	3.793313	2.24	<b>There is a mixture effect</b>
Conditioning	1	0.00333	0.003333	0.037825	4.07	No conditioning effect
Interaction	7	0.07333	0.010476	0.118879	2.24	No interaction effect
Error	32	2.82000	0.088125			
Total	47					

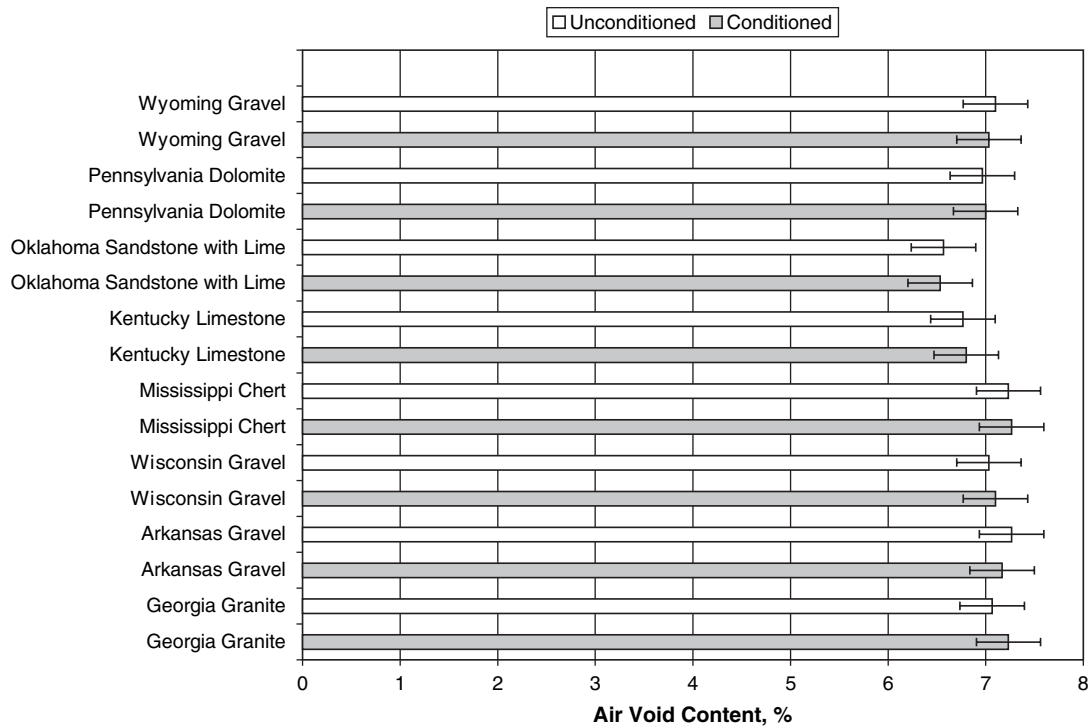


Figure 25. ASTM D4867 testing air void contents.

(36). At a significance level of 5 percent, this test found the saturation level in the Georgia granite mixture was higher than all other mixtures except the Oklahoma sandstone with lime. Figure 28 presents a plot of tensile strength ratio as a function of saturation level. Because of its extreme value, the point for the Georgia granite mixture has a significant effect on the relationship between degree of saturation and tensile

strength ratio. When this point is excluded, the data exhibit poor correlation. However, it is possible that the data for the Georgia granite were affected by the higher saturation level obtained in this mixture.

The last analysis that was conducted on the ASTM D4867 results was a series of hypothesis tests to determine whether the conditioned tensile strengths were significantly lower

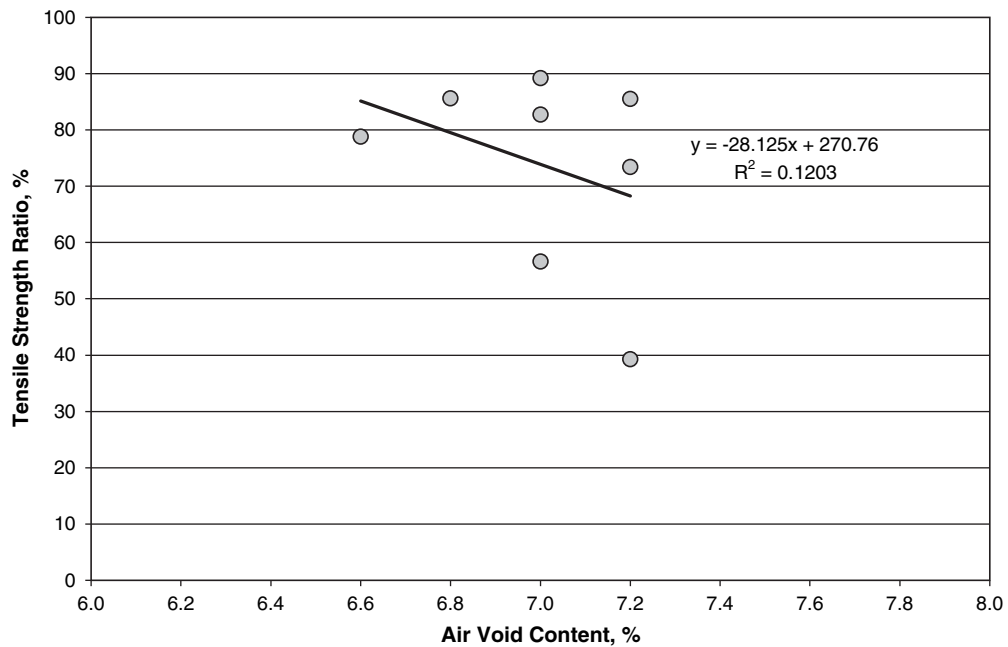


Figure 26. Scatter plot of tensile strength ratio versus air voids.

**Table 32. One-way analysis of variance for saturation in the ASTM D4867 testing.**

Source	Degrees of Freedom	Sum of Squares	Mean Squares	F Statistic	Critical F 95% Significance Level	Conclusion
Mixture	7	577.69290	82.52756	6.65433	2.66	There is a mixture effect
Within	16	198.43333	12.40208			
Total	23					

than the unconditioned tensile strengths. The following hypothesis test for two means was used (36):

Null Hypothesis:  $\mu_1 = \mu_2$

Alternative Hypothesis:  $\mu_1 > \mu_2$

Test Statistic: 
$$t = \frac{\bar{X}_1 - \bar{X}_2}{s \left( \frac{1}{n_1} + \frac{1}{n_2} \right)^{0.5}} \quad (8)$$

$$s = \left[ \frac{(n_1 - 1)s_1^2 + (n_2 - 1)s_2^2}{(n_1 + n_2 - 2)} \right]^{0.5} \quad (9)$$

Rejection Region:  $t > t_\alpha$  for  $(n_1 + n_2 - 2)$  degrees of freedom

where

$\mu$  = mean of population,

$\bar{X}_1$  = unconditioned average tensile strength,

$\bar{X}_2$  = conditioned average tensile strength,

$s$  = pooled standard deviation,

$s_1$  = unconditioned tensile strength standard deviation,

$s_2$  = conditioned tensile strength standard deviation,

$n_1$  = number of samples in the unconditioned set,

$n_2$  = number of samples in the conditioned set,

$t$  = value of t-distribution, and

$\alpha$  = level of significance.

The results are summarized in Table 33. The conditioned strengths were significantly lower for all mixtures tested except for the Pennsylvania dolomite. This mixture had the highest tensile strength ratio at 89.2 percent and the lowest amount of visual damage. Figure 29 is a graphical illustration of this finding. It presents average unconditioned and conditioned tensile strengths for all of the mixtures tested. The error bars shown are 95-percent confidence intervals based on the pooled standard deviation from the conditioned and unconditioned tests on each mixture.

In summary, the ASTM D4867 testing found visual evidence of damage in all of the mixtures. It also found all mixtures except the Pennsylvania dolomite to have significantly lower tensile strengths after conditioning. Although all of the air void

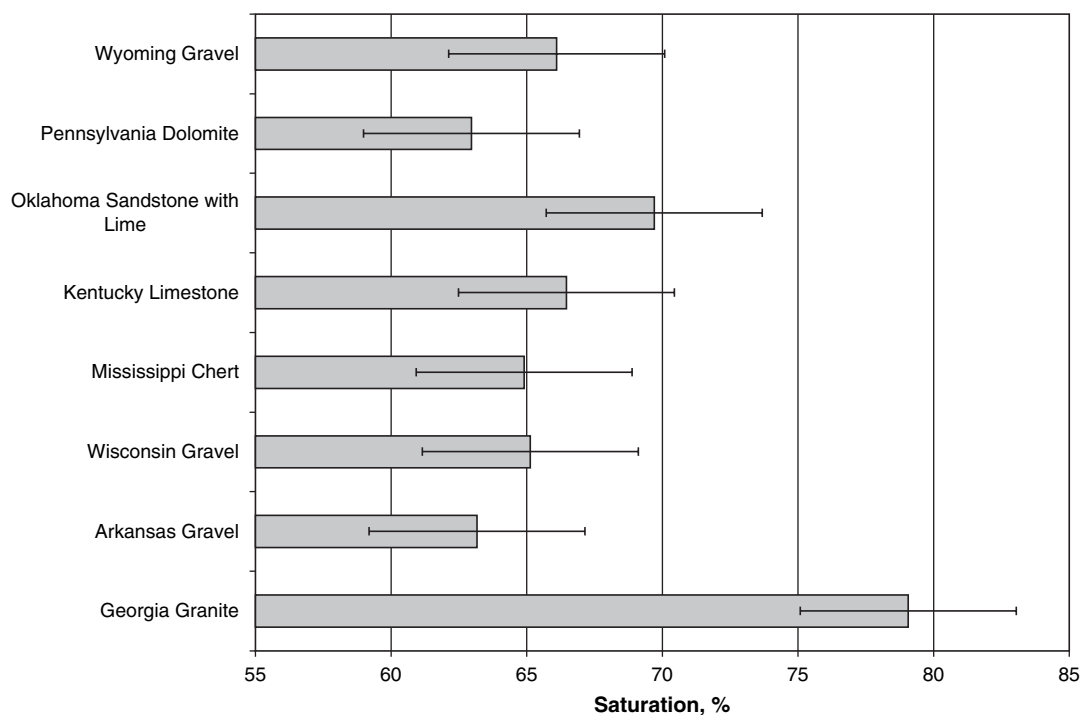


**Figure 27. ASTM D4867 testing saturation levels.**

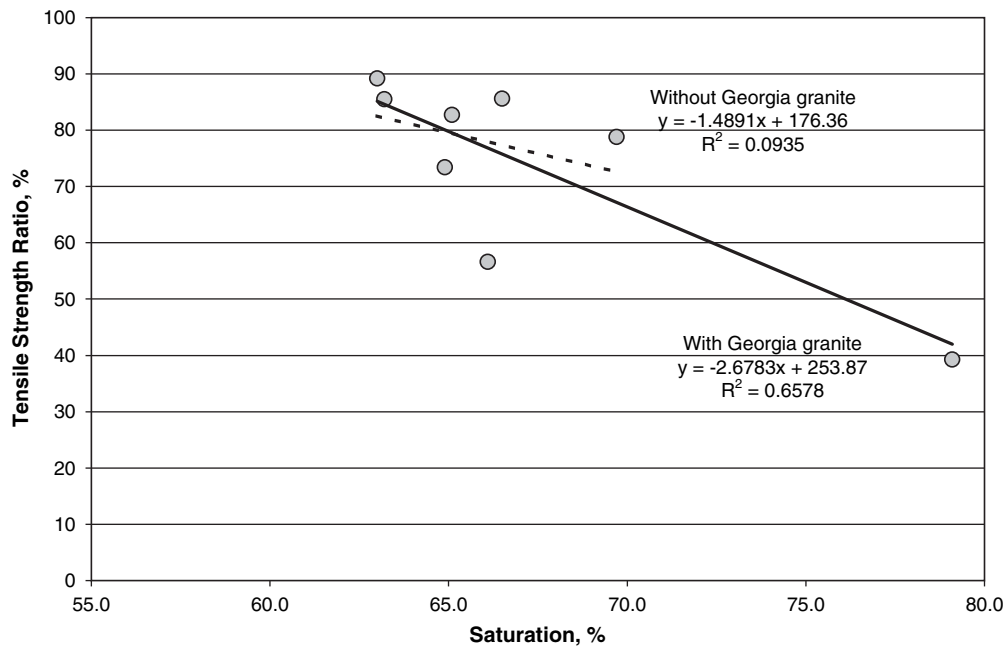


Figure 28. Scatter plot of tensile strength ratio versus saturation level.

contents and saturation levels were within the ASTM D4867 limits of 6 to 8 percent for air voids and 55 to 80 percent for saturation, there were differences in air voids and saturation levels for the mixtures tested. Only the mixtures with the highest and lowest air voids were significantly different, and it appears that this difference did not affect the results of the testing. The Georgia granite mixture had a significantly higher degree of saturation compared to the other mixtures tested. It also had the lowest tensile strength ratio. With the available data, it was not possible to conclude whether the higher saturation for the Georgia granite affected the results of the testing.

The ASTM D4867 test results did not agree with the reported field performance of the mixtures tested. Using the AASHTO M323 tensile strength criterion of 80 percent,

ASTM D4867 correctly identified the performance of five of the eight mixtures tested. It incorrectly identified Oklahoma sandstone with lime—which was reported to perform well—as being susceptible to moisture damage. More importantly, however, it identified the reportedly poor-performing Kentucky limestone and Arkansas gravel mixtures as having acceptable resistance to moisture damage. Using visual damage estimates, ASTM D4867 correctly identified all of the reportedly poor-performing mixtures and the Pennsylvania dolomite mixture, reported to perform well. This criterion, however, incorrectly identified the Oklahoma sandstone with lime and the Wisconsin gravel mixtures as being moisture sensitive. Combining both criteria results in the same rankings as using only the visual criterion.

Table 33. Hypothesis test results for difference in tensile strength for conditioned and unconditioned specimens.

Mixture	Tensile Strength Ratio	t-Statistic	Critical t-Statistic		Conclusion
			95 percent	99 percent	
Georgia Granite	39.3	20.10	2.78	4.60	Conditioned strength significantly less at 99-percent level
Arkansas Gravel	85.5	4.14	2.78	4.60	Conditioned strength significantly less at 95-percent level
Wisconsin Gravel	82.7	3.67	2.78	4.60	Conditioned strength significantly less at 95-percent level
Mississippi Chert	73.4	9.60	2.78	4.60	Conditioned strength significantly less at 99-percent level
Kentucky Limestone	85.6	3.86	2.78	4.60	Conditioned strength significantly less at 95-percent level
Oklahoma Sandstone with Lime	78.8	4.66	2.78	4.60	Conditioned strength significantly less at 99-percent level
Pennsylvania Dolomite	89.2	2.32	2.78	4.60	Conditioned strength not significantly less
Wyoming Gravel	56.6	27.20	2.78	4.60	Conditioned strength significantly less at 99-percent level



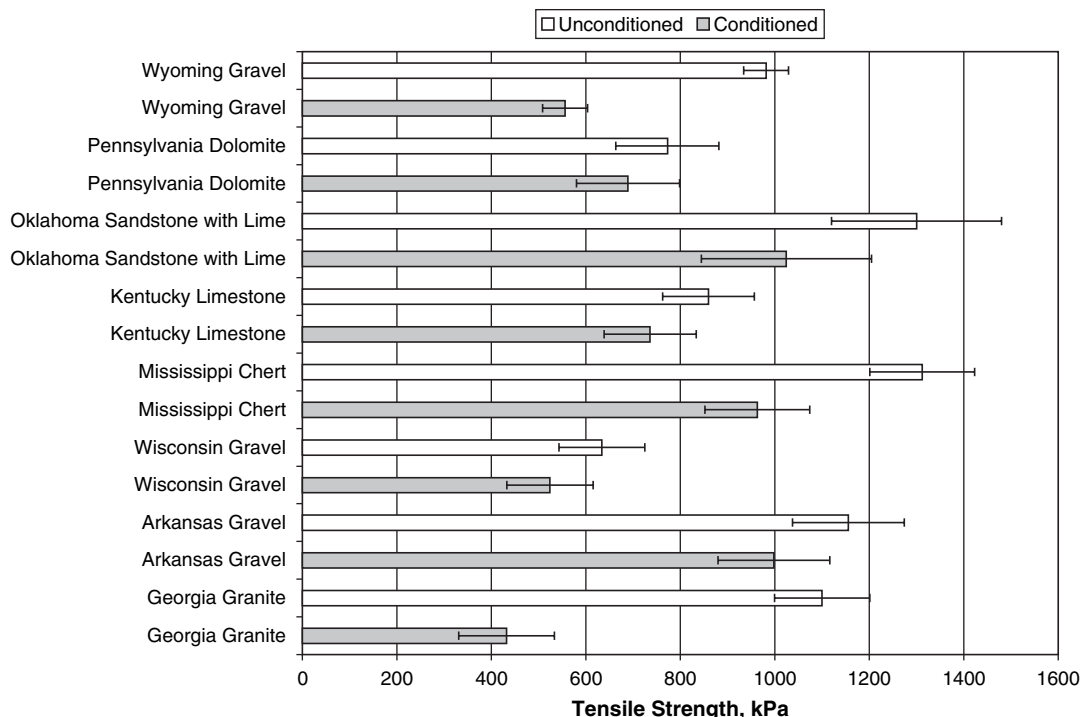


Figure 29. Comparison of average tensile strengths.

### 3.3 The Hamburg Wheel Tracking Test

#### 3.3.1 Comparing Slab Specimens with Superpave Gyrotory Compactor (SGC) Specimens

During the early stages of Phase IA tests with the HWTD, the research team was directed by the project panel to make a comparison between results from tests on specimens prepared with the SGC and results from tests on slab specimens. To meet this goal, two sets of loose mixtures for Oklahoma sandstone and Georgia granite were prepared by AAT and sent to Koch Pavement Solutions, Inc., where slab specimens were prepared and tested.

Figures 30 and 31 show the Georgia granite results for the slabs and cylindrical specimens (SGC specimens), respectively. While the numerical values from the two tests are different, both have identified the tested mixture as a failing mix.

The HWTD results on the slab specimens of Oklahoma sandstone mix (see Figure 32) indicate a strong-performing mix, as was also demonstrated by the HWTD results on the SGC specimens of this mix (see Figure 33). For this mix, the results from slab and cylindrical specimens are extremely close, both indicating an excellent mix.

A study by Izzo and Tahmoressi (37) on repeatability and reproducibility of the HWTD has shown that the testing configuration using cylindrical specimens provides results similar to the results obtained with slabs. In that research, no significant

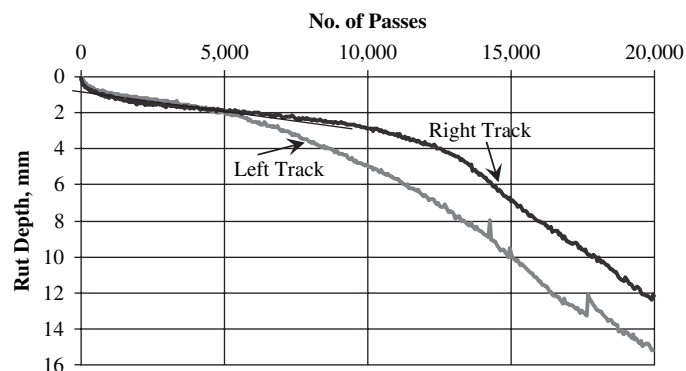


Figure 30. Rut depth versus wheel passes from HWTD on slab specimens for Georgia granite mix at 50 °C.

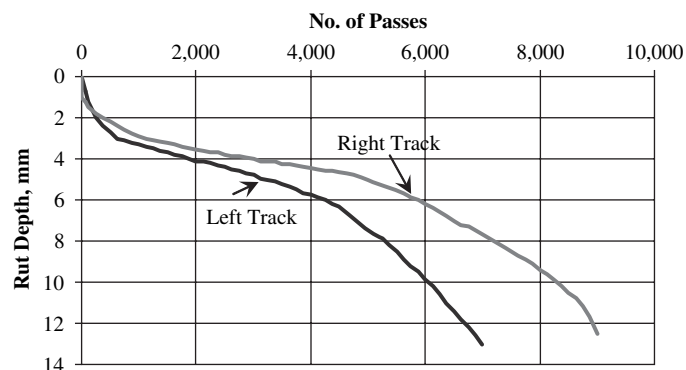
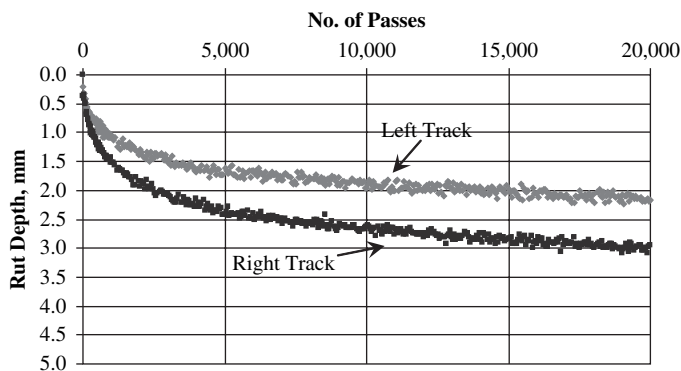
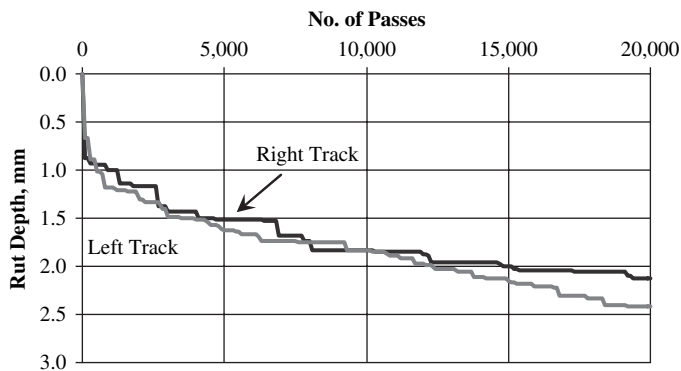


Figure 31. Rut depth versus wheel passes from HWTD on SGC specimens for Georgia granite mix at 50 °C.



**Figure 32.** Rut depth versus wheel passes from HWTB on slab specimens for Oklahoma sandstone mix at 50°C.



**Figure 33.** Rut depth versus wheel passes from HWTB on SGC specimens for Oklahoma sandstone mix at 50°C.

difference was seen in the standard deviation for each test parameter. The results indicated that the level of performance for both mixtures could be predicted with either a slab or SGC test specimen.

Based on the results obtained from the two sets of tests conducted under this study, as well as results from past research, it was decided to continue testing the remaining mixes of Phase IA using SGC specimens.

### 3.3.2 Results for Cylindrical Specimens

The summary of results from HWTB tests are presented in Appendix C. These results indicate that in five out of the eight tested mixtures, the results from the HWTB tests match the reported field performance (see Table 34).

The Georgia mix indicated a very poor performance in HWTB, consistent with the reported field performance. The average stripping inflection point was at approximately 5,160 cycles, with 12.5 mm of deformation reached after only 7,000 and 9,000 passes for the left and right tracks, respectively.

The Arkansas mix exhibited good performance in HWTB. The material easily passed the PG 64-22 requirements based

**Table 34.** Comparison of HWTB performance versus field performance.

Source	HWTB Result	Reported Field Performance
GA Granite	Poor	Poor
AR Gravel	Good	Poor
WI Gravel	Poor	Good
MS Chert	Good	Poor
KY Limestone	Poor	Poor
OK Sandstone	Good	Good
PA Dolomite	Good	Good
WY Gravel	Poor	Poor

on a Texas Department of Transportation (TxDOT) specification. It also passed the PG 70-22 requirement and was borderline passing for PG 76-22. The mix had been prepared with no lime or liquid antistripping additive. Good performance of this mix in HWTB is consistent with the results obtained for tensile strength ratio (TSR) from ASTM D4867. However, this is in contradiction to the reported field performance for this material. This mix was used on US 59 and IH 20 in Texas several years ago and showed severe stripping within 6 months of placement.

The results for the Wisconsin mix showed significant deformation at the test temperature (50°C). This was expected since the binder was a PG 58-28. Judging the moisture susceptibility of this mix based on these results would be difficult because a major portion of the observed deformation is the result of using a soft binder rather than the effect of moisture damage in HWTB. The Hamburg tracking was possibly too severe considering the soft binder. The reported field performance for this mix is good.

The Mississippi mix showed an average permanent deformation of 5.7 mm at 10,000 passes and 6.8 mm after 20,000. This mix is considered a passing mix considering the TxDOT criteria. No stripping inflection point was observed for this mix, implying no stripping effect. The behavior of this mix in HWTB was in conflict with its field performance, which was reported to be poor without lime or antistripping agents.

The results for the Kentucky mix indicated that it is susceptible to stripping and rutting. Based on the stripping inflection point data, it appeared that stripping took control after about 6,000 passes of the wheel. The limiting rut depth of 12.5 mm was reached between 7,000 and 8,000 cycles. This observation matches the reported field behavior of this mix.

The results for the Oklahoma mix indicate that it is highly resistant to rutting and moisture damage. This mixture experienced very little permanent deformation, and a stripping inflection point was not observed through 20,000 passes. The performance of this mixture in the HWTB is in agreement with reports of its excellent field performance.

The results for the Pennsylvania dolomite mix exhibit acceptable performance based on the TxDOT criteria for a PG

64-22 binder. The performance of this mixture in the HWTD is in agreement with reports of its good field performance.

The results for the Wyoming mix exhibit a failed performance based on the TxDOT criteria for a PG 64-22 binder. The performance of this mixture in the HWTD is in agreement with reports of its poor field performance.

### 3.4 Dynamic Modulus Testing

#### 3.4.1 Results from Load Level Study

The experimental plan that was followed to establish conditioning load levels was discussed in Chapter 2. Table 35 summarizes the test results from this experimental study. This table includes resilient strains, computed resilient moduli, permanent strains measured after 9,500 cycles, and permanent strains extrapolated to 68,400 cycles (as used in the ECS procedure). The load levels in the Phase IA work plan were based on permanent to resilient strain ratios computed using the model proposed for the AASHTO mechanistic empirical pavement design guide. The last column in Table 35 presents the ratio of the extrapolated permanent strain at 68,400 cycles to the measured permanent strain at 9,500 cycles. Figure 34 presents a plot of the measured permanent strain after 9,500 load cycles as a function of the measured resilient strain for each specimen tested in the load level verification study. Also shown in this figure are the best-fit regression lines through the origin. These lines represent the permanent to resilient strain ratio for the various binder grades. Considering the scatter in the data, there appears to

be two relationships, one for the unmodified PG 58 and 64 binders and one for the polymer-modified PG 76 binder. In computing the slope for the polymer-modified binder data, one point was considered an outlier. There is a definite relationship between the permanent strains and resilient strains, but contrary to Kaloush's previous work (31), the relationship does not appear to be the same for unmodified and modified binders. For the same resilient strain level, modified binders result in lower permanent deformation, which is rational considering recent field studies that have shown that for the same grade, modified binders have less permanent deformation than neat binders.

##### 3.4.1.1 Analysis Based on Constant Dynamic Strain

Knowing the resilient modulus of the mixtures, the loads required to produce a constant resilient strain level are given by Equation 10:

$$P = \epsilon \times M_r \times A \quad (10)$$

where

$P$  = load,

$\epsilon$  = selected strain level,

$M_r$  = resilient modulus, and

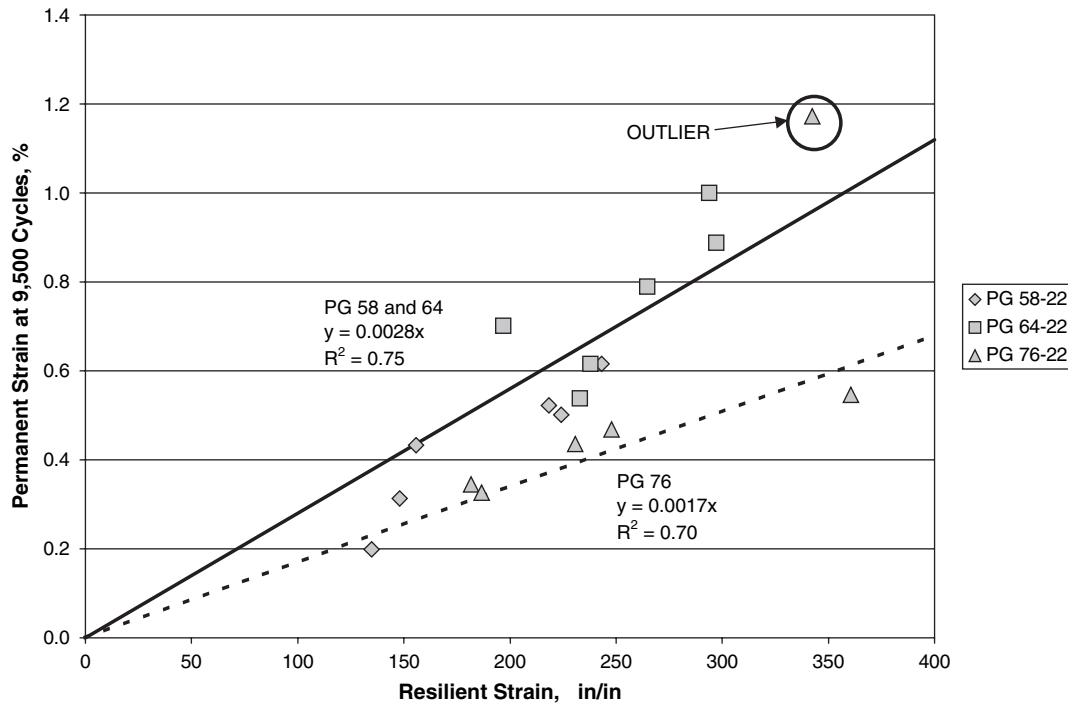
$A$  = cross-sectional area of the specimen.

Table 36 summarizes experimentally determined load levels required to produce constant dynamic strains at 60°C for the three binder grades used in the load level experiment. Past research with the ECS has shown a conditioning load of 200

**Table 35. Summary data from the load level verification study.**

Specimen ID	Binder Grade	Load, lb	Resilient Strain, $\mu\text{in/in}$	Resilient Modulus, ksi	Permanent Strain, %		Ratio
					9,500	64,800	
310-3	58-28	130	148	70	0.31	0.47	1.50
310-4	58-28	130	156	66	0.43	0.50	1.16
310-5	58-28	168	224	60	0.50	0.91	1.82
310-6	58-28	168	218	61	0.52	0.93	1.78
310-1	58-28	180	135	106 <sup>1</sup>	0.20	0.29	1.47
310-2	58-28	180	243	59	0.62	0.93	1.51
PG 58-28 Average				63			1.54
309-3	64-22	190	197	77	0.70	1.11	1.58
309-4	64-22	190	233	65	0.54	1.11	2.06
309-5	64-22	210	294	57	1.00	1.50	1.50
309-6	64-22	210	265	63	0.79	1.46	1.85
309-1	64-22	240	297	64	0.89	1.31	1.47
309-2	64-22	240	238	80	0.62	1.53	2.49
PG 64-22 Average				68			1.83
308-3	76-22	240	182	105	0.34	0.51	1.49
308-4	76-22	240	187	102	0.33	0.48	1.46
308-5	76-22	280	248	90	0.47	0.71	1.52
308-6	76-22	280	231	97	0.44	0.65	1.48
308-1	76-22	410	361	90	0.55	0.73	1.34
308-2	76-22	410	342	95	1.17	1.63	1.39
PG 76-22 Average				97			1.45

<sup>1</sup>Data not used in computation of average.



**Figure 34.** Permanent strain as a function of resilient strain for the load level study specimens.

lb to be appropriate for PG 58 binders. Based on this previous work and Table 36, the resilient strain during conditioning was limited to about 250  $\mu\text{in./in.}$ , resulting in loads of 200, 215, and 305 lb for PG 58, 64, and 76 binders, respectively.

### 3.4.1.2 Analysis Based on Constant Mechanical Damage

In this analysis, the loads are chosen based on a constant level of permanent strain in Figure 34. The extrapolated data in Table 35 result in permanent strains at 64,800 cycles (i.e., the number of cycles during the ECS procedure) that average 1.5 times the measured permanent strain at 9,500 cycles (i.e., the number of cycles used in the load level study). Thus, if we want to limit the maximum permanent strain at 64,800 cycles so as not to exceed 1 percent, then the strain at 9,500 cycles should be limited to 0.667 percent. From the slopes given in Figure 34, the corresponding resilient strains are 240  $\mu\text{in./in.}$  for unmodified binders and 395  $\mu\text{in./in.}$  for modified binders. Substituting these strains into Equation 10 yields

load levels of 190, 205, and 465 lb for PG 58, 64, and 76 binders, respectively. This analysis results in similar load levels as the constant dynamic strain analysis for the unmodified binders, but requires much higher conditioning loads for modified binders due to the lower slope of the permanent to resilient strain relationship.

### 3.4.1.3 Recommended Approach

After careful consideration of the findings from the two analyses and the comments received from the project panel on the Phase IA work plan, the research team adopted the constant dynamic strain approach as the basis for determination of the conditioning loads. Using this approach, the conditioning loads were adjusted to account for the different binder grades used in different environmental regions. This adjustment was made to result in approximately the same dynamic strain level in the specimens since stiffer binders are selected in hotter climates. The conditioning loads were not adjusted to remove the beneficial effect that binder modifica-

**Table 36.** Summary of conditioning loads for various dynamic strain levels.

Binder	$M_r$ , psi	Conditioning Load, lb				
		150 $\mu\text{in./in.}$	175 $\mu\text{in./in.}$	200 $\mu\text{in./in.}$	225 $\mu\text{in./in.}$	250 $\mu\text{in./in.}$
PG 58	63,000	119	139	158	178	198
PG 64	68,000	128	150	171	192	214
PG 76	97,000	183	213	244	274	305

tion or grade bumping may have on the damage level induced in the specimen during the ECS procedure.

The load magnitudes developed under this laboratory experiment were based only on the analysis of a single mixture with specific binders used in this study. As an extension to this work, existing empirical models were utilized to determine load magnitudes based on the analysis of representative mixtures. Two approaches were considered for performing this analysis. The first was the Witczak dynamic modulus equation that was described in Chapter 2. The conditioning loads given in Table 15 in Chapter 2 were estimated using the Witczak dynamic modulus equation. The second approach used was the recently developed Hirsch model (38). Equations 11 and 12 present the Hirsch model, which allows estimation of the modulus of the mixture from binder stiffness data and volumetric properties of the mixture.

$$|E^*|_{\text{mix}} = P_c \left[ 4,200,000 \left( 1 - \frac{VMA}{100} \right) + 3 |G^*|_{\text{binder}} \left( \frac{VFA \times VMA}{10,000} \right) \right] + \frac{1 - P_c}{\left[ \frac{\left( 1 - \frac{VMA}{100} \right)}{4,200,000} + \frac{VMA}{3 VFA |G^*|_{\text{binder}}} \right]} \quad (11)$$

where

$$P_c = \frac{\left( 20 + \frac{VFA \times 3 |G^*|_{\text{binder}}}{VMA} \right)^{0.58}}{650 + \left( \frac{VFA \times 3 |G^*|_{\text{binder}}}{VMA} \right)^{0.58}}; \quad (12)$$

VMA = Voids in mineral aggregates, %;

VFA = Voids filled with asphalt, %;

$|G^*|_{\text{binder}}$  = shear complex modulus of binder, psi; and

$|E^*|_{\text{mix}}$  = dynamic modulus of the mix.

Moisture sensitivity specimens are usually prepared to a level of 7-percent air voids. Using this level of air voids and a typical effective volumetric binder content of 10 percent results in VMA of approximately 17 percent and VFA of approximately 60 percent. Table 37 presents representative

**Table 37. Representative binder  $G^*$  values at 60°C and 10 Hz for RTFOT aging.**

Binder Grade	$G^*$ , kPa	$G^*$ , psi
52-34	5	0.7
58-28	10	1.4
64-22	20	2.9
70-22	30	4.4
76-22	45	6.5
82-22	70	10.2

**Table 38. Representative mixture moduli and estimated conditioning loads using the Hirsch model.**

Binder Grade	10 Hz Modulus, psi	Estimated Conditioning Load, lb
52-34	36,624	174
58-28	42,114	200
64-22	51,736	246
70-22	60,148	286
76-22	71,292	338
82-22	87,330	415

60°C binder complex shear modulus values for a loading rate of 10 Hz (62.8 rad/sec) for rolling thin film oven test (RTFOT) conditions. Table 38 summarizes mixture moduli computed for representative moisture sensitivity specimens using the Hirsch model and the representative binder moduli in Table 37. Table 38 also includes conditioning load levels based on a ratio of the mixture moduli using 200 lb as the standard for PG 58-28.

Figure 35 compares conditioning loads calculated using the Witczak dynamic modulus equation and the Hirsch model with those determined experimentally using the constant dynamic strain analysis discussed above. In all cases, the results are plotted using the temperature at the midpoint of the specific binder grade. The loads calculated with the Witczak equation are those from Table 15 adjusted to a load of 200 lb for PG 58 binders. As shown, conditioning load from the Witczak equation appears to overestimate the binder grade effect measured in this project. In fact, for the PG 76 binder, the estimated conditioning load is similar to that determined from constant damage analysis. The Hirsch model results are in better agreement. This model, along with the site impact, was used to determine conditioning loads for the project sites, as discussed below.

#### 3.4.1.4 Site Impact on Load Levels

The study conducted to establish conditioning loads provided a valuable guide. However, an important consideration in finalizing the conditioning load level should be the site conditions. The emphasis of this research study is on determining how well results from the ECS/dynamic modulus system correlate to the observed field performance. For this reason, it is important to maintain the same load level for all the mixtures that are under the same climatic conditions. Conditioning loads for each of the sites were estimated using the Hirsch model results. Equation 13 presents the conditioning load as a function of temperature.

$$P = 0.0066T^{2.51} \quad (13)$$

where

$P$  = ECS conditioning procedure load, lb, and

$T$  = site pavement temperature, °C.

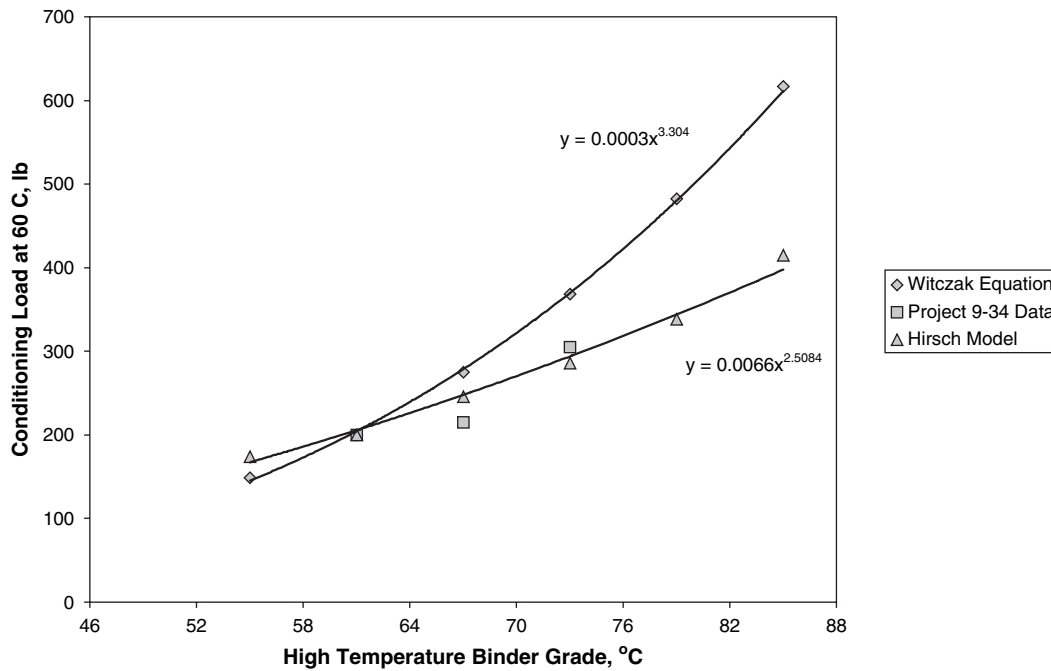


**Figure 35. Comparison of conditioning loads estimated using the Witczak Dynamic Modulus Equation, the Hirsch Model, and measured specimen responses.**

For each location, the pavement temperature has been determined and then used to establish the required PG grade for that site. LTPP Bind Program Version 2 was used for this purpose. This temperature is used in Equation 13 to determine the load level to be used for that site. For example, the Arkansas gravel mix was used in a project with known field performance in Atlanta, TX. The 98-percent reliability high temperature for binder PG selection at this site is almost 62°C. Using Equation 13, this temperature provides a load level of about 210 lb for conditioning in the ECS/dynamic modulus system. Similarly, load levels were established for

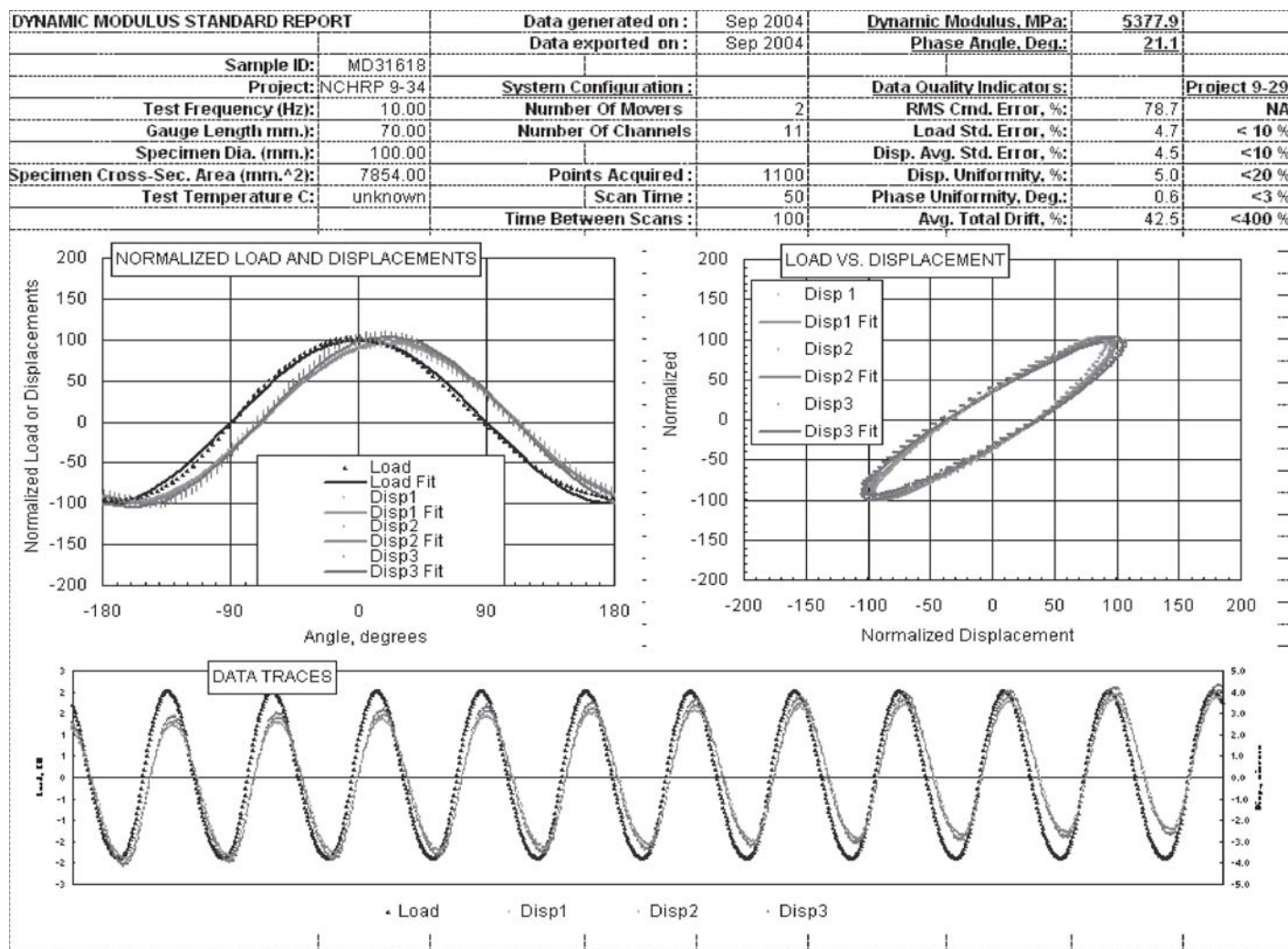
other mixtures, as shown in Table 39. This way, the selected load levels are site specific. The loads presented in Table 39 were finally used for conditioning the mix for a specific site regardless of the stiffness of the mix used at that site.

### 3.4.2 Dynamic Modulus Results

Figure 36 presents a typical dynamic modulus summary report in the NCHRP Project 9-29 format for the 10-Hz frequency testing. This report provides a graphical display of the raw dynamic modulus test data, the computed modulus and

**Table 39. Load levels for mixes used at different locations.**

Mixture	Construction Location	Longitude/Latitude	Pavement Temperature, °C, 98% Reliability	Load Level, lb
1 – GA Granite	Northwestern GA	34.03/ 84.62	60	190
2 – AR Gravel	Atlanta, TX	33.07/ 94.09	62	210
3 – WI Gravel	Janesville, WI	42.40/ 89.01	57	170
4 – MS Chert	Covington, MS	31.37/ 89.32	61	200
5 – KY Limestone	Southwestern KY	37.00/ 88.00	59	185
6 – OK Sandstone	Atlanta, TX	33.07/ 94.09	62	210
7 – PA Dolomite	North-central PA	40.73/ 77.96	55	155
8 – WY Gravel	Southwestern WY	41.86/ 105.40	55	155



Data Quality Indicators:	Project 9-29 L
RMS Cmd. Error, %:	78.7
Load Std. Error, %:	4.7
Disp. Avg. Std. Error, %:	4.5
Disp. Uniformity, %:	5.0
Phase Uniformity, Deg.:	0.6
Avg. Total Drift, %:	42.5

Figure 36. Dynamic modulus summary report for one of the specimens of Oklahoma sandstone.

phase angle, and the data quality statistics. The quality of the data from every test at each frequency was investigated, as presented in Figure 36, to ensure that the data were within the acceptable range. As shown for this specific specimen, the variability from measurements of the three LVDTs is well below the acceptable limit.

As mentioned before, every specimen was tested for dynamic modulus at three conditions: dry, short-term conditioned (partial saturation through 30-min vacuum application), and fully conditioned in ECS. Detailed results and basic statistical parameters from dynamic modulus measurements for both laboratories are presented in Appendix D. Tables 40 and 41 present the summary of dynamic modulus results obtained at PSU and

UTEP, respectively. The results are discussed further in the following sections.

### 3.4.3 Retained Dynamic Modulus

In general, a drop in modulus was observed for all specimens after full conditioning. Figure 37 shows this drop for different conditions for one of the mixes that was reported to perform poorly. A significant drop in modulus is observed for this mix after accelerated conditioning. The ratio of the modulus of a fully conditioned specimen to the modulus of that specimen in dry condition is presented in Figure 38 for two of the mixes, one reported to perform poorly and one reported

**Table 40. Summary of dynamic modulus results from PSU laboratory tests.**

Mix No. and Source	Freq. Hz	Modulus Before Conditioning <sup>(1)</sup> , MPa			Modulus After Static Saturation <sup>(2)</sup> , MPa			Modulus After Full Conditioning <sup>(3)</sup> , MPa			Moduli Ratio <sup>(4)</sup> After/Before Cond		
		Avg.	S.D.	C.V. <sup>(5)</sup>	Avg.	S.D.	C.V.	Avg.	S.D.	C.V.	Avg.	S.D.	C.V.
1 GA Granite	25	6032	340.9	5.7	5774	434.1	7.5	3611	259.2	7.2	0.60	0.06	10.1
	10	4965	351.4	7.1	4718	416.5	8.8	2756	288.9	10.5	0.56	0.07	12.8
	5	4192	312.0	7.4	3943	384.4	9.7	2123	248.0	11.7	0.51	0.07	14.3
	2	3232	261.1	8.1	3002	318.5	10.6	1463	181.8	12.4	0.46	0.07	14.8
	1	2597	216.5	8.3	2385	265.1	11.1	1080	135.6	12.5	0.42	0.06	15.1
2 AR Gravel	25	6465	441	6.8	6292	444.2	7.1	NA	NA	NA	NA	NA	NA
	10	5086	434	8.5	4929	433.8	8.8	NA	NA	NA	NA	NA	NA
	5	4084	408	10.0	3938	388.9	9.9	NA	NA	NA	NA	NA	NA
	2	2901	348	12.0	2764	305.3	11.0	NA	NA	NA	NA	NA	NA
	1	2135	279	13.0	2034	288.4	14.2	NA	NA	NA	NA	NA	NA
3 WI Gravel	25	4146	127.1	3.1	3828	116.4	3.0	3026	41.0	1.4	0.73	0.03	3.5
	10	3115	108.7	3.5	2847	86.4	3.0	2105	96.4	4.6	0.68	0.05	7.6
	5	2419	87.0	3.6	2181	67.9	3.1	1522	76.3	5.0	0.63	0.05	7.6
	2	1676	77.7	4.6	1491	61.2	4.1	954	47.6	5.0	0.57	0.05	8.3
	1	1233	62.0	5.0	1080	50.2	4.7	655	31.6	4.8	0.53	0.05	8.8
4 MS Chert	25	8125	175.4	2.2	7723	235.5	3.0	NA	NA	NA	NA	NA	NA
	10	6664	140.0	2.1	6313	181.1	2.9	NA	NA	NA	NA	NA	NA
	5	5615	108.6	1.9	5288	140.9	2.7	NA	NA	NA	NA	NA	NA
	2	4359	62.7	1.4	4065	129.7	3.2	NA	NA	NA	NA	NA	NA
	1	3439	38.5	1.1	3201	65.9	2.1	NA	NA	NA	NA	NA	NA
5 KY Limestone	25	NA	NA	NA	NA	NA	NA	NA	NA	NA	NA	NA	NA
	10	4725	200.2	4.2	4620	143.2	3.1	3527	138.4	3.9	0.75	0.0	2.3
	5	3833	188.0	4.9	3752	134.9	3.6	2749	118.6	4.3	0.72	0.0	2.8
	2	2799	159.6	5.7	2706	117.8	4.4	1858	100.8	5.4	0.66	0.0	3.4
	1	2075	126.8	6.1	1976	107.1	5.4	1330	80.2	6.0	0.64	0.0	4.6
6 OK Sandstone	25	NA	NA	NA	NA	NA	NA	NA	NA	NA	NA	NA	NA
	10	5555	253.7	4.6	5391	175.8	3.3	4711	246.9	5.2	0.84	0.01	1.3
	5	5033	464.7	9.2	4864	170.2	3.5	4000	246.0	6.1	0.82	0.02	2.1
	2	4103	536.7	13.1	3940	169.8	4.3	3083	239.3	7.8	0.79	0.03	3.5
	1	3324	417.9	12.6	3175	172.5	5.4	2469	213.2	8.6	0.78	0.03	3.8
7 PA Dolomite	25	NA	NA	NA	NA	NA	NA	NA	NA	NA	NA	NA	NA
	10	5373	307.8	5.7	5261	200.3	3.8	4210	168.4	4.0	0.79	0.05	6.2
	5	4588	402.3	8.8	4500	187.6	4.2	3379	139.7	4.1	0.77	0.05	5.9
	2	3517	473.0	13.4	3375	154.9	4.6	2363	109.1	4.6	0.72	0.04	6.1
	1	2647	335.5	12.7	2516	125.0	5.0	1734	87.1	5.0	0.70	0.05	7.4
8 WY Gravel	25	NA	NA	NA	NA	NA	NA	NA	NA	NA	NA	NA	NA
	10	5060	248.0	4.9	4447	220.8	5.0	3110	232.3	7.5	0.62	0.05	7.8
	5	4374	320.3	7.3	3839	196.5	5.1	2494	210.2	8.4	0.59	0.05	8.2
	2	3409	351.7	10.3	2952	151.7	5.1	1842	167.0	9.1	0.57	0.05	9.1
	1	2726	216.7	7.9	2387	76.7	3.2	1414	138.6	9.8	0.54	0.05	9.9

<sup>1</sup>Results for the dry unconditioned specimen.<sup>2</sup>Results for vacuum applied partial saturated specimen.<sup>3</sup>Results for long-term ECS-procedure specimen.<sup>4</sup>Ratio of modulus after full conditioning to modulus of unconditioned specimen.<sup>5</sup>Avg., S.D., and C.V. refer to Average, Standard Deviation, and Coefficient of Variation, respectively.

NA = not available.

to perform well. The mix that was reported to perform well has retained 85 percent of its original value at the 10-Hz frequency, while the mix reported to perform poorly has dropped to a retained value of 55 percent. The ratio also tends to be lower for the tests conducted at lower frequencies for both mixes even though the drop of modulus with decreasing frequency is more significant for the mix reported to perform poorly (see Figure 38).

The dynamic modulus values for dry specimens for both laboratories (PSU and UTEP) are presented in Figure 39 and the ratios of moduli are presented in Figure 40. The results follow the same trend. Arkansas gravel and Mississippi chert are missing from Figure 40 due to excessive deformation during conditioning. It appears that a ratio of 75 or 80 percent is the dividing line between mixes reported to perform poorly and mixes reported to perform well (except WI Gravel). Sim-



**Table 41. Summary of dynamic modulus results from UTEP laboratory tests.**

Mix and Source	Freq. Hz	Modulus Before Conditioning <sup>(1)</sup> , MPa			Modulus After Static Saturation <sup>(2)</sup> , MPa			Modulus After Full Conditioning <sup>(3)</sup> , MPa			Moduli Ratio <sup>(4)</sup> After/Before Cond		
		Avg.	S.D.	C.V. <sup>(5)</sup>	Avg.	S.D.	C.V.	Avg.	S.D.	C.V.	Avg.	S.D.	C.V.
		1	25	NA	NA	NA	NA	NA	NA	NA	NA	NA	NA
GA Granite	10	6056	708.5	11.7	6688	735.5	11.0	3478	833.3	24.0	0.57	0.1	25.6
	5	5118	666.9	13.0	5648	727.3	12.9	2972	710.8	23.9	0.57	0.1	25.9
	2	3794	560.9	14.8	4172	649.5	15.6	2244	627.7	28.0	0.58	0.2	32.2
	1	3122	521.2	16.7	3405	570.5	16.8	1882	589.0	31.3	0.58	0.2	30.8
2 AR Gravel	25	NA	NA	NA	NA	NA	NA	NA	NA	NA	NA	NA	NA
	10	6654	758.8	11.4	7366	1045.5	14.2	NA	NA	NA	NA	NA	NA
	5	5427	687.7	12.7	6138	947.4	15.4	NA	NA	NA	NA	NA	NA
	2	3867	541.4	14.0	4476	725.6	16.2	NA	NA	NA	NA	NA	NA
3 WI Gravel	25	NA	NA	NA	NA	NA	NA	NA	NA	NA	NA	NA	NA
	10	3905	446.8	11.4	4341	419.6	9.7	2329	344.6	14.8	0.59	0.1	19.1
	5	3188	430.3	13.5	3638	340.9	9.4	1780	256.2	14.4	0.56	0.1	19.5
	2	2247	350.1	15.6	2655	248.5	9.4	1213	185.4	15.3	0.55	0.1	19.8
4 MS Chert	25	NA	NA	NA	NA	NA	NA	NA	NA	NA	NA	NA	NA
	10	7626	1421.2	18.6	8888	1193.0	13.4	NA	NA	NA	NA	NA	NA
	5	6558	1109.5	16.9	7656	1093.6	14.3	NA	NA	NA	NA	NA	NA
	2	5264	889.1	16.9	6137	739.2	12.0	NA	NA	NA	NA	NA	NA
5 KY Limestone	25	NA	NA	NA	NA	NA	NA	NA	NA	NA	NA	NA	NA
	10	4783	153.3	3.2	5006	154.4	3.1	2971	145.0	4.9	0.62	0.0	4.9
	5	3944	146.6	3.7	4088	119.4	2.9	2381	167.5	7.0	0.60	0.0	7.0
	2	2781	119.5	4.3	2893	84.8	2.9	1608	106.5	6.6	0.58	0.0	7.0
6 OK Sandstone	25	NA	NA	NA	NA	NA	NA	NA	NA	NA	NA	NA	NA
	10	5270	228.2	4.3	5604	230.2	4.1	4316	244.4	5.7	0.82	0.0	3.9
	5	4530	252.4	5.6	4850	304.1	6.3	3672	229.1	6.2	0.81	0.0	2.3
	2	3368	203.4	6.0	3634	257.8	7.1	2764	185.3	6.7	0.82	0.0	2.1
7 PA Dolomite	25	NA	NA	NA	NA	NA	NA	NA	NA	NA	NA	NA	NA
	10	5164	244.4	4.7	5742	369.1	6.4	4759	248.7	5.2	0.92	0.0	3.6
	5	4205	230.4	5.5	4659	352.4	7.6	3836	258.7	6.7	0.91	0.0	2.9
	2	3135	170.1	5.4	2887	1261.7	43.7	2785	212.4	7.6	0.89	0.0	3.8
8 WY Gravel	25	NA	NA	NA	NA	NA	NA	NA	NA	NA	NA	NA	NA
	10	4722	140.3	3.0	5375	1081.4	20.1	3307	104.9	3.2	0.70	0.0	3.9
	5	4002	152.2	3.8	4272	237.7	5.6	2647	127.3	4.8	0.66	0.0	4.2
	2	3038	167.2	5.5	3255	171.0	5.3	1924	74.8	3.9	0.63	0.0	4.3
1	2418	127.6	5.3	2332	738.5	31.7	1435	78.8	5.5	0.59	0.0	5.2	

<sup>1</sup>Results for the dry unconditioned specimen.

<sup>2</sup>Results for vacuum applied partial saturated specimen.

<sup>3</sup>Results for long-term ECS-procedure specimen.

<sup>4</sup>Ratio of modulus after full conditioning to modulus of unconditioned specimen.

<sup>5</sup>Avg., S.D., and C.V. refer to Average, Standard Deviation, and Coefficient of Variation, respectively.

NA = not available.

ilar results are obtained if the results from both laboratories are combined (see Figure 41).

### 3.4.4 Behavior during Conditioning

The 18-h load/water conditioning of the specimen starts at the same time the target temperature of the chamber is set at 60°C. Therefore, at early stages, water permeating through

the specimen is not yet at the 60°C equilibrium temperature. As a result of a lower temperature for the initial cycles, the material exhibits a stiffer response. As time progresses and the specimen temperature rises, higher strain is achieved for each cycle of load. At a higher number of cycles, once the temperature is established at 60°C, the specimen demonstrates strain hardening, as shown from the hysteresis loops in Figure 42.

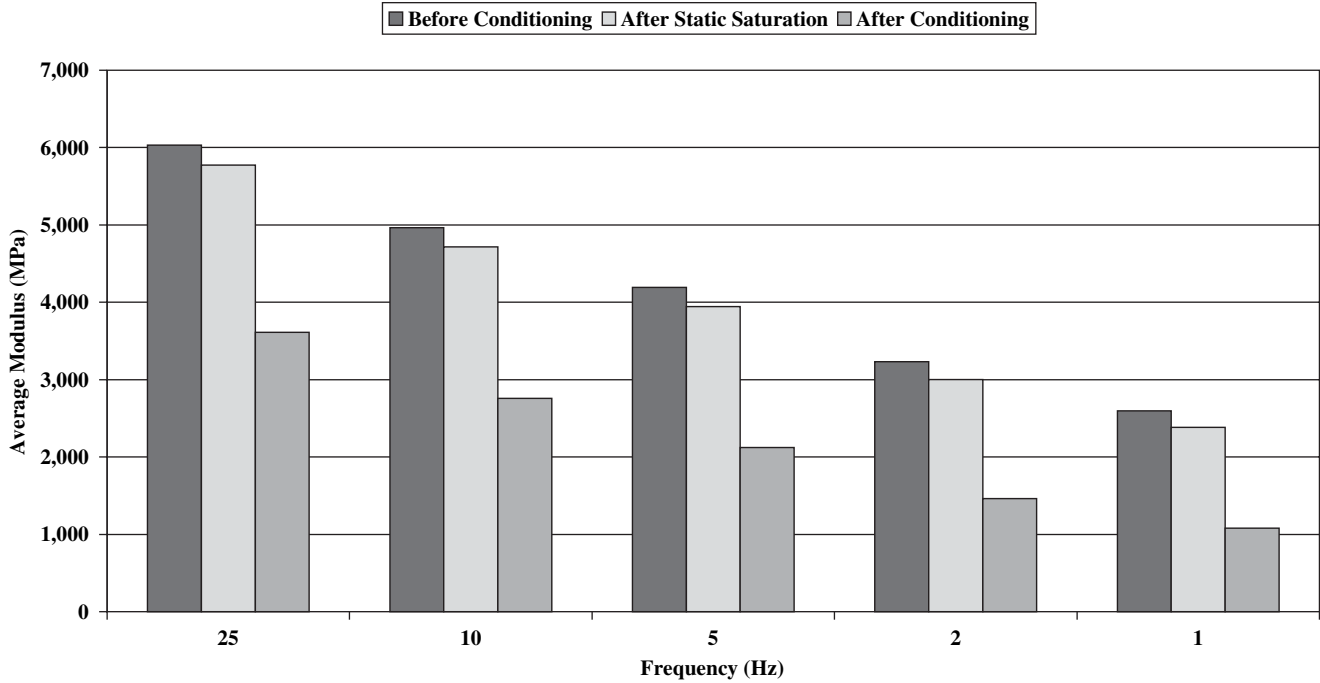


Figure 37. Dynamic modulus for a poorly performing mix at different conditioning levels.

The calculated strain used to present the results in Figure 42 is the average value from three LVDTs mounted on the specimen. Typical responses from individual LVDTs are presented in Figure 43.

Permanent deformation is induced in the specimen during the 18 h that water and load conditioning is imposed on the specimen. This duration of conditioning results in 64,800 cycles of loading. Two of the mixes (Arkansas gravel and Mississippi chert) exhibited excessive deformation during conditioning and could not be conditioned for the complete 18 h. The remaining six mixtures demonstrated permanent deformation in the range of about 0.2 percent (Oklahoma sandstone and Pennsylvania dolomite) to about 1.5 percent (Georgia granite). Figure 44 exhibits permanent deformation as a function of cycles for one of the specimens of Wisconsin gravel. The change in the temperature of the specimen is also presented in this graph as time progresses. From this figure,

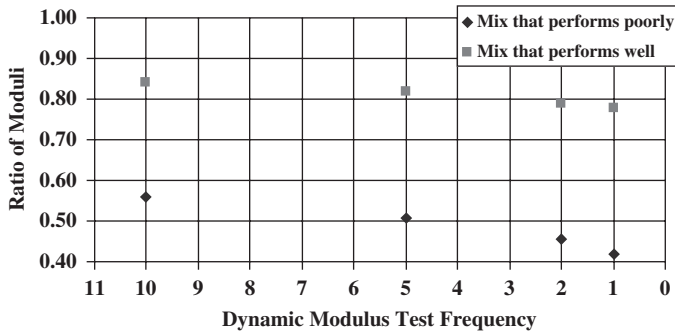


Figure 38. The ratio of moduli at different frequencies.

it appears that after 20,000 cycles there is a slight decrease in permanent deformation (a reduction of approximately 22 microns, equivalent to 0.03 percent). This reduction exists because the repeated loading starts at the same time the temperature setting is changed from 25°C to 60°C. It takes time for the temperature to reach the equilibrium temperature, as shown in Figure 44, resulting in thermal expansion of the specimen and affecting permanent deformation. Furthermore, the deformation measuring transducers (LVDTs) also

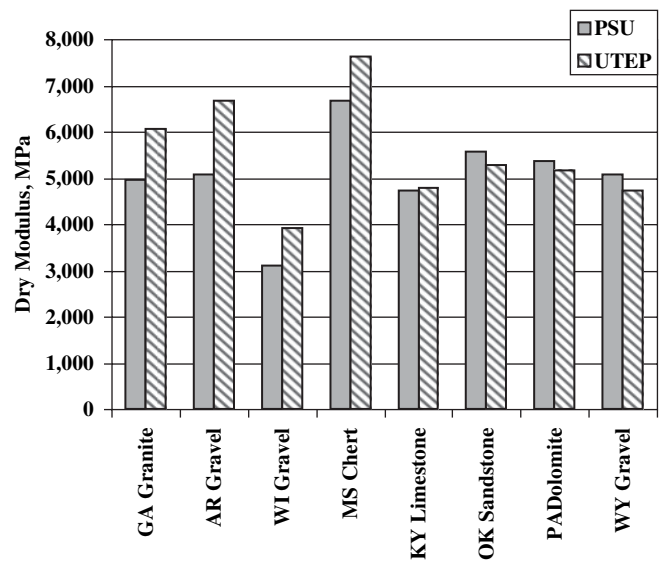
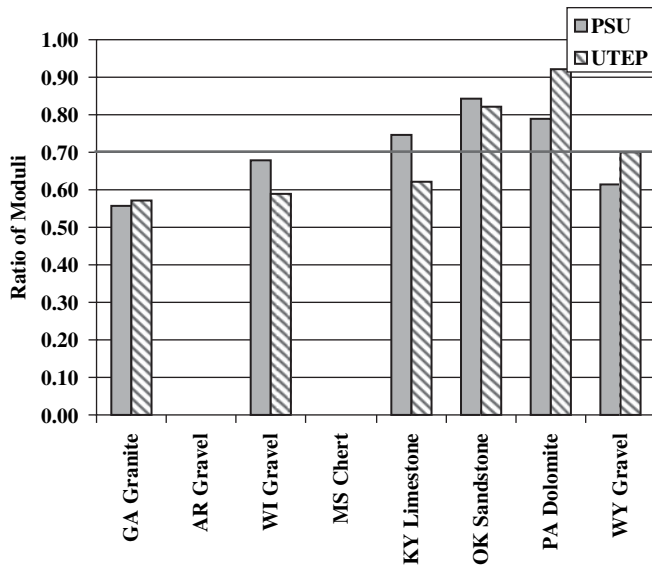
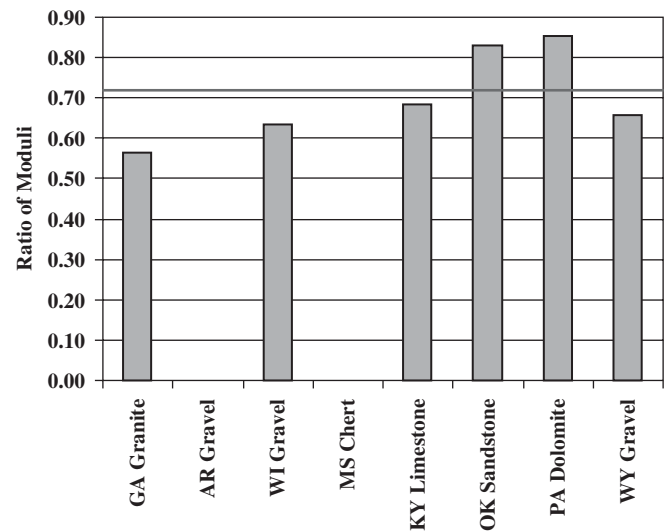


Figure 39. Moduli of dry tested specimens for different mixes.



**Figure 40.** Ratio of modulus after accelerated conditioning to modulus before conditioning for different mixes.



**Figure 41.** Ratio of modulus after accelerated conditioning to modulus before conditioning for different mixes (average from both laboratories).

experience this cycle of temperature change, slightly affecting the measurements. However, these effects are relatively minor compared to the total permanent deformation.

In general, the mixtures susceptible to moisture damage indicated a higher level of permanent deformation than those resistant to moisture damage. The specimens shown in Figure 45, from left to right, are Arkansas gravel (report to perform poorly) and Oklahoma sandstone (reported to perform

well). The excessive deformation in Arkansas gravel is obvious in this figure.

### 3.4.5 Visual Investigation of Moisture Damage for Conditioned Specimens

After completion of ECS/dynamic modulus tests, all of the specimens were split and visually investigated for signs of

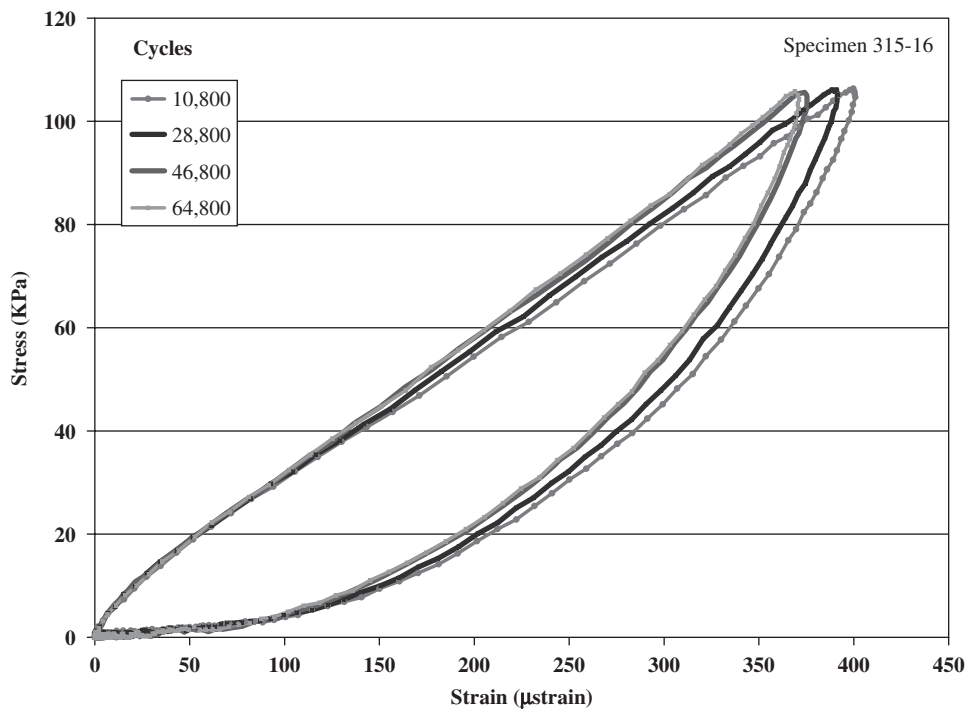


**Figure 42.** Stress-strain hysteresis loops at different cycles during load/water conditioning (stress-controlled test).

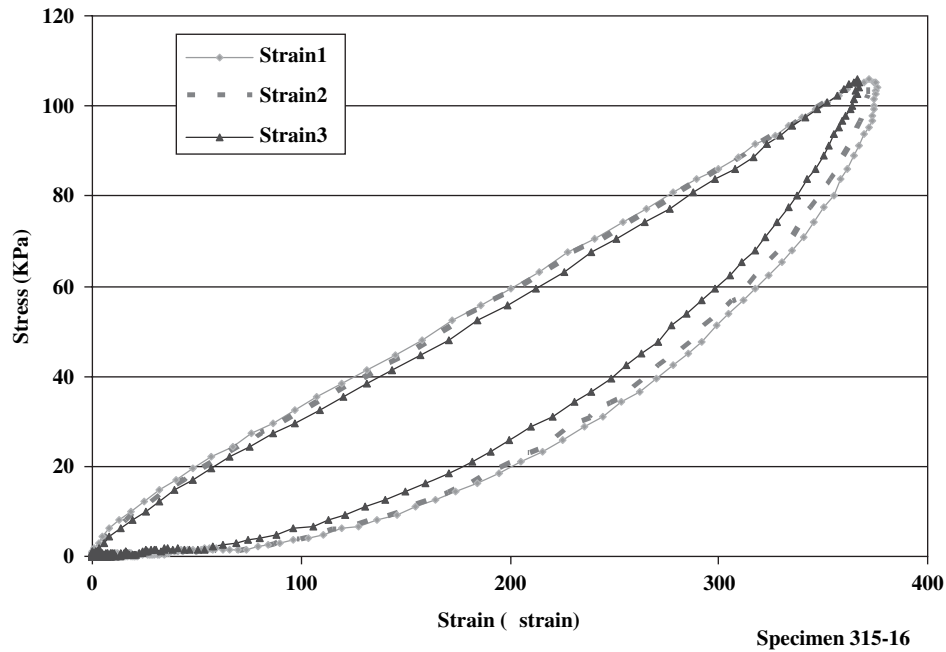


**Figure 43.** Stress-strain hysteresis loops from different transducers at the same cycle of loading during water/load conditioning (stress-controlled test).

moisture damage and stripping. Unfortunately, the specimens were not split immediately after completion of dynamic modulus tests. In some cases, several months had passed before the specimens were broken. It is not clear if any “re-wetting” or re-bonding might have occurred because of this time lag. Pictures of split specimens are provided in Appendix E. Table 42 summarizes the results of the visual inspections of the ECS/dynamic modulus tested specimens.

### 3.5 Statistical Analysis of Dynamic Modulus Test Results

#### 3.5.1 Important Considerations

The main response variable in the statistical analyses presented here is the ratio of the modulus after conditioning to the modulus before conditioning. There are several points to

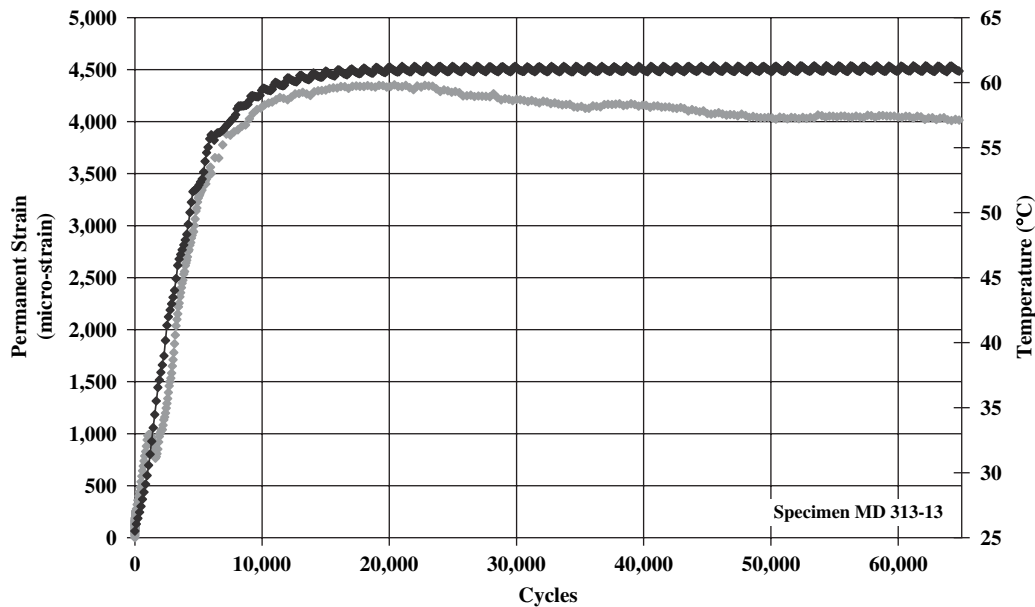


**Figure 44.** Accumulation of permanent deformation during conditioning.

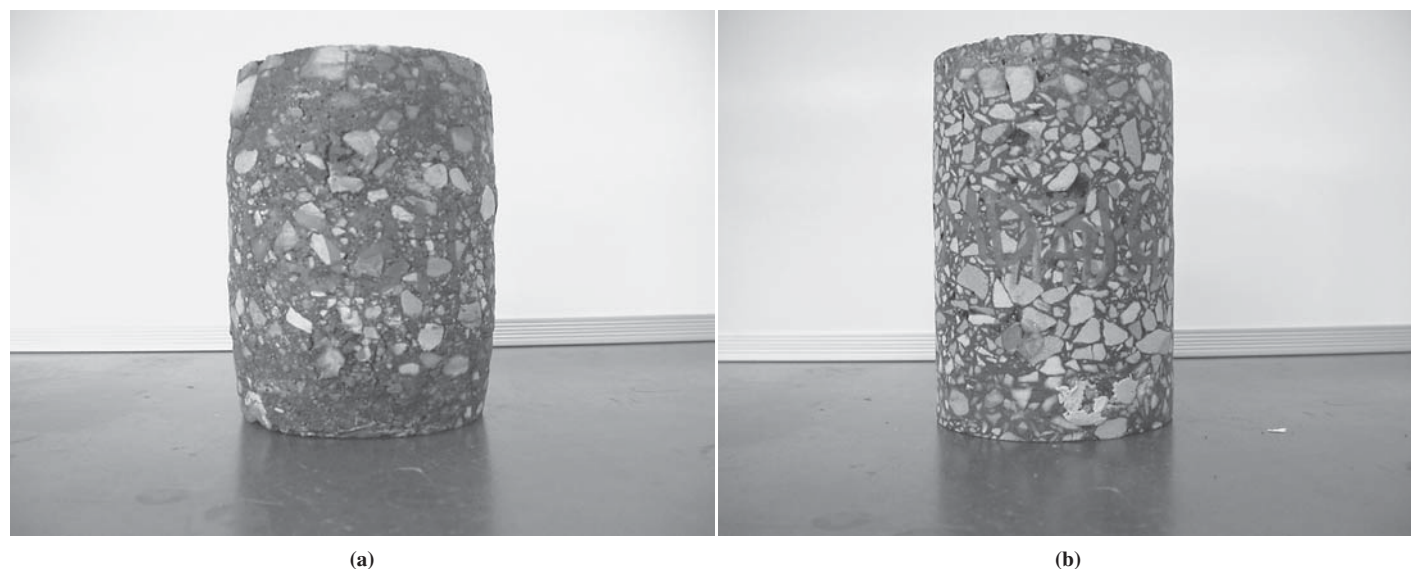


**Figure 45.** Specimens from a mix reported to perform poorly (a) and a mix reported to perform well (b) after accelerated conditioning.

be considered when interpreting the results for the analyses presented, as discussed below.

For each mix, there were a total of six replicate specimens tested at each laboratory (i.e., a total of 12 replicate specimens). However, for some of the mixes, not all six replicate specimens from each laboratory were included in calculation of the statistical parameters such as averages and standard deviations. Several factors contributed to the reduction of replicates used in analyses. For example, there were conditioning problems with a few of the specimens, and, for a few others, the modulus values were found to be simply outliers. Details of which specimens were excluded are provided as footnotes to the tables presenting results in Appendix D. In no case, however, were fewer than four specimens included from each laboratory.

Another point of consideration is the number of mixes used in the statistical analyses. Two of the moisture-susceptible mixes (Arkansas gravel and Mississippi chert), based on reported field performance, exhibited excessive deformation during conditioning in the laboratory and, therefore, could not be tested for dynamic modulus after conditioning. Since

testing could not be completed for these two mixes, they were not included in the statistical analysis. Furthermore, it was suspected that for one of the mixes (Wisconsin gravel), a proper conditioning load was not selected, and, therefore, the specimens of this mix were excessively damaged during conditioning. Testing on this mix resulted in a significantly lower ratio than expected. This low ratio of moduli could be due to excessive conditioning load rather than the moisture damage susceptibility of the mix. As a result, this mix was also excluded from analysis. Therefore, the following analysis was mainly limited to five of the mixes, three reported to perform poorly in the field and two reported to perform well in the field.

It is expected that if this procedure (after modifications) is adopted for routine testing, only one testing frequency will be used (even though, in this research, tests were conducted at multiple loading frequencies). It appears that if only one testing frequency is to be used, 10 Hz is commonly selected. For this reason, the statistical analyses presented in the following section are for 10-Hz loading frequency only.

### 3.5.2 Laboratory Effect

The statistical model that will allow for the best evaluation of any differences in the testing in the two different laboratories (the lab effect) is given as

$$\text{Ratio of Moduli} = \text{Place of Testing} + \text{Mix} + \text{Error} \quad (14)$$

With this model, place of testing will have two values (PSU and UTEP) and mix will have five values (five different mixes: Georgia granite, Wisconsin gravel, etc.). Details of analysis for this linear model are presented in Appendix F. The summary of results is shown in Table 43.

**Table 42.** Assessment of visual evaluation of stripping.

Mixture	Level of Stripping
Georgia Granite	Slight to Moderate
Arkansas Gravel	Moderate
Wisconsin Gravel	Slight
Mississippi Chert	Moderate
Kentucky Limestone	Slight
Oklahoma Sandstone	Almost none
Pennsylvania Dolomite	Almost none
Wyoming Gravel	Moderate

**Table 43. Analysis of variance for moduli ratios.**

Source	Degrees of Freedom	Mean Sum of Squares	F-Ratio	P-Value
Place of Test	1	0.00451	0.87	0.36
Mix Type	4	0.17010	32.71	<0.0001
Error	49	0.00520		

There was no reason to believe that the testing in the two places would produce any important differences in the results, and the statistical analysis (P-Value for a difference due to Place of Testing = 0.36) gives us the assurance that this is the case. The specimens were all prepared in the AAT laboratory, and a random selection from each mix was sent to PSU and UTEP, thus ensuring that the specimen preparation was not a part of any laboratory effect. Of course, the mix effect is quite large ( $F = 32.71$ ) and highly significant. This is as it should be because these mixes were quite different, ranging from poor to good in reported moisture damage susceptibility.

### 3.5.3 Statistical Comparison of Mean Modulus Before and After Conditioning

The modulus measurements were conducted on the same specimen before and after conditioning. Therefore, for each mix, comparison of the mean modulus before conditioning to the mean modulus after conditioning yields itself well to a paired t-test. The data can be considered paired because each modulus measurement before conditioning can be naturally paired with one modulus measurement after conditioning. The null and alternative hypotheses to be tested are as follows:

$$H_0: \mu_{\text{before}} = \mu_{\text{after}}$$

$$H_0: \mu_{\text{before}} > \mu_{\text{after}}$$

Where  $\mu_{\text{before}}$  and  $\mu_{\text{after}}$  refer to the true mean of the modulus before conditioning and the true mean of the modulus after conditioning, respectively, for the mix under consideration. The paired sample t-test is used to test for the differences of these two means. The difference between paired measurements ( $d$ ) is calculated as

$$d_i = x_i - y_i \quad (i = 1, \dots, N) \quad (15)$$

where  $x_i$  and  $y_i$  refer to paired measurements for specimen  $i$  before and after conditioning, respectively, and  $N$  presents the number of replicate measurements. The mean and standard deviation of the differences ( $\bar{d}$  and  $S_d$ , respectively) are then calculated as

$$\bar{d} = \frac{1}{N} \sum_{i=1}^N d_i \quad (16)$$

$$\text{and } S_d = \sqrt{\frac{1}{N-1} \sum_{i=1}^N (d_i - \bar{d})^2} \quad (17)$$

The test statistic  $t$  is determined as

$$t = \frac{\bar{d}}{S_d / \sqrt{N}} \quad (18)$$

Since earlier analysis indicated that there was no significant difference between the results from the two laboratories (analysis of lab effect), the data from the laboratories were pooled together. Results are presented in Table 44, indicating that in all cases, there is a significant difference between the modulus before and after conditioning.

### 3.5.4 Components of Variance for the Ratio

In this section, the results of a components of variance (CV) analysis will be considered. From such analysis, it will be possible to provide an answer to this question: "If a measured value of the ratio is 0.70, then what is the probability that the mix will be a 'good' mix?"

It is assumed that the true value for the ratio of moduli (after conditioning to before conditioning) for the class of "good" mixes is from a normal distribution with the mean of  $\mu_{\text{GOOD}}$  and a standard deviation of  $\sigma_{\text{GOOD}}$ . Likewise the true value for the ratio of moduli for the "poor" mixes will have a mean of  $\mu_{\text{poor}}$  and a standard deviation of  $\sigma_{\text{poor}}$ . It is also assumed that the measured ratio values for a given "good" mix are from a normal distribution with the mean  $\mu_{\text{GOOD}}$  and a standard deviation of  $S_{g\text{-measured}}$  and likewise for the "poor" mixes with the standard deviation of the measured ratios as  $S_{p\text{-measured}}$ . CV analysis is used to develop estimates for all of the preceding quantities. The statistical model that is assumed for the data from the "good" mixes is

$$\rho(I, J) = \mu_{\text{GOOD}} + \text{MIX}(I) + \text{ERROR}(I, J) \quad (19)$$

where

$\mu_{\text{GOOD}}$  = the true mean for the ratio for good mixes,

$\text{MIX}(I)$  = the effect of the  $I$ th good mix,

$\text{ERROR}(I, J)$  = the error in the measured ratio for the  $J$ th specimen of the  $I$ th mix, and

$\rho(I, J)$  = ratio of moduli for  $J$ th specimen of the  $I$ th mix.

A similar model will be used for the "poor" mixes.

With this structure, it is assumed that the data are for a random selection of "good" mixes and a random selection of "poor" mixes. Furthermore, it is assumed that for the set of such "good" mixes, the component  $\text{MIX}(I)$  will be a normal random variable with a mean of 0 and variance of  $\text{Var}(\text{Good Mixes})$  and that  $\text{ERROR}(I, J)$  will be a normal random variable with a mean of 0 and variance of  $\text{Var}(\text{Err}|\text{Good Mixes})$ . Both of these components are useful in planning future studies or future operations of the testing process, as well as in the analyses in the following section. The same assumptions

**Table 44. Results from statistical comparison of modulus before and after conditioning.**

Mixture	Average Modulus before Condition. MPa	Average Modulus after Condition. MPa	t-Statistic	Critical t-Statistic at $\alpha = 0.05$ level		Conclusion
				One-tailed	Two-tailed	
GA Granite	5,549	3,117	9.53	1.83	2.26	Conditioned modulus different from unconditioned modulus
AR Gravel	85.5	NA	NA	NA	NA	NA
WI Gravel	3,515	2,206	8.06	1.81	2.23	Conditioned modulus different from unconditioned modulus
MS Chert	73.4	NA	NA	NA	NA	NA
KY Limestone	4,759	3,193	14.25	1.83	2.26	Conditioned modulus different from unconditioned modulus
OK Sandstone with Lime	5,419	4,495	22.32	1.81	2.23	Conditioned modulus different from unconditioned modulus
PA Dolomite	5,243	4,509	5.53	1.81	2.23	Conditioned modulus different from unconditioned modulus
WY Gravel	4,876	3,208	17.02	1.80	2.20	Conditioned modulus different from unconditioned modulus

regarding the model will define the  $Var(Poor\ Mixes)$  and the  $Var(Err|Poor\ Mixes)$ .

With this model and the present data, the results of the Proc Nested (a SAS procedure) are provided in Appendix F. A summary of the results is given in Table 45.

These results will be useful in several settings. The CV percentage ( $Err|Good\ Mixes$ ) of 6.9 percent is a good estimate since the  $Var(Err|Good\ Mixes)$  had 21 degrees of freedom, and the CV percentage ( $Err|Poor\ Mixes$ ) of 12.7 percent is a very good estimate since the  $Var(Err|Poor\ Mixes)$  had 29 degrees of freedom. These values could be useful in the future as a base for selecting the number of specimens to be tested in the evaluation of a given mix. The CV percentages in Table 45 are reported for a single specimen (individual observation) to indicate the noise level associated with a single measurement. For decision mak-

ing, more than one specimen is tested, and, in this case, the CV percentage for the average of the specimens will vary as one over the square root of the number of specimens. For example, if four specimens are tested, the CV percentage for their average for good specimens would be 3.45 percent and the CV percentage for their average for poor specimens would be 6.1 percent.

The CV percentages for the mixes, both good and poor, appear to be reasonable, but caution should be exercised because the values are based only on samples of two mixes reported to perform well and three mixes reported to perform poorly.

### 3.5.5 Comparison of the Mixes Reported to Perform Well and the Mixes Reported to Perform Poorly

Using the results from the general linear model analysis, a statistical test was conducted to determine whether the modulus ratios for the mixes reported to perform well and the mixes reported to perform poorly were statistically different. The null and alternative hypotheses were

$$H_0: X_{\text{good}} = X_{\text{poor}}$$

$$H_1: X_{\text{good}} \neq X_{\text{poor}}$$

where  $X_{\text{good}}$  and  $X_{\text{poor}}$  present the mean ratio of moduli for the mixes reported to perform well and the mixes reported to perform poorly (reported field performance), respectively. Because of a large value for degrees of freedom (49, as given in Appendix F), the Z test was selected.

**Table 45. Results of a CV analysis for the ratio of moduli.**

Results for "Good" Mixes		Results for "Poor" Mixes	
Var(Good Mixes)	0.00035	Var(Poor Mixes)	0.00262
Std(Good Mixes) <sup>1</sup>	0.019	Std(Poor Mixes)	0.052
Var(Err Good Mixes)	0.0034	Var(Err Poor Mixes)	0.0065
Std(Err Good Mixes)	0.058	Std(Err Poor Mixes)	0.081
CV%(Good Mixes)	2.24%	CV%(Poor Mixes)	8.06%
CV%(Err Good Mixes)	6.9%	CV%(Err Poor Mixes)	12.7%
E(Ratio Good Mixes) <sup>2</sup>	0.848	E(Ratio Poor Mixes) <sup>3</sup>	0.635

<sup>1</sup>Std = standard deviation.

<sup>2</sup>E(Ratio|Good Mixes) = mean ratio of moduli for good mixes.

<sup>3</sup>E(Ratio|Poor Mixes) = mean ratio moduli for poor mixes.

**Table 46. Statistical comparison of mixes reported to perform well and mixes reported to perform poorly.**

Reported Mix Performance	Mean Ratio of Moduli	Standard Deviation (Error) of the Mean	Pooled Standard Deviation of the Mean	z	Pr ( Z <= z )
Good	0.85	0.018	0.038	5.59	< 0.001
Poor	0.64	0.033			

$$Z = \frac{X_{\text{good}} - X_{\text{poor}}}{S_p} \quad (20)$$

The pooled standard error ( $S_p$ ) or, standard deviation of the mean, was calculated as

$$S_p = \sqrt{S_{n1}^2 + S_{n2}^2} \quad (21)$$

where  $S_{n1}$  and  $S_{n2}$  present the estimates of the standard deviations of the means for the good and poor mixes, respectively. The results are shown in Table 46, clearly indicating a significant difference between the mixes reported to perform well and the mixes reported to perform poorly.

To assess the variability of the results, statistical 95-percent confidence intervals were established for ratios of moduli for each mix. The ratios of moduli for pooled data from both laboratories are presented in Figure 46. The error bars indicate the 95-percent confidence intervals for the ratio of moduli for the pooled data. Arkansas gravel and Mississippi chert are absent from this graph because their failure and excessive deformation during conditioning made it impossible to establish a ratio. In a way, it could be argued that the ratio of moduli for these two failing mixes is close to zero (both were reported to have poor field performance) because the failed specimen during conditioning would yield an extremely low dynamic modulus after conditioning. It can be seen that the lower limit for the true mean of the ratio for the Pennsylvania dolomite and Oklahoma sandstone mixes exceeds 0.80.

These two mixes were reported to have good field performance. The upper limit for the three mixes reported to perform poorly is less than 0.72. The poor ECS/dynamic modulus performance of Wisconsin gravel, reported to perform well, is probably caused by the presence of a soft PG 58-28 binder.

### 3.5.6 Impact of Saturation Level

It was explained in Chapter 2 that short-term water conditioning of the specimens was accomplished through application of a vacuum to the specimen for 30 min at 25°C. There are two options available to induce partial saturation to the specimen. One is controlling the degree of saturation through a vacuum, as is used in AASHTO T283 or ASTM D4867. The second approach is controlling the time duration of the vacuum application. This second approach was used in this research because it was included in the original EDS system as well as in the Texas modified version of the ECS.

It can be observed that the degree of saturation varies among mixes and within the replicate specimens of the same mix (see Tables 47 and 48). The variability in saturation level for specimens conditioned at UTEP is lower than that at PSU. For both laboratories, statistical one-way analysis of variance indicates that not all mixes have similar saturation levels (see Tables 49 and 50).

Figures 47 and 48 indicate the saturation level for different mixes. The error bars shown are 95-percent confidence inter-

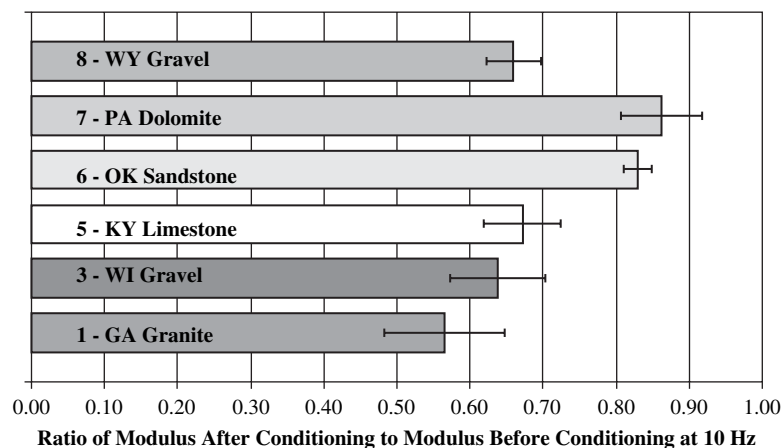


**Figure 46. Ratios of moduli for different mixes along with 95-percent confidence intervals.**



**Table 47. Degree of saturation for different mixes tested at PSU.**

Specimen #	GA Gravel	AR Gravel	WI Gravel	MS Chert	KY Limestone	OK Sandstone	PA Dolomite	WY Gravel
1	77	76	80	79	79	57	63	85
2	79	81	83	80	81	60	71	91
3	77	82	75	77	77	67	80	89
4	85	82	81	76	81	67	76	78
5	74	71	80	90	84	67	80	84
6	75	73	74	78	83	64	74	76
<b>Average</b>	<b>78</b>	<b>78</b>	<b>79</b>	<b>80</b>	<b>81</b>	<b>64</b>	<b>74</b>	<b>84</b>
<b>Std. Dev.</b>	<b>3.9</b>	<b>4.8</b>	<b>3.5</b>	<b>5.1</b>	<b>2.6</b>	<b>4.3</b>	<b>6.4</b>	<b>5.9</b>

**Table 48. Degree of saturation for different mixes tested at UTEP.**

Specimen #	GA Gravel	AR Gravel	WI Gravel	MS Chert	KY Limestone	OK Sandstone	PA Dolomite	WY Gravel
1	72	73	74	68	74	70	75	79
2	74	80	74	72	76	71	71	78
3	71	77	73	72	73	71	70	74
4	72	73	73	68	72	73	77	76
5	73	72	74	71	73	75	73	72
6	72	75	73	69	72	72	77	73
<b>Average</b>	<b>72</b>	<b>75</b>	<b>74</b>	<b>70</b>	<b>73</b>	<b>72</b>	<b>74</b>	<b>75</b>
<b>Std. Dev.</b>	<b>1.0</b>	<b>3.0</b>	<b>0.5</b>	<b>1.9</b>	<b>1.5</b>	<b>1.8</b>	<b>3.0</b>	<b>2.8</b>

**Table 49. One-way analysis of variance for degree of saturation for ECS/dynamic modulus specimens (PSU).**

Source	Degrees of Freedom	Sum of Squares	Mean Square	F Statistic	P-value	Critical F at 95% Significant Level
Mixture	7	1566	223.7	10.030	3.62E-07	2.249
Within Groups	40	892.1	22.3			
<b>Total</b>	<b>47</b>	<b>2458</b>				

**Table 50. One-way analysis of variance for degree of saturation for ECS/dynamic modulus specimens (UTEP).**

Source	Degrees of Freedom	Sum of Squares	Mean Square	F Statistic	P-value	Critical F at 95% Significant Level
Mixture	7	124.3	17.8	3.8965787	0.0025	2.249
Within Groups	40	182.3	4.6			
<b>Total</b>	<b>47</b>					

vals for each mixture. It is obvious from Figure 47 that the Oklahoma sandstone mix and the Wyoming gravel mix have significantly different saturation levels compared to other mixes tested at PSU. In Figure 48, these two mixes also exhibit the lowest saturation level and the highest saturation level, respectively, among the mixes tested at UTEP, even though the difference is not as large as the difference observed at PSU.

Scatter plots in Figures 49 and 50 exhibit the relationship between the saturation level and the observed ratio of moduli. It can be seen that no particular trend could be established for such a relationship. The results for individual mixes also

verify this conclusion. Figure 51, for example, shows the Wyoming gravel mix exhibiting no particular trend.

### 3.5.7 A Bayesian Analysis for the 10-Hz Ratio of After/Before Modulus

The analysis presented in this section was conducted to provide a better explanation of the test results than a simple fail or pass response for the tested mixtures. The retained modulus after conditioning, indicated by a value between 0 and 100 percent, can be the basis for determining the probability that

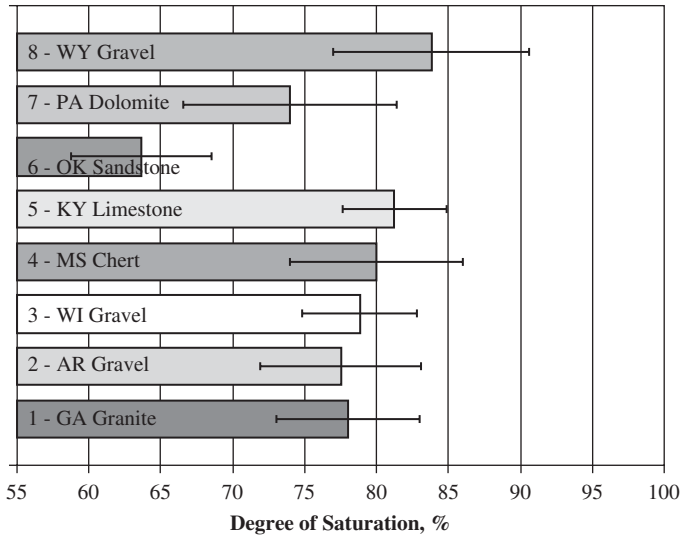


**Figure 47. Degree of saturation after vacuum application for various mixes along with 95-percent confidence intervals (PSU specimens).**

a specific mix will be among the class of mixes that performs well or among the class of mixes that performs poorly. The Bayesian structure, taking advantage of the results presented in the CV analysis above, allows one to do this in the most effective manner.

The present set of mixes reported to perform well is regarded as a sample of such mixes from the population of good mixes. For the case of n measurements of the ratio (i.e., using n specimens), an average value,  $\bar{x}_g$ , could be determined. Considering the variability in the population of good mixes

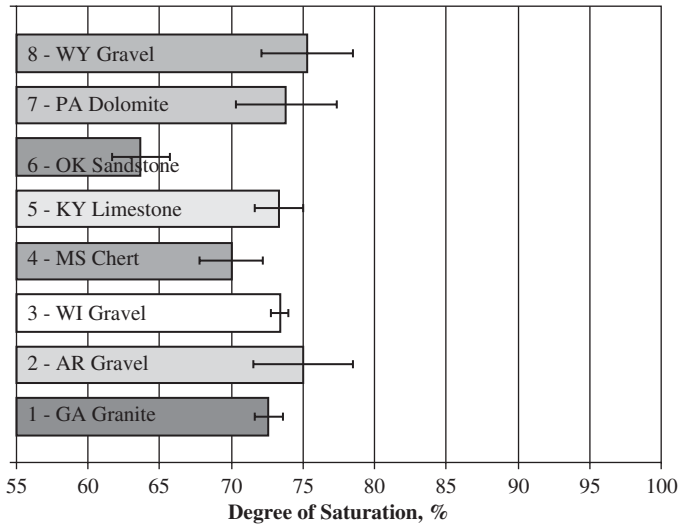


**Figure 48. Degree of saturation after vacuum application for various mixes along with 95-percent confidence intervals (UTEP specimens).**

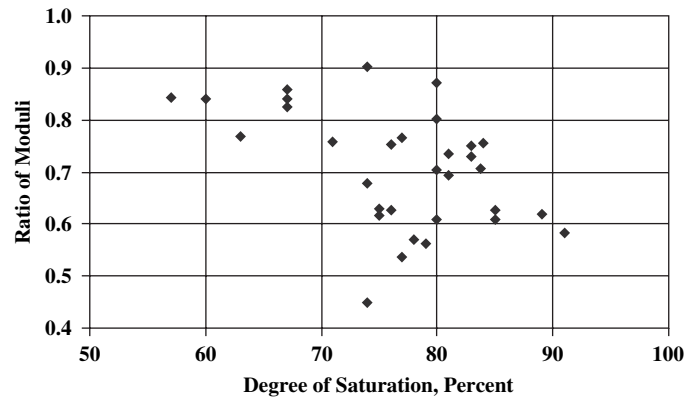


**Figure 49. Scatter plot of ratio of moduli versus saturation level for ECS/dynamic modulus specimens (PSU).**

and the variability in the measured ratios, the variance of such an average would be presented as

$$Var(\bar{x}_g) = Var(Mix|Good) + Var(Err|Good)/n \quad (22)$$

If the values from the CV analysis for four such measurements are used, the result would be

$$Var(\bar{x}_g) = 0.000349 + 0.00339/4 = 0.0011965 \text{ and } STD(\bar{x}_g) = 0.03459$$

Similarly, from the CV for the poor mixes, the variance of the average of four ratio measurements from a random member of such mixes could be determined as

$$Var(\bar{x}_p) = 0.002622 + 0.006487/4 = 0.0042437 \text{ and } STD(\bar{x}_p) = 0.06514$$

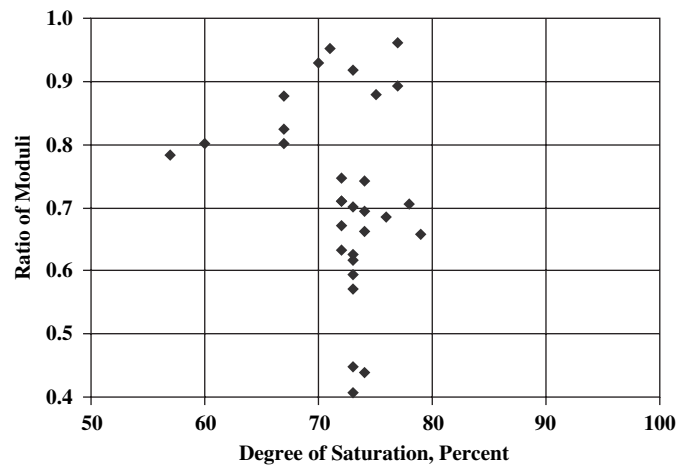


**Figure 50. Scatter plot of ratio of moduli versus saturation level for ECS/dynamic modulus specimens (UTEP).**

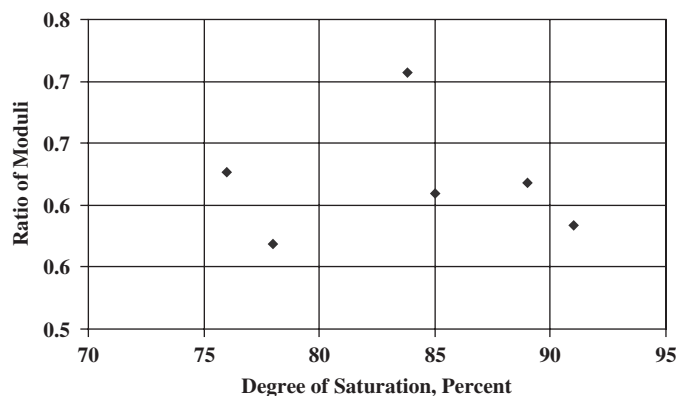


**Figure 51. Scatter plot of ratio of moduli versus saturation level for ECS/dynamic modulus specimens (Wyoming gravel tested at PSU).**

Earlier analysis, as suggested by the CV, has provided expected values for  $\bar{x}_g$  and  $\bar{x}_p$  as 0.8478 and 0.6351, respectively. Now, it is assumed that the probability ( $P$ ) or frequency with which good mixtures ( $G$ ) arrive in the laboratory for testing is presented as  $P(G)$ . Using the normal density function,  $ND(X, \mu, \sigma)$ , with mean  $\mu$  and standard deviation  $\sigma$ , it follows from Bayes' Rule that using the average of  $n$  measured ratios for a mix, say  $X$ , the probability that the mixture being tested is from the set of good mixtures is  $Pr(Good|X)$  where

$$Pr(Good|X) = \frac{P(G) \times ND(X, \bar{x}_g, STD(\bar{x}_g))}{P(G) \times ND(X, \bar{x}_g, STD(\bar{x}_g)) + (1 - P(G)) \times ND(X, \bar{x}_p, STD(\bar{x}_p))} \quad (23)$$

The importance and utility of this formula should be well known. Using expected values of  $\bar{x}_g$  and  $\bar{x}_p$  (0.8478 and 0.6351, respectively), the standard deviations of  $\bar{x}_g$  and  $\bar{x}_p$  (0.0346 and 0.0651, respectively), an assumed  $P(G)$  of 0.5, and an average ratio of 0.8 for four specimens of a given mixture, the probability that the mix in question is good will be given by Equation 23.

$$Pr(Good|X = .80) = \frac{.5 \times ND(.80, .8478, .0346)}{.5 \times ND(.80, .8478, .0346) + .5 \times ND(.80, .6351, .0651)} = .93$$

This mix would be declared to be among the good mixes. Such a result is not at all surprising if it is true that the mean ratio for the good mixes is 0.8478 and the mean ratio for the poor mixes is 0.635.

For an average ratio of 0.75 for four specimens, the calculated probability for the mix to be among good ones would be 0.22 (i.e.,  $Pr(Good|X = 0.75) = 0.22$ ) and for the mix to be among the poor ones the probability is 0.78 ( $Pr(Poor|X = 0.75) = 0.78$ ).

As another example, if the average ratio for four specimens is found to be 0.77, then  $Pr(Good|X = 0.77) = 0.61$  and  $Pr(Poor|X = 0.77) = 0.39$ . In this case, we might be inclined to believe this mix will be among the moisture-resistant mixes, but it is quite uncertain.

Using an average of 0.70 rather than 0.77 results in  $Pr(Good|X = .70) = 0.001$ , which would surely allow us to declare that this mixture belongs to the poor group.

The preceding calculations by means of the Bayes Theorem include all of the information that can be obtained in regard to the laboratory and the mix to be tested. Examples of such information include the following:

- The frequency (prior probability) with which mixes tested in a specific laboratory are, in fact, moisture-resistant mixes (mixes that perform well);
- The variation in the true ratio values for the mixes from the population of good mixes, and likewise for the poor mixes, that is, the  $STD(Mix|Good)$  and  $STD(Mix|Poor)$ ; and
- The test variation for good and poor mixes, that is, the standard deviation of the testing measurements and the number of specimens tested.

To the extent that correct values are entered, the resulting Bayesian Probability provides an excellent manner to present the results. If good data collection and follow-up of performance are practiced, then this method of testing and evaluation will be an excellent test procedure.

Since typically most of the mixes tested in a specific laboratory are, in fact, good, a value higher than 0.5 should be applied for  $P(G)$ . For example, if 80 percent of the mixes tested in the past have been found to be good mixes, then  $P(G)$  should be 0.8 in the formula above, and, in this case, the result would be  $Pr(Good|X = 0.75) = 0.53$ , which may be compared to the 0.22 resulting from  $P(G) = 0.5$  for probability of good mixes. The probability result of 0.53 makes it uncertain whether the mix can be considered to be truly from the group of good mixes.

A brief table constructed from the above results will help provide insight into the impact of  $P(G)$  on the outcome (i.e., the probability of the mix belonging to the good or the poor group). (See Table 51.) It is assumed that the average ratio measurement is for four samples. The data from the project are used as the averages and variances for analyses and are noted in Table 51 for convenience.

### 3.5.8 Summary of Results from the Statistical Analyses

The statistical analyses of the data from this experiment make it clear that the test is quite sensitive to the moisture

**Table 51. Probability of a mix belonging to the good or the poor group based on the Bayes method.**

$P(G)$	$\bar{x}_g$	$\bar{x}_p$	Average Ratio from Lab Measurements	$Pr(Good)$	$Pr(Poor)$
0.5	0.8478	0.6353	0.70	0.001	0.999
0.5	0.8478	0.6353	0.75	0.22	0.78
0.5	0.8478	0.6353	0.77	0.61	0.39
0.5	0.8478	0.6353	0.80	0.93	0.07
0.8	0.8478	0.6353	0.75	0.53	0.47

susceptibility of an asphalt mix. It is desirable that the test will result in a measured value for deciding moisture susceptibility. From this measured value, a decision in the form of a “yes” or “no” can be made on the acceptability of the mix. These test results may also be used in a Bayesian Decision Rule, which will provide a probability statement regarding whether the mix will be found to be good if it is used in a future project.

The test was found to have good repeatability properties. The variability in the ratios due to the measurement errors as given by the within-specimen CV percentage were 6.9 percent for the good specimens and 12.2 percent for the poor specimens. These numbers are for a single specimen, and the test will be done with more than one specimen, perhaps with four or more if little is known about the performance of the mix in regard to its moisture susceptibility. It is clear from the Bayesian analysis that some mixes will get a quick acceptance, some will get a quick fail, and others will be in a somewhat uncertain state when the tests are completed. These uncertain

outcomes may be all that is needed for a decision, but if not, additional tests may be required.

The Bayesian framework for the development of good decision rules has been developed and illustrated for this important problem. These decision rules may be updated at any laboratory simply by keeping good records of the results of ongoing tests. This active updating would provide the very best of decision rules for any laboratory doing these tests.

While the structure of the Bayesian Decision Rule is developed by a mathematical process, the nature of the rule is easy to comprehend. If a given laboratory is finding that a high percentage of the mixes being tested are good in their field performances, then they should be more inclined to consider the somewhat doubtful cases to be, in fact, good. This enters into the rule as the number  $P(G)$  and has a strong influence on the calculated  $PR(Good)$ . Also, of course, the closer the observed average is to the prior average of the good mixes, the higher the calculated  $PR(Good)$  will be.

## CHAPTER 4

# Interpretation, Appraisal, and Applications

During Phase I of this research project, three simple performance tests, i.e., flow number, flow time, and dynamic modulus, were evaluated under water/load conditioning with the ECS. Among these tests, the dynamic modulus test proved to be the most promising in identifying hot-mix asphalt mixtures prone to moisture damage. Dynamic modulus, under ECS, was further investigated during Phase IA of the research. This chapter provides interpretation, appraisal, and applications of the results of this research.

### 4.1 Interpretation of the Results

Unsuccessful results from the flow tests conducted under Phase I of this research imply only that flow tests are not suitable for moisture damage detection as they were used in this research. It is possible that the flow number test could produce acceptable results if the ECS procedure were modified to perform this test during the conditioning process. However, it should be pointed out that the flow number test has been shown to have a high level of variability in other studies. This may result in the test having poor sensitivity for detecting changes due to moisture conditioning. The high level of variability in this test is a result of the flat slope of the permanent deformation curve for a large number of cycles prior to flow. This flat slope makes it very difficult to detect the exact point when flow occurs in most mixtures.

During Phase IA, the results from the ECS/dynamic modulus tests were compared with those from the Hamburg wheel tracking tests (HWTD and Tex-242-F) and indirect tensile tests (ASTM D4867). The success of the developed ECS/dynamic modulus procedure was not determined on the basis of how well the results from this procedure compared to those from HWTD or ASTM D4867. Rather, success was determined on the basis of the procedure's ability to predict reported field performance for each mix.

Procurement of detailed information regarding construction and performance of selected mixes for this study was a

great challenge. In most cases, lack of detailed performance data prevented reliable ranking of the mixtures in terms of moisture damage resistance. Furthermore, construction data and in-place density were not available to interpret the results in the light of such information. Three of the mixes reported to perform poorly that were selected for this study had been historically poor performers with regard to moisture damage regardless of in-place air voids. However, for the other two mixes (Arkansas gravel and Kentucky limestone), reported moisture damage problems were associated with specific projects, and in-place density data for these projects could have produced better interpretation of results.

Table 52 provides a summary of results from all three tests. Among the presented procedures, the ECS/dynamic modulus procedure appears to best match the reported field performances. The inability to correctly predict performance for the Wisconsin gravel with the ECS/dynamic modulus procedure appears to be the result of using excessive conditioning load for a mixture with a soft PG 58-28 binder rather than truly being the result of moisture damage.

### 4.2 Appraisal of the ECS/Dynamic Modulus Test Procedure

The need to explore new test procedures for moisture damage is justified because of the shortcomings of the current procedures. Test methods ASTM D4867 and AASHTO T283 are still the procedures most widely used to assess the moisture susceptibility of asphalt mixes. A major concern with these tests is their reproducibility and ability to predict moisture susceptibility with reasonable confidence. State highway agencies have reported mixed success with these methods. Some of the problems with AASHTO T283 were identified in a comprehensive research project by Epps et al. (4). Problems with these test methods triggered several state highway agencies' use of wheel tracking devices for identifying moisture damage. The main disadvantage of the wheel tracking tests is

**Table 52. Summary of results for all mixes tested under Phase IA research.**

Mix	TSR	HWTD	ECS/Dynamic Modulus	Reported Field Performance
GA Granite	Poor	Poor	Poor	Poor
AR Gravel	<u>Good</u> <sup>1</sup>	<u>Good</u>	Poor	Poor
WI Gravel	Good	<u>Poor</u>	<u>Poor</u>	Good
MS Chert	Poor	<u>Good</u>	Poor	Poor
KY Limestone	<u>Good</u>	Poor	Poor	Poor
OK Sandstone	<u>Poor</u>	Good	Good	Good
PA Dolomite	Good	Good	Good	Good
WY Gravel	Poor	Poor	Poor	Poor

<sup>1</sup>Underlined items refer to test predictions that did not match reported field performance.

that they do not provide fundamental material properties, and it has been shown that the test may give false positive and false negative results (39)

For the reasons discussed above, there is certainly a place for the researched ECS/dynamic modulus system. There are several advantages to using such a system. First, the ECS was extensively researched and improved during SHRP and during a multiyear research project at the University of Texas at El Paso. Second, the dynamic modulus test has become the dominant test among the three original simple performance tests and appears to be the test proposed as part of future mix design procedures. Another advantage of the ECS/dynamic modulus system is that the repeated load/water conditioning used in this procedure simulates, to some extent, the combined effect of traffic and water on the asphalt pavement, a feature lacking in AASHTO T283 and ASTM D4867 procedures. The results in Table 52 indicate that the procedure used with ECS/dynamic modulus in this research identified the mixture quality in terms of moisture susceptibility seven out of eight times.

In spite of the advantages outlined above, there are several shortcomings that need to be addressed before the ECS/dynamic modulus system can be used as a routine mix design test to identify the moisture damage susceptibility of the mix. These problems are mostly associated with the duration of water/load conditioning, temperature at the time of conditioning, and the magnitude of the conditioning load.

The current conditioning time of 18 h appears to be long for routine testing because at a minimum, to have reliable results, three replicate specimens are needed, and each needs to be subjected to 18 h of conditioning. Further investigation is needed to determine whether the conditioning time could be reduced.

Current conditioning temperature, for both water and specimen, is 60°C. Such a high conditioning temperature is desirable because, on the one hand, it is close to actual pavement temperature, and, on the other hand, it accelerates the effect of moisture damage. However, test duration would be shortened if testing could be conducted at a lower temperature without increasing the conditioning time. Since the dynamic modulus testing is conducted at 25°C, conditioning

at a temperature lower than 60°C reduces the time needed to reach the 25°C temperature after conditioning is completed.

The peak magnitude of the haversine load during conditioning has not been adequately addressed yet. In the past, a constant load of 200 lb has been utilized. During this research, a good faith attempt was made to develop a procedure for determination of a reasonable conditioning load, as discussed in Chapters 2 and 3. However, it appears that with the recommended approach, the load level selected was too high for the mix with the PG 58-28 binder since the retained modulus after water/load conditioning was significantly lower than the modulus of the dry, unconditioned specimen. Having the proper load level during conditioning is very important because of the need to control the level of damage associated with the load and to ensure that it is of a similar magnitude to the load-induced damage in the field. Excessive conditioning load could damage the specimen beyond reasonable levels, reducing the measured modulus and, therefore, the moduli ratio. In this case, the results would not be truly indicative of the damage imposed by the presence of moisture. However, if the load is too low, then the pumping/suction effect in the presence of water may not be fully induced.

### 4.3 Applications

The developed ECS/dynamic modulus testing procedure has the potential to be used in the hot-mix asphalt design phase. As mentioned previously, modifications to the system are needed before it can be used as a routine mix design procedure. A great benefit of this testing system is that it is focused on measuring a widely used engineering property, i.e., asphalt modulus. The technicians and engineers who will be conducting Superpave mix design will need to become familiar with the dynamic modulus test once it becomes part of the Superpave mix design system. As a result, it makes sense to utilize this testing with water/load conditioning to evaluate moisture damage. Of course, for routine testing, the procedure could be limited to just one frequency of loading (for example, 10 Hz) rather than using different frequencies, as was done in this research.

Another important application of the results of this testing system will be with the developed mechanistic empirical pavement design guide (ME-PDG) used for pavement performance predictions. The pavement response models in the ME-PDG utilize the dynamic modulus as one of the important input parameters. The modulus of the unconditioned specimen, as well as the retained modulus after the ECS/dynamic modulus testing, could be used in the pavement response models to determine the impact of moisture damage on developed distresses (rutting and fatigue cracking). An example of this application is presented here for a project built in the northern part of the Pennsylvania in 2001. An analysis was conducted using ME-PDG (version 0.900), available on the Web site of the Transportation Research Board. A 20-yr design life was considered for analysis. The pavement structure used for this analysis is shown in Figure 52.

To evaluate the effect of dynamic modulus on predicted performance, the measured moduli of different layers were first used as input in the models. Afterward, the moduli were reduced at different levels, and the analyses were repeated.

Figures 53 and 54 indicate how rutting and fatigue cracking predictions are influenced as a result of reduction in the modulus for the particular pavement structure and input used in this analysis. As shown in these figures, 75-percent retained modulus after conditioning resulted in a 10-percent increase in rutting, and a 50-percent increase in fatigue cracking. A 50-percent modulus reduction resulted in a 30-percent increase in rutting and a 150-percent increase in fatigue cracking.

The significance of the impact of modulus on the results is evident considering the models used in the ME-PDG. Rutting is determined as a summation of permanent deformation of different layers as given in the following equation:

$$RD = \sum_{i=1}^n (\epsilon_p)_i h_i \quad (24)$$

where

$RD$  = total rutting,

$(\epsilon_p)_i$  = permanent deformation of layer  $i$ ,

$h_i$  = thickness of layer  $i$ , and

$n$  = number of layers used in the analysis.

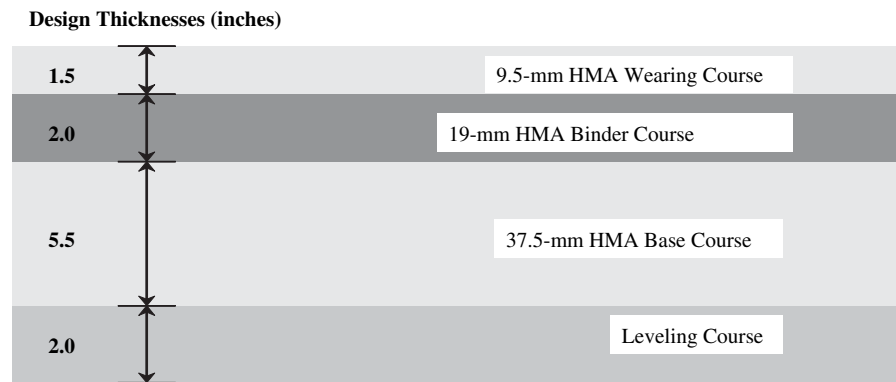


Figure 52. Pavement layer information used as input with ME-PDG for performance prediction.

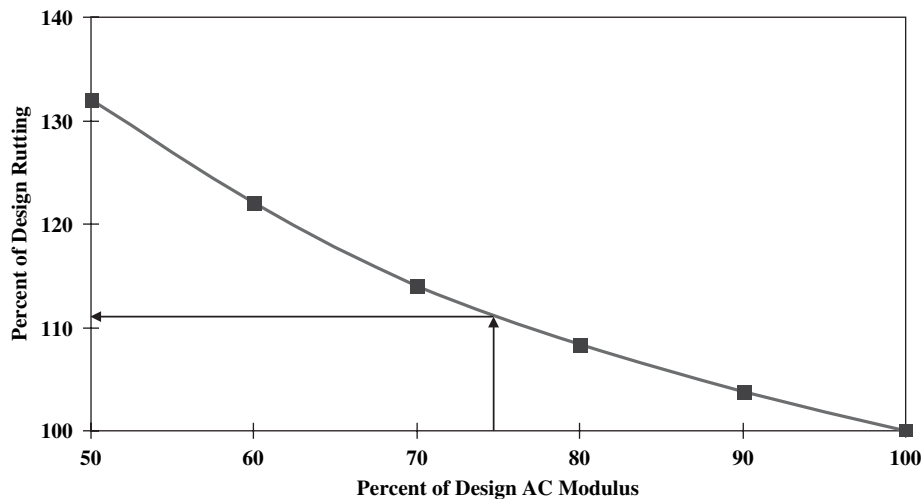
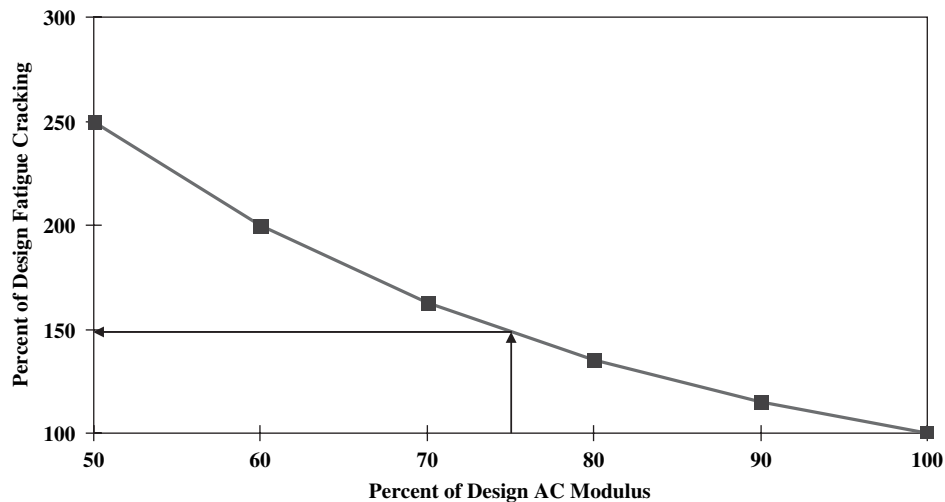


Figure 53. The impact of changes in asphalt concrete modulus on predicted rutting.



**Figure 54. The impact of changes in asphalt concrete modulus on predicted fatigue cracking.**

$\epsilon_p$  is related to the resilient strain  $\epsilon_r$  through

$$\epsilon_p = \epsilon_r (a_1 T^{a_2} N^{a_3}) \quad (25)$$

where

$\epsilon_r$  = resilient strain,  
 $T$  = layer temperature,  
 $N$  = number of load repetitions, and  
 $a_1$ ,  $a_2$ , and  $a_3$  are calibration coefficients.

Resilient strain  $\epsilon_r$  at each pavement layer is inversely proportional to the modulus of that layer.

For fatigue cracking, fatigue life is determined from the following equation:

$$N_f = K_1 \left[ \frac{1}{\epsilon_t} \right]^{k_2} \left[ \frac{1}{E} \right]^{k_3} \quad (26)$$

where

$N_f$  = number of load repetitions to fatigue cracking,  
 $\epsilon_t$  = tensile strain at the critical location,  
 $E$  = asphalt modulus, and  
 $K_1$ ,  $k_2$ , and  $k_3$  = constants determined from the experiment.

Critical tensile strain,  $\epsilon_t$ , is inversely proportional to the layer modulus (see Figure 55). Both the rutting model and the fatigue model indicate the importance of the modulus and its direct impact on the predicted performance.

#### 4.4 Cost of the ECS/Dynamic Modulus Set-Up

The total cost of the ECS/dynamic modulus testing equipment depends on the cost of its individual units, i.e., the cost of the equipment for conducting dynamic modulus testing

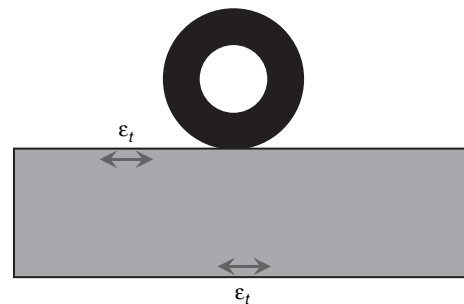


**Figure 55. Critical tensile strain in a pavement layer under load.**

and repeated loading during conditioning and the cost of the device for water conditioning. Commercial servo-hydraulic units, which are currently manufactured for conducting simple performance tests, are quite capable of addressing the needs of the ECS/dynamic modulus system. Such simple performance testers cost approximately \$55,000.

To the best of the authors' knowledge, at the time of preparing this report, there was only one manufacturer of the ECS. During SHRP, several of these units were manufactured. However, production of ECS units during the post-SHRP period progressed slowly, and very few units with improvements over the original equipment were produced. A recent inquiry into the cost of improved units indicates a cost of under \$12,000. This includes the flow control unit equipped with water drain tanks, flow meter, pressure control vacuum gauge and regulator, pressure transducers, digital pressure displays, water reservoir, and several other pieces. The unit also includes a water heating unit with a digital temperature controller and a capacity to heat 20 liters of water to 90°C.



## CHAPTER 5

# Conclusions and Recommendations

### 5.1 Conclusions

This research study was focused on utilizing and improving a laboratory testing system for reliable prediction of moisture damage in asphalt concrete. For this purpose, the test procedures developed for dynamic modulus, flow number, and flow time under NCHRP Projects 9-19 and 9-29 were applied to specimens conditioned with the ECS. Mixes with known field performance were procured and tested with this system. It was concluded during Phase I of this research that the flow number and flow time tests did not provide satisfactory results in predicting HMA moisture damage potential, while the results from the dynamic modulus test were promising. This test was further evaluated during Phase IA of the project. During Phase IA, the mixes tested included those demonstrating resistance against moisture damage and those susceptible to moisture damage. The tests were conducted at two different laboratories (PSU and UTEP). For comparison, indirect tensile strength of conditioned and unconditioned specimens was also determined by Advanced Asphalt Technologies, LLC, according to ASTM D4867. All mixes were also tested in the Hamburg Wheel Tracking Device (HWTd) at PaveTex Engineering and Testing, Inc.

The results indicated that for seven of the eight mixes researched in Phase IA of NCHRP Project 9-34, the ECS/dynamic modulus system was able to identify the mix quality in terms of moisture damage. This was a higher level of performance prediction than ASTM D4867 and the HWTd. The test protocol should be further modified to be used as a routine test for evaluating moisture-induced damage.

It was also shown that determining the change in asphalt concrete modulus as a result of moisture damage had the potential to be utilized with the mechanistic empirical design for performance prediction purposes.

### 5.2 Recommendations

The ECS/dynamic modulus procedure developed under this research has demonstrated a great ability in discriminating between mixes that perform well and those that perform poorly in resisting moisture damage. However, it is unlikely that the developed procedure, in its current form, will be accepted as a routine test in design of hot-mix asphalt concrete. The procedure needs to be simplified and shortened before it can be widely adopted. The major area of concern is the time it takes to complete the test. Specifically, further work is needed in regard to the duration of water/load conditioning, temperature at the time of conditioning, and the magnitude of the conditioning load.

One approach for reducing the testing time and simplifying the procedure is measuring and utilizing modulus or deformation of the specimen during the conditioning as a deciding factor rather than using measurements before and after completion of conditioning. With this approach, the modulus (or strain) of the specimen is monitored while conditioning is in progress, and once the value of the modulus drops below a threshold (or once deformation exceeds a certain level), excessive damage is indicated and the test is stopped. If the threshold is not met during a specified number of conditioning load cycles, the mix is considered moisture-damage resistant. A careful investigation is needed to determine how reliable measurement of deformation during water/load conditioning could be made because this deformation would be utilized in determination of the specimen modulus.

It was mentioned that unsuccessful results from the flow tests conducted in this research were probably due to the way the tests were conducted. Further research could be conducted to evaluate the results when the flow number procedure is applied during conditioning. However, it is recommended that the criteria be based on the permanent deformation from

the test after conditioning rather than the number of load cycles to tertiary creep (flow number). As was discussed earlier, high variability in flow number makes this parameter unsuitable as a criterion in a moisture conditioning test.

Further exploration into the conditioning phase of the test could be extremely valuable in improving the procedure used in this research. It is recommended that in addition to the water/load conditioning that was applied in this research, an experiment be conducted to explore the effect of load conditioning and water conditioning separately. In other words, replicate specimens should be subjected to three levels of conditioning: a combination of load and water (as in this research), load only, and water only. With this approach, a distinction could be made between the damage induced by load and the damage induced by water. In addition, the load/water interaction effect is taken into account with this approach.

In this research, the authors have been concentrating on different load levels, assuming that temperature will remain constant regardless of the binder grade and assuming that for softer grades, the load could be reduced enough to counterbalance the effect of higher temperature. The authors' assumption has been that using a lower load level and higher temperature might have the same effect as using a higher load level and lower temperature. However, time and the budget

of the project did not allow for validation of this assumption. It would be worth investigating the load-temperature relationship in a future project to achieve similar damage levels after conditioning.

It is also recommended that the materials studied under Phase IA of the research be evaluated for fundamental properties. For example, the Western Research Institute has been testing the hypothesis that asphalt/aggregate mixtures that form insoluble calcium salts of asphalt components are the least prone to moisture damage. Since the field performance of the mixes used in this research is known, the results could be used in validating this hypothesis. In addition, recent research on the relationship between moisture damage and asphalt/aggregate surface energy by the Texas Transportation Institute could be extended to the mixes used in the NCHRP Project 9-34 study.

Distilled water was used for conditioning of specimens in this study. Researchers are not aware of any study that investigated mix behavior after being conditioned with different types of water containing various dissolved chemicals and salts. Since rain water and underground water, major contributors to asphalt moisture damage, can contain different types of salts in different parts of the country, it may be important to consider the effect of water types on asphalt moisture damage.

---

# References

1. Hicks, R. G. *NCHRP Synthesis of Highway Practice 175: Moisture Damage in Asphalt Concrete*. Transportation Research Board, National Research Council, Washington, DC, 1991.
2. Solaimanian, M., T. W. Kennedy, and W. E. Elmore. *Long-Term Evaluation of Stripping and Moisture Damage in Asphalt Pavements Treated with Lime and Antistripping Agents*. Report CTR 0-1286-1F. Texas Department of Transportation, Center for Transportation Research, University of Texas at Austin, 1993.
3. Kiggundu, B. M. and F. L. Roberts. *Stripping in HMA Mixtures: State-of-the-Art and Critical Review of Test Methods*. NCAT Report No. 88-2. National Center for Asphalt Technology, Auburn University, Auburn, AL 1988.
4. Epps, J. A., P. E. Sebaaly, J. Penaranda, M. R. Maher, M. B. McCann, and A. J. Hand. *NCHRP Report 444: Compatibility of a Test for Moisture-Induced Damage with Superpave Volumetric Mix Design*. Transportation Research Board, National Research Council, Washington, DC, 2000.
5. Johnson, D. L. *Debonding of Water-Saturated Asphaltic Concrete Caused by Thermally Induced Pore Pressure*. MSCE Thesis. University of Idaho, Moscow, 1969.
6. Schmidt, R. J. and P. E. Graf. "The Effect of Water on the Resilient Modulus of Asphalt Treated Mixes." *Proceedings, Association of Asphalt Paving Technologists*, Vol. 41, 1972, pp. 118–162.
7. Jimenez, R. A. "Testing for Debonding of Asphalt from Aggregates." *Transportation Research Record 515*. Transportation Research Board, National Research Council, Washington, DC, January 1974, pp. 1–17.
8. Lottman, R. P. *NCHRP Report 192: Predicting Moisture-Induced Damage to Asphaltic Concrete*. Transportation Research Board, National Research Council, Washington, DC, 1978.
9. Tunnicliff, D. G. and R. Root. "Antistripping Additives in Asphaltic Concrete—State-of-the-Art 1981." *Proceedings, Association of Asphalt Paving Technologists*, Vol. 51, 1982, pp. 265–293.
10. Lottman, R. P. *NCHRP Report 246: Predicting Moisture-Induced Damage to Asphaltic Concrete: Field Evaluation*. Transportation Research Board, National Research Council, Washington, DC, 1982.
11. Aschenbrener, T. "Evaluation of Hamburg Wheel-Tracking Device to Predict Moisture Damage in Hot Mix Asphalt." *Transportation Research Record 1492*. Transportation Research Board, National Research Council, Washington DC, 1995, pp. 193–201.
12. Aschenbrener, T., and G. Currier. *Influence of Testing Variables on the Results from the Hamburg Wheel-Tracking Device*. CDOT-DTD-R-93-22. Colorado Department of Transportation, Denver, CO, 1993.
13. Aschenbrener, T., R. Terrel, and R. Zamora. *Final Report: Comparison of the Hamburg Wheel Tracking Device and the Environmental Conditioning System to Pavements of Known Stripping Performance*. Colorado Department of Transportation, Denver, CO, 1994.
14. Aschenbrener, T., R. B. McGennis, and R. L. Terrel. "Comparison of Several Moisture Susceptibility Tests to Pavement of Known Field Performance." *Journal of the Association of Asphalt Paving Technologists*, 1995, pp. 163–208.
15. Al-Swailmi, S. and R. Terrel. *Water Sensitivity of Asphalt-Aggregate Mixtures: Test Selection*. Report SHRP-A-403. Strategic Highway Research Program, National Research Council, Washington, DC, 1994.
16. Al-Swailmi, S. and R. L. Terrel. "Evaluation of Water Damage of Asphalt Concrete Mixtures Using the Environmental Conditioning System (ECS)." *Journal of the Association of Asphalt Paving Technologists*, Vol. 61, 1992, pp. 405–445.
17. Al-Swailmi, S., T. V. Scholz, and R. L. Terrel. "Development and Evaluation of Test System to Induce and Monitor Moisture Damage to Asphalt Concrete Mixtures." *Transportation Research Record 1353*. Transportation Research Board, National Research Council, Washington, DC, 1992, pp. 39–45.
18. Vemuri, N. *Evaluation and Modification of Environmental Conditioning System to Predict the Moisture Susceptibility of Hot Mix Asphalt Concrete*. M.S. Thesis. University of Texas at El Paso, 1996.
19. Tandon, V., N. Vemuri, S. Nazarian, and M. Tahmoressi. "A Comprehensive Evaluation of Environmental Conditioning System." *Journal of the Association of Asphalt Paving Technologists*, Vol. 66, 1997, pp. 187–210.
20. Tandon, V. and S. Nazarian. *Modified Environmental Conditioning System: Validation and Optimization*. Research Report TX - 01/1826 - 1F. Center for Highway Materials Research, University of Texas at El Paso, 2001.
21. Alam, M. M. *A Test Method for Identifying Moisture Susceptible Asphalt Concrete Mixes*. M.S. Thesis. The University of Texas at El Paso, 1997.
22. Witzcak, M. W., K. Kaloush, T. Pellinen, M. El-Basyouny, and H. Von Quintus. *NCHRP Report 465: Simple Performance Test for Superpave Mix Design*. Transportation Research Board, National Research Council, Washington, DC, 2002.
23. Collins, R. *Status Report on the Use of Hydrated Lime in Asphaltic Concrete Mixtures in Georgia*, Georgia Department of Transportation, Materials and Research Report. Atlanta, GA, June 13, 1988.
24. Tunnicliff, D. G. and R. E. Root. *NCHRP Report 373: Use of Antistripping Additives in Asphaltic Concrete Mixtures: Field Evaluation*. Transportation Research Board, National Research Council, Washington, DC, 1995.

25. *Mix Design Methods for Asphalt Concrete and Other Hot-Mix Types*. Manual Series Number 2. (MS-2). Asphalt Institute, Lexington, KY, 1979.
  26. Witzczak, M. W., R. Bonaquist, H. Von Quintus, and K. Kaloush. "Specimen Geometry and Aggregate Size Effects in Uniaxial Compression and Constant Height Shear Tests." *Journal of the Association of Asphalt Paving Technologists*, Vol. 68, 2000, pp. 733–793.
  27. Bonaquist, R. F., D. W. Christensen, and W. Stump. *NCHRP Report 513: Simple Performance Tester for Superpave Mix Design: First-Article Development and Evaluation*. Transportation Research Board of the National Academies, Washington, DC, 2003.
  28. Pellinen, T. K. *Investigation of the Use of Dynamic Modulus as an Indicator of Hot-Mix Asphalt Performance*. Ph.D. Dissertation. Arizona State University, Tempe, May 2001.
  29. Dougan, C. E., J. E. Stephens, J. Mahoney, and G. Hansen. *E\*-DYNAMIC MODULUS Test Protocol—Problems and Solutions*. Report CT-SPR-0003084-F-03-3. University of Connecticut, Storrs, April 2003.
  30. Terrel, R. L. and S. Al-Swailmi. *Water Sensitivity of Asphalt–Aggregate Mixes*. Report SHRP-A-403. Strategic Highway Research Program, National Research Council, Washington, DC, 1994.
  31. Kaloush, K. *Simple Performance Test for Permanent Deformation of Asphalt Mixtures*. Ph.D. Dissertation. Arizona State University, Tempe, 2001.
  32. Andrei, E., M. W. Witzczak, and M. W. Mirza. "NCHRP Inter Team Report 1-37A: Development of a Revised Predictive Model for the Dynamic (Complex) Modulus of Asphalt Mixtures," University of Maryland, College Park, 1999.
  33. Spellerberg, P., D. Savage, and J. Pielert. *Web Document 54: Precision Estimates of Selected Volumetric Properties of HMA Using Non-Absorptive Aggregate*. [http://onlinepubs.trb.org/onlinepubs/nchrp/nchrp\\_w54.pdf](http://onlinepubs.trb.org/onlinepubs/nchrp/nchrp_w54.pdf). Transportation Research Board of the National Academies, Washington, DC, February 2003.
  34. American Association of State Highway and Transportation Officials. AASHTO Materials Reference Laboratory. [www.amrl.net/Portal/PublicDocs/PspStatistics/Index.asp](http://www.amrl.net/Portal/PublicDocs/PspStatistics/Index.asp). Accessed September 2005.
  35. Stuart, K. D. *Evaluation of Procedures Used to Predict Moisture Damage in Asphalt Mixtures*. Report FHWA/RD-86/091. FHWA, U.S. Department of Transportation, March 1986.
  36. McCuen, R. H. *Statistical Methods for Engineers*. Prentice-Hall, Inc., Englewood Cliffs, NJ, 1985.
  37. Izzo, R. P. and M. Tahmoressi. "Testing Repeatability of the Hamburg Wheel-Tracking Device and Replicating Wheel-Tracking Devices among Different Laboratories." *Journal of the Association of Asphalt Paving Technologists*, Vol. 68, 1999, pp. 589–612.
  38. Christensen, D. W., T. Pellinen, R. F. Bonaquist. "Hirsch Model for Estimating the Modulus of Asphalt Concrete." *Journal of the Association of Asphalt Paving Technologists*, Vol. 72, 2003, pp. 97–121.
  39. Lu, Q. and J. T. Harvey. "Evaluation of Hamburg Wheel-Tracking Device Test with Laboratory and field Performance Data." *Transportation Research Record: Journal of the Transportation Research Board*, No. 1970, 2006, pp. 25–44.
-

## APPENDIXES

Appendixes to the contractor's final report for NCHRP Project 9-34, "Improved Conditioning Procedure for Predicting the Moisture Susceptibility of HMA Pavements" are available on the TRB website at [http://trb.org/news/blurp\\_detail.asp?id=8113](http://trb.org/news/blurp_detail.asp?id=8113). The appendixes are the following:

- Appendix A ECS/Dynamic Modulus Procedure for Phase IA
  - Appendix B Test Specimen Identification and Air Void Content
  - Appendix C HWTD Data and Graphs
  - Appendix D ECS/Dynamic Modulus Results
  - Appendix E Visual Inspection
  - Appendix F Statistical Analysis of Dynamic Modulus Results.
-

*Abbreviations and acronyms used without definitions in TRB publications:*

AAAE	American Association of Airport Executives
AASHO	American Association of State Highway Officials
AASHTO	American Association of State Highway and Transportation Officials
ACI-NA	Airports Council International-North America
ACRP	Airport Cooperative Research Program
ADA	Americans with Disabilities Act
APTA	American Public Transportation Association
ASCE	American Society of Civil Engineers
ASME	American Society of Mechanical Engineers
ASTM	American Society for Testing and Materials
ATA	Air Transport Association
ATA	American Trucking Associations
CTAA	Community Transportation Association of America
CTBSSP	Commercial Truck and Bus Safety Synthesis Program
DHS	Department of Homeland Security
DOE	Department of Energy
EPA	Environmental Protection Agency
FAA	Federal Aviation Administration
FHWA	Federal Highway Administration
FMCSA	Federal Motor Carrier Safety Administration
FRA	Federal Railroad Administration
FTA	Federal Transit Administration
IEEE	Institute of Electrical and Electronics Engineers
ISTEA	Intermodal Surface Transportation Efficiency Act of 1991
ITE	Institute of Transportation Engineers
NASA	National Aeronautics and Space Administration
NASAO	National Association of State Aviation Officials
NCFRP	National Cooperative Freight Research Program
NCHRP	National Cooperative Highway Research Program
NHTSA	National Highway Traffic Safety Administration
NTSB	National Transportation Safety Board
SAE	Society of Automotive Engineers
SAFETEA-LU	Safe, Accountable, Flexible, Efficient Transportation Equity Act: A Legacy for Users (2005)
TCRP	Transit Cooperative Research Program
TEA-21	Transportation Equity Act for the 21st Century (1998)
TRB	Transportation Research Board
TSA	Transportation Security Administration
U.S.DOT	United States Department of Transportation